小型磁気圏形成とそのダイポール磁場強度依存性に関する考察

臼井 英之 [1]; 沖 知起 [2]; 三宅 洋平 [3]
[1] 神戸大・システム情報; [2] 神大・システム・計算; [3] 神戸大学

The formation of a small magnetosphere and its dependence on the dipole field intensity

Hideyuki Usui[1]; Satoki Oki[2]; Yohei Miyake[3]
[1] System informatics, Kobe Univ; [2] Kobe Univ.; [3] Kobe Univ.

The objective of this research is to understand the formation of small magnetospheres of weakly magnetized bodies such as asteroid, lunar magnetic anomaly and Mercury by taking the intensity of the intrinsic magnetic field as a physical parameter. We define D_p as the distance from the dipole center to the point at which the dynamic pressure of the solar wind and the dipole magnetic pressure are equal. When the ratio D_p/L_i is much larger than the unity where L_i denotes the ion inertia length, the formation of the magnetosphere can be examined with the fluid plasma approximation.However, the D_p/L_i becomes close to the unity, the kinetic effect such as finite Lamor radius in plasma cannot be ignored in the formation of the magnetosphere. Blanco-Cano et al. (2003) examined the effect of finite ion scale lengths on the formation of planetary magnetospheres by performing two-dimensional hybrid particle simulations with different D_p/L_i values. Ashida et al. (2014) examined the formation of small magnetospheres for the cases where D_p/ L_i is equal or less than the unity by performing three-dimensional full particle plasma simulations.In the present study, considering the previous studies, we started to examine the formation of small magnetospheres for the cases where D_p/L_i is slightly larger than the unity by performing three-dimensional full particle simulations. We would like to understand how each region of the magnetosphere will change when we vary D_p/L_i values. When D_p/L_i is close to the unity, we found the formation of a small magnetosphere and the asymmetric structure of the plasma density distribution in the magnetic equator. We are interested to know how these phenomena vary when we increase the D_p/L_i value. We would like to keep increasing the D_p/L_i so that we will be able to contribute to the understanding of the Mercury's magnetosphere in the near future.

本研究の目的は、小惑星や月面磁気異常、水星など、地球よりも十分弱い磁場を持つ天体と太陽風との相互作用により形成される小型磁気圏について、ダイポール磁場強度をパラメータとして理解することである。天体固有磁場の磁気ダイポール中心から磁気圧と太陽風動圧が釣り合う点までの距離を D_p とすると、D_p が太陽風イオン慣性長 L_i に対して十分大きい場合は、地球磁気圏のように、太陽風を流体近似した形で磁気圏形成を議論できる。しかし、天体磁場の磁気モーメントが小さくなり D_p が L_i やイオンラーマ半径などに近づくと磁気圏形成において太陽風の運動論的効果が無視できなくなる。先行研究の一つとして、Blanco-Cano et al. (2003) により、磁気圏形成における D_p/L_i 依存性について、イオンの運動論的効果を含めた 2 次元ハイブリッド粒子シミュレーションを用いて解析が行われた。また、Ashida et al.(2014) により、電子も粒子として扱う全粒子プラズマシミュレーションを用いて、D_p の太陽風イオンラーマ半径に対する比が 1 以下の場合における磁気圏形成の解析が行われた。

本講演では、これらの先行研究を踏まえた上で、D_p/L_i が 1 から数倍の範囲の場合における小型磁気圏形成に着目する。幾つかの違う D_p を用いて、電子及びイオンを粒子として扱う全粒子プラズマモデルによる小型磁気圏形成シミュレーションを行い、磁気圏各領域形成の D_p/L_i 依存性について電子ダイナミクスを考慮して明らかにする。D_p が L_i に近いモデルを用いたシミュレーション結果により、小型磁気圏の形成、朝方夕方の磁気圏構造の非対称性、昼間側磁気圏境界層幅の IMF 方向の依存性などが明らかになった。これらの現象が、D_p/L_i 値にどのように依存するかについて考察を行う。今後、磁気ダイポールを強めることにより、D_p/L_i 値を 10 以上にし、最終的には水星磁気圏環境を再現しその理解につなげていきたい。

ベピコロンボ水星探査計画の現状と新たな科学課題の整理

村上 豪 [1]; 藤本 正樹 [2]; 早川 基 [3]; BepiColombo MMO SWG 村上 豪 [4]; BepiColombo MMO プロジェクトチーム 早川　基 [4]
[1] ISAS/JAXA; [2] 宇宙研; [3] 宇宙研; [4] -

Current status and updated science goals of Mercury exploration project BepiColombo

Go Murakami[1]; Masaki Fujimoto[2]; Hajime Hayakawa[3]; Go Murakami BepiColombo MMO SWG[4]; HAYAKAWA, Hajime BepiColombo MMO Project team[4]
[1] ISAS/JAXA; [2] ISAS, JAXA; [3] ISAS/JAXA; [4] -

After the successful observation by the first Mercury orbiter MESSENGER ended in 2015, Mercury becomes one of the most curious planets to investigate. MESSENGER raised new science issues, such as the northward offset of planetary dipole magnetic filed, the highly dynamic magnetosphere, and the year-to-year constant exosphere. These outstanding discoveries still remains as open issues due to some limitations of instruments onboard MESSENGER and its extended elliptical orbit with apherm in southern hemisphere. The next Mercury exploration project BepiColombo will address these open issues. BepiColombo is an ESA-JAXA joint mission to Mercury with the aim to understand the process of planetary formation and evolution as well as to understand Mercury's extreme environment in the solar system. Two spacecraft, i.e. the Mercury Planetary Orbiter (MPO) and the Mercury Magnetospheric Orbiter (MMO), will be launched in October 2018 by an Ariane-5 launch vehicle and arrive at Mercury in December 2025. The mechanical test in a complete stack configuration has been performed in the ESA test center and successfully finished. Here we present the latest development status of BepiColombo and updated science goals addressed by MMO.

Io-related electron heating in the Io plasma torus: effect of local plasma density around Io

Fuminori Tsuchiya[1]; Kazuo Yoshioka[2]; Masato Kagitani[3]; Tomoki Kimura[4]; Go Murakami[5]; Atsushi Yamazaki[6]; Hiroaki Misawa[7]; Yasumasa Kasaba[8]; Ichiro Yoshikawa[9]; Takeshi Sakanoi[10]; Ryoichi Koga[11]; Ryo Arakawa[12]; Fumiharu Suzuki[13]; Reina Hikida[14]

[1] Planet. Plasma Atmos. Res. Cent., Tohoku Univ.; [2] The Univ. of Tokyo; [3] PPARC, Tohoku Univ; [4] RIKEN; [5] ISAS/JAXA; [6] ISAS/JAXA; [7] PPARC, Tohoku Univ.; [8] Tohoku Univ.; [9] EPS, Univ. of Tokyo; [10] Grad. School of Science, Tohoku Univ.; [11] Geophysics, Tohoku Univ.; [12] Geophysics, Tohoku Univ.; [13] Complexity Science, Univ. of Tokyo; [14] Frontier Sciences, Tokyo Univ.

http://pparc.gp.tohoku.ac.jp/

HISAKI observation of Io plasma torus (IPT) with extreme ultraviolet (EUV) wavelength range is a useful probe to access plasma environment in inner magnetosphere of Jupiter. Emissions from sulfur and oxygen ions in EUV range are caused by electron impact excitation and their intensity is well correlated with the electron temperature distribution in IPT. Previous IPT observation with HISAKI showed that the brightness was enhanced downstream of the satellite Io, indicating that efficient electron heating takes place at Io and/or just downstream of Io. Detailed analysis of the emission intensity shows that the brightness depends on the magnetic longitude at Io and primary and secondary peaks appear in the longitude ranges of 100-130 and 250-340 degrees, respectively [Tsuchiya et al. 2015]. Io's orbit crosses the center of the IPT around these longitudes. The peak position and amplitude are slightly different between dawn and dusk sides. Here, we introduce inhomogeneous IPT density model in order to investigate relation between the emission intensity and local plasma density around Io in detail. An empirical IPT model [Bagenal 1994] is used for radial distribution of ion and electron density in the equatorial plane. The density distribution along magnetic field lines is calculated by solving diffusive equilibrium [Mei et al. 1995], where we do not consider longitude dependence of ion temperatures here. To include longitude and local time asymmetry in IPT, we consider (1)dawnward shift of IPT due to global convection electric field, (2) offset of Jupiter's dipole magnetic field, and (3) tilt of IPT with respect to Io's orbital plane. From the empirical IPT model, electron densities at the position of Io when the satellite is located at dawn and dusk sides are derived. The modeled electron density as a function of magnetic longitude at Io shows similar profile with the ion emission intensity derived from HISAKI. This result suggests that energy extracted around Io and/or efficiency of electron heating is closely related to the plasma density around Io and longitude and local time dependences is explained by the spatial inhomogeneity of plasma density in IPT. A part of the energy extracted around Io could be transferred to the Jovian ionosphere along the magnetic field line and cause bright aurora spots and strong radio emissions. We plan to update the model by including (1) longitude dependence of ion temperatures which also causes longitudinal inhomogeneity of plasma density and (2) spatial density distributions of neutral particles and newly picked up ions which are a primary energy source of local electron heating.

ひさき衛星によって観測された木星衛星イオの酸素原子中性雲の空間分布

古賀 亮一 [1]; 土屋 史紀 [2]; 鍵谷 将人 [3]; 坂野井 健 [4]; 米田 瑞生 [5]; 吉川 一朗 [6]; 吉岡 和夫 [7]; 村上 豪 [8]; 山崎 敦 [9]; 木村 智樹 [10]
[1] 東北大・理・地物; [2] 東北大・理・惑星プラズマ大気; [3] 東北大・理・惑星プラズマ大気研究センター; [4] 東北大・理; [5] なし; [6] 東大・理・地惑; [7] 東大・理; [8] ISAS/JAXA; [9] JAXA・宇宙研; [10] RIKEN

Spatial distribution of Io's oxygen neutral cloud observed by Hisaki/EXCEED

Ryoichi Koga[1]; Fuminori Tsuchiya[2]; Masato Kagitani[3]; Takeshi Sakanoi[4]; Mizuki Yoneda[5]; Ichiro Yoshikawa[6]; Kazuo Yoshioka[7]; Go Murakami[8]; Atsushi Yamazaki[9]; Tomoki Kimura[10]
[1] Geophysics, Tohoku Univ.; [2] Planet. Plasma Atmos. Res. Cent., Tohoku Univ.; [3] PPARC, Tohoku Univ; [4] Grad. School of Science, Tohoku Univ.; [5] none; [6] EPS, Univ. of Tokyo; [7] The Univ. of Tokyo; [8] ISAS/JAXA; [9] ISAS/JAXA; [10] RIKEN

We analyzed azimuthal and radial distribution of atomic oxygen ultraviolet emission surrounding the Jovian moon Io's torus using Hisaki/EXCEED (Extreme Ultraviolet Spectroscope for Exospheric Dynamics) to show the spatial distribution of an oxygen neutral cloud. The atmosphere of a Jovian moon Io has been thought to be mainly supported by volcanism and sublimation of frost (reviewed by Lellouch et al, [2007]). Dominant atomospheric gases are sulfur dioxide, and its dissociative products such as atomic oxygen and sulfur (electron impact dissociation and photolysis). The atoms escape from the exobase and form corona and neutral clouds mainly due to atmospheric sputtering. The spatial distribution of oxygen and sulfur neutral clouds is important to know the source of Io plasma torus. However, the spatial distribution of them was not understood because atomic oxygen (130.4 nm, 135.6 nm and 630.0 nm) and sulfur (129.9 nm and 142.9 nm) emissions are faint (several Rayleighs (R)). Hisaki satellite on board the extreme ultraviolet spectrometer called EXCEED observed Io plasma torus continuously in 2014-2015 and we found the detail distribution of atomic oxygen emission at 130.4 nm from a neutral cloud for the first time.

We investigated the Io phase angle (IPA) dependence of atomic oxygen emission in the Io plasma torus averaged over the distance range of 4.5-6.5 Jovian radii from Jupiter on the dawn and dusk sides during the volcanially quiet period (day of year (DOY) 331 to 365 of 2014). The emission strongly depends on IPA and has a maximum at IPA of 60-90 degrees on the dawn side, and at 240-270 degrees on the dusk side, respectively. The emission distribution also shows asymmetry and the intensity averaged for IPA 60-90 degrees (14.0 R) is larger than that for IPA 90-120 degrees (10.5 R) on the dusk side. There is the similar tendency on the dusk side. This shows that more oxygen atoms spread the leading side of Io rather than the trailing side. Weak atomic oxygen emission (4 R) uniformly exists not depending on IPA. We also examined the radial distribution in the same period and found that there is an emission peak near Io's orbit with decreasing the intensity up to 8.0 Jupiter radii.

We suggest the following model to explain the above observation results. The banana-shaped the thick region of an oxygen neutral cloud spreads mainly leading side of Io. In addition, the thin region distributes uniformly in the azimuthal direction up to 8 Jovian radii and decreases toward the outside. According to the model of Smyth and Marconi, [2003], the gradient of radial distribution of neutral clouds is represented by power law. We fit the power law curve to the radial distribution observed by Hisaki/EXCEED to show the number density distribution of an oxygen neutral cloud.

私たちはひさき衛星を用いてイオ起源の酸素原子発光の動径および方位角分布を解析し、イオ酸素原子中性雲の分布を明らかにした。木星衛星イオは表面の昇華と火山活動によって薄い大気を形成している。この大気は二酸化硫黄が主成分であり、電子や光と衝突することで解離して、酸素や硫黄原子が生成される。これらの原子は主に外部から飛来するイオンとの衝突による大気スパッタリングによって大気からコロナや重力圏外である中性雲 (5.8 イオ半径より外側) の領域まで広がる。酸素や硫黄中性雲の空間分布はイオプラズマトーラスの供給源を知る上で重要であるが、酸素 (130.4 nm, 135.6 nm, 630.0 nm) や硫黄原子発光 (129.9 nm, 142.9 nm) が暗い (数レイリー (R) 程度) ために今まで観測で明らかにされていなかった。しかし、ひさき衛星の数か月に及ぶイオプラズマトーラスの連続観測によって、中性雲由来の 130.4 nm 酸素原子発光の詳細な分布を解析することがはじめて可能となった。

私たちは火山活動が静穏な 2014 年の DOY (day of year) 331-365 のデータを用いて、dawn 側と dusk 側の木星中心から 4.5-6.5 木星半径の領域の酸素原子発光がイオ位相角によってどのように変動するかを調べた。その結果、酸素原子発光の明るさはイオ位相角に強く依存し、dawn 側ではイオの位相角が 60-90 度のとき、dusk 側では 240-270 度の時に最大になることが分かった。酸素原子発光はイオの近くでは非対称性を示し、dawn 側ではイオ位相角 90-120 度の時 (10.5 R) より 60-90 度の時 (14.0 R) の方が明るかった。Dusk 側でも同様の傾向が見られた。これらは酸素原子がイオの反対方向より進行方向に広がっていることを示している。一方、弱い発光 (4 R 程度) が dawn 側と dusk 側両方にイオがすべての位相角にいるときに存在した。また私たちは同時期の動径方向の分布も明らかにした。酸素原子発光はイオの軌道で最大となり、イオ軌道から遠ざかるにしたがって減少した。酸素原子の発光は木星中心から 8.0 木星半径程度まで確認できた。

これらの解析結果は次のような酸素原子中性雲のモデルで説明できると考えられる。イオ付近ではバナナ型の濃い領域がおもにイオの進行方向に広がっている。一方、それ以外の薄い領域が方位各方向に一様に、動径方向にイオ軌道から遠ざかるにしたがって減少しながら広がっている。Smyth and Marconi, [2003] のモデルによると、中性雲の動径分布の勾配はイオ軌道をピークにべき乗根で減少することが予想されている。発表ではこのひさき衛星の観測で得られた動径分布にべき乗根の関数をフィットさせ、酸素原子中性雲の数密度分布を示す。

ひさき衛星が取得した惑星大気・プラズマの観測データに対するLassoを用いた時系列解析

鈴木 文晴 [1]; 岡田 真人 [1]; 吉岡 和夫 [2]; 益永 圭 [3]; 吉川 一朗 [4]
[1] 東大・新・複雑; [2] 東大・理; [3] 東大・理
; [4] 東大・理・地惑

Time Series Analysis Using Lasso of Atmospheric and Magnetospheric Data Obtained by HISAKI

Fumiharu Suzuki[1]; Masato Okada[1]; Kazuo Yoshioka[2]; Kei Masunaga[3]; Ichiro Yoshikawa[4]
[1] Complexity Science, Univ. of Tokyo; [2] The Univ. of Tokyo; [3] Univ. Tokyo; [4] EPS, Univ. of Tokyo

http://www.astrobio.k.u-tokyo.ac.jp/yoshikawa/

Thanks to recent progress in technology related to observation instruments, we can obtain various data on planetary science. In such a privileged situation, it should be pointed out that we should use analysis methods suitable for dealing with a large number of data.

For example, in the periodic analysis, the intensity of many frequency components can be obtained by prolonging the observation period and improving the temporal resolution. However, it is inappropriate to treat all of them as meaningful signals in terms of physical interpretation. Furthermore, when fitting by using the least squares method such as Fourier transform to derive frequency components, it is impossible to prevent 'overfitting' to noise-containing data. So frequency components are erroneously estimated.

To solve the above problem, 'sparse modeling' used in the analysis of big data becomes a breakthrough. This method can extract only important variables after handling a large number of data. It is very effective against the above problem.

In this study, we show the results of analyzing by applying "Lasso" (Least Absolute Selection and Shrinkage Operator) [Tibshirani et al., 1996] to the optical observation data of HISAKI. Lasso is a mathematical method which is modeling in which a 'penalty term' is added to the least squares method. Lasso has the advantage that it can extract important variables and prevent overfitting. Lasso is widely used in information science and natural sciences such as medicine and astronomy, but it is not used in data analysis of planetary science. In this presentation, we introduce that Lasso gives better interpretive results than conventional methods.

近年、国内外の観測機器によって惑星科学に関する様々なデータが蓄積されている。このような恵まれた状況では、多数のデータの取り扱いに最適な解析方法の必要性が議論されるべきである。

例えば周期解析では、観測期間や時間分解能の向上により多数の周期成分が得られるようになるが、その全てを意味のある信号として取り扱うことは物理的解釈の上で不適切である。さらに、従来手法である離散フーリエ変換のように最小二乗法を用いたフィッティングによる周期成分の導出では、誤差を含むデータへの「過剰適合」を防げない。そのため結果として得られる偽の周期成分を排除できない危険性がある。

上記の問題に対しては、情報科学分野でビッグデータの解析に用いられるスパースモデリングが突破口となる。これは多数のデータを同等に扱った上で重要な変数のみを抽出する手法であり、上記のような惑星科学衛星のデータ解析における問題に対して非常に効果的であると考えられる。

本研究では、ひさき衛星の光学観測データに対しスパースモデリングの一種である“Lasso”（Least Absolute Selection and Shrinkage Operator）[Tibshirani et al., 1996] を適用して解析した結果を示す。この数理手法は、フィッティング手法として一般的に用いられる最小二乗法に特定の「罰則項」を加えたモデリングであり、過剰適合の防止や重要な変数の抽出が可能であるという利点を持つ。Lassoは情報科学だけでなく医学や天文学などの自然科学分野でも広く用いられているが、惑星観測衛星のデータ解析に適用された例はない。Lassoを用いることで、従来手法に比較して解釈性に優れ、物理現象の説明に役立つ結果が得られた。

CubeSat project for the investigation of the beaming structures of Jupiter's decametric radio emissions

Kazumasa Imai[1]; Lkhagvadorj Sukhtsoodol[1]; Mizuki Ando[2]; Nobuto Hirakoso[3]; Taku Takada[4]; Kentarou Kitamura[5]; Charles A. Higgins[6]; James R. Thieman[7]
[1] NIT, Kochi; [2] NIT, Gunma; [3] NIT,Gunma; [4] Kochi-CT; [5] NIT,Tokuyama.; [6] Middle Tennesee State University; [7] University of Maryland Baltimore County

Since the discovery of Jupiter's radio emissions in 1955, important details of its radiation mechanism have not yet been elucidated. Jupiter radio waves are powerful enough to easily observe on the earth, because large particle energies generated in the Jovian magnetosphere are converted into radio wave radiation energy. In order to investigate the beaming concept of Jupiter radio waves, which is important for clarifying this Jupiter radio emission mechanism, we will launch a 2U-size CubeSat for observation of Jupiter radio waves and observe simultaneously in outer space and on the ground. The purpose of this project is to measure the emission delay time by using a correlation analysis method.

It is estimated that the beaming structure of the S bursts of the short Jovian radio bursts (S bursts), has a large angle with respect to the Jovian magnetic field lines and has a narrow beam thickness. The delay time can be measured by the correlation analysis of waveform data obtained by simultaneous observations of Jupiter radio S bursts between this satellite and the ground. If the beam of Jupiter radio S bursts is moving together with the rotation of Jupiter, we can calculate a time difference of about 70 milliseconds at the base line length of 8000 km. Using the proposed simultaneous observations it is possible to test whether the Jovian S bursts are emitted like a 'beacon', rotating with Jupiter's magnetic field and sweeping by the Earth, or like a 'flashlight', an instantaneous emission with a 0 millisecond time delay. This result is very important information to determine the nature of the Jupiter radio emission mechanism.

The development of a 2U-CubeSat for Jupiter's decametric radio observation has been made by the collaboration with 8 colleges that belong to KOSEN-Space-Renkei Group. The students and teachers have been collaborating to develop the 2U-size CubeSat. This CubeSat is being considered to be launched from the International Space Station (ISS). The duration of the possible observation is estimated to be more than 50 days. During this period we are considering the measurement of the delay time between the CubeSat and ground observatories for the detection of Jovian S-bursts. The worldwide ground-based observations will be supported by the NASA RadioJOVE project, an education and outreach program for planetary radio astronomy.

We will show the design of the CubeSat for the observation of Jupiter's radio emissions, including the data acquisition system using a Raspberry Pi Zero with a GPS module, and the deployment of the antenna system. This Raspberry Pi Zero is a microcomputer board with Linux installed; it is considered to be suitable for this mission because of the small size and low power consumption. In order to observe Jupiter's radio waves, it is necessary to deploy a 3.6 m antenna at 20 MHz. We propose an antenna deployment mechanism using biometal fiber (BMF). BMF is a thread-like form in which fibers of Ti-Ni alloy have the property of contracting when voltage is applied. This antenna deployment mechanism using BMF has been tested and shows good function.

The measurement of the delay time between the CubeSat and ground observatories by the correlation analysis of Jupiter's S bursts is proposed to reveal the beaming structure of Jupiter's radio emissions. The elucidation of the radiation mechanism of Jupiter radio waves, which is the ultimate goal of Jupiter radio research, may lead to a better understanding of particle-wave energy generation mechanisms and their applications. From this point of view the contribution of this mission is believed to be significant.

This project is supported by the Coordination Funds for Promoting AeroSpace Utilization the Ministry of Education, Culture, Sports, Science and Technology (MEXT), JAPAN.

Recent Observations of Radio and Plasma Waves by Juno and Cassini in Their Similar Orbits at Jupiter and Saturn

W.S. Kurth[1]; D.A. Gurnett[1]; G.B. Hospdarsky[1]; S. Ye[1]; J.D. Menietti[1]; A.M. Persoon[1]; A. Sulaiman[1]; M. Imai[1]; S. Tetrick[1]; P. Zarka[2]; L. Lamy[2]; B. Cecconi[2]; C. Louis[2]; A. Lecacheux[2]; W.M. Farrell[3]; G. Fischer[4]; J.-E. Wahlund[5]; M. Morooka[5]; M.K. Dougherty[6]; S.J. Bolton[7]; J.E.P. Connerney[3]; S.M. Levin[8]; P. Louarn[9]; P. Valek[7]; F. Allegrini[7]; B.H. Mauk[10]

[1] Univ. of Iowa; [2] Observatoire de Paris; [3] GSFC; [4] Austrian Academy of Sciences; [5] IRF-U; [6] Imperial College; [7] SWRI; [8] JPL; [9] IRAP; [10] APL

Cassini entered its 'Grand Finale' orbits beginning in late April 2017 with perikrones between the atmosphere and the D ring. The orbit inclination is approximately 63^0, hence, the orbits sometimes take Cassini close to or through the source regions of Saturn Kilometric Radiation (SKR). The Grand Finale orbits also carry the spacecraft across magnetic field lines connecting the ring system with the planet, providing the opportunity to investigate electromagnetic connections between the planet and its ring system. The orbits allow for in situ observations of Jupiter's topside ionosphere for the first time with the possibility of penetrating even deeper on its descent into the atmosphere at the end of its mission, depending on how long telemetry can be maintained. Dust apparently eroded from the main ring system is also found in this region, although the number of micron size particles is much less than in the E ring.

Juno is simultaneously orbiting Jupiter in similar orbits. Juno is in a 90^0 inclination orbit with perijoves between Jupiter's atmosphere and its ring system. Juno has already skimmed through or close to Jupiter's auroral radio emission sources and provided in situ examples of the cyclotron maser instability in operation and the electron distributions driving them. Juno also observes plasma waves of various types on auroral field lines, allowing comparison with terrestrial auroral plasma waves and the possibility to understand the acceleration of auroral charged particles. In addition, Juno has scanned, pole-to-pole, the very innermost region of Jupiter's magnetosphere, inviting comparisons of radio and plasma waves within the inner magnetospheres of these two giant planets. In the case of Jupiter, low-dispersion whistlers are commonly observed at mid-latitudes clearly indicating convective storms including lightning below the spacecraft. Because of the general lack of convective storm activity on Saturn since the Great White Spot storm in late 2010 and the first half of 2011, whistlers have not been observed by Cassini. Juno has observed Jupiter's topside ionosphere near its perijove and dust between the Jovian ring and the atmosphere.

Observations of non-terrestrial in situ auroral radio generation are important in the study of the cyclotron maser instability (CMI) in different planetary settings, so such observations from both Juno and Cassini are of critical interest. Another exciting aspect of these orbits at both planets is the exploratory nature of observing plasma waves in a region not previously sampled with the possibility of investigating interactions between the rings and atmosphere.

Brightening of Jupiter’s aurora observed by the Hisaki satellite and Hubble Space Telescope during Juno’s approach phase

Tomoki Kimura[1]; Chihiro Tao[2]; Go Murakami[3]; Atsushi Yamazaki[4]; Fuminori Tsuchiya[5]; Kazuo Yoshioka[6]; Hajime Kita[7]; Ichiro Yoshikawa[8]; Masaki Fujimoto[9]
[1] RIKEN; [2] NICT; [3] ISAS/JAXA; [4] ISAS/JAXA; [5] Planet. Plasma Atmos. Res. Cent., Tohoku Univ.; [6] The Univ. of Tokyo; [7] Tohoku Univ.; [8] EPS, Univ. of Tokyo; [9] ISAS, JAXA

In early 2014, continuous monitoring with the Hisaki satellite discovered transient auroral emission at Jupiter during a period when the solar wind was relatively quiet for a few days. Simultaneous imaging made by the Hubble Space Telescope (HST) suggested that the transient aurora is associated with a global magnetospheric disturbance that spans from the inner to outer magnetosphere. However, the temporal and spatial evolutions of the magnetospheric disturbance were not resolved because of the lack of continuous monitoring of the transient aurora simultaneously with the imaging. Here we report the coordinated observation of the aurora and plasma torus made by Hisaki and HST during the approach phase of the Juno spacecraft in mid-2016. On day 142, Hisaki detected a transient aurora with a maximum total H2 emission power of 8.5 TW. The simultaneous HST imaging was indicative of a large dawn storm, which is associated with tail reconnection, at the onset of the transient aurora. The outer emission, which is associated with hot plasma injection in the inner magnetosphere, followed the dawn storm within less than two Jupiter rotations. The monitoring of the torus with Hisaki indicated that the hot plasma population increased in the torus during the transient aurora. These results imply that the magnetospheric disturbance is initiated via the tail reconnection and rapidly expands toward the inner magnetosphere, followed by the hot plasma injection reaching the plasma torus. This corresponds to the radially inward transport of the plasma and/or energy from the outer to the inner magnetosphere.

電離圏ポテンシャルソルバーによる木星内部磁気圏電場の太陽風応答の研究

寺田 綱一朗 [1]; 垰 千尋 [2]; 寺田 直樹 [3]; 笠羽 康正 [4]; 北 元 [5]; 中溝 葵 [6]; 吉川 顕正 [7]; Ohtani Shinichi[8]; 土屋 史紀 [9]; 鍵谷 将人 [10]; 坂野井 健 [11]; 村上 豪 [12]; 吉岡 和夫 [13]; 木村 智樹 [14]; 山崎 敦 [15]; 吉川 一朗 [16]
[1] 東北大・理・地物; [2] 情報通信研究機構; [3] 東北大・理・地物; [4] 東北大・理; [5] 東北大・理・惑星プラズマ大気; [6] NICT; [7] なし; [8] なし; [9] 東北大・理・惑星プラズマ大気; [10] 東北大・理・惑星プラズマ大気研究センター; [11] 東北大・理; [12] ISAS/JAXA; [13] 東大・理; [14] RIKEN; [15] JAXA・宇宙研; [16] 東大・理・地惑

Study of the solar wind influence on the Jovian inner magnetosphere using an ionospheric potential solver

Koichiro Terada[1]; Chihiro Tao[2]; Naoki Terada[3]; Yasumasa Kasaba[4]; Hajime Kita[5]; Aoi Nakamizo[6]; Akimasa Yoshikawa[7]; Shinichi Ohtani[8]; Fuminori Tsuchiya[9]; Masato Kagitani[10]; Takeshi Sakanoi[11]; Go Murakami[12]; Kazuo Yoshioka[13]; Tomoki Kimura[14]; Atsushi Yamazaki[15]; Ichiro Yoshikawa[16]
[1] Geophysics, Tohoku Univ.; [2] NICT; [3] Dept. Geophys., Grad. Sch. Sci., Tohoku Univ.; [4] Tohoku Univ.; [5] Tohoku Univ.; [6] NICT; [7] ICSWSE/Kyushu Univ.; [8] The Johns Hopkins University Applied Physics Laboratory; [9] Planet. Plasma Atmos. Res. Cent., Tohoku Univ.; [10] PPARC, Tohoku Univ; [11] Grad. School of Science, Tohoku Univ.; [12] ISAS/JAXA; [13] The Univ. of Tokyo; [14] RIKEN; [15] ISAS/JAXA; [16] EPS, Univ. of Tokyo

The solar wind hardly influences the plasma convection in the Jovian inner magnetosphere ($<30R_J$), because the corotation of magnetospheric plasma dominates the convection there. However, Hisaki satellite observed that the brightness intensity and distribution of the Io plasma torus (IPT) located in the vicinity of Io's orbit (~$6R_J$) changed asymmetrically between the dawn and the dusk sides. Furthermore, it was confirmed that this asymmetric change coincided with a rapid increase in the solar wind dynamic pressure. This asymmetric change can be explained by the existence of a dawn-to-dusk electric field of ~4-9 mV/m around Io's orbit [Murakami et al., 2016]. The dawn-to-dusk electric field shifts the position of IPT toward dawn side by ~0.1-0.3R_J. The plasma in the IPT is heated adiabatically at dusk and cooled at dawn, which makes the dawn-dusk brightness asymmetry. The following processes have been suggested as a possible cause of the dawn-to-dusk electric field. First, the Jovian magnetosphere is compressed by the increase of solar wind dynamic pressure. Then, the magnetosphere-ionosphere coupling current system is modified, and the field-aligned current (FAC) at the high-latitude ionosphere increases. As a result, the ionospheric electric field increases and penetrates to low-latitude regions. It is mapped to the equatorial plane of the inner magnetosphere along the magnetic field line, and the dawn-to-dusk electric field is created around Io's orbit.

We have constructed a 2-D ionospheric potential solver in order to demonstrate this scenario quantitatively. We use a time-averaged intensity of the total FAC obtained from Galileo observations [Khurana, 2001] and adopt a Gaussian function for its horizontal distribution in a similar way to the Earth's ionospheric model. Also, we model the ionospheric conductivities from collision frequencies, cyclotron frequencies and density distribution in the upper atmosphere. We deduce the collision frequencies from ion-H_2 and electron-H_2 collisions [Tao, 2009]. The intensity of the dawn-to-dusk electric field at Io's orbit depends on the global distribution of the ionospheric conductivities, because Io's orbit connects to the ionosphere at a lower latitude region than the FAC and aurora regions. The limited area of the ionosphere was observed by Galileo and Voyager, therefore we use a Jovian thermosphere-ionosphere-magnetosphere coupling model [Tao et al., 2014] to obtain the global distributions of the ionospheric density. The model considers ionization caused by the solar extreme ultraviolet and aurora electrons precipitation at the downward FAC region to estimate the global conductivity distribution. We use the magnetic field model of Ray et al. [2014] when we map the ionospheric potential to the magnetospheric equatorial plane. This model considers the local time variation of the footprint. This variation is of importance in connecting IPT and ionospheric potential distribution, because the ionospheric potential distributes asymmetrically between the dawn and the dusk sides.

We calculate the ionospheric electric potential distribution and the magnetospheric dawn-to-dusk electric field with the aforementioned FAC and conductivity distributions, assuming that the plasma in the IPT drifts along the equipotential lines. The calculated dawn-to-dusk electric field was an order of magnitude larger than that expected from the Hisaki observations. We consider that this difference would be caused by the uncertainties in the ionospheric conductivities and electron density (cf. Majeed et al. [1999]). Then, we investigated the distribution of the ionospheric electron density that accounts for the dawn-to-dusk electric field intensity expected from Hisaki. We will discuss the influence of these uncertainties on the conductivities and the dawn-to-dusk electric field.

木星内部磁気圏は約 $30R_J$ に至るまでプラズマ共回転が対流を支配する領域で、この領域のプラズマ対流には太陽風の影響が及びにくいとする考え方が一般的である。しかし最近、ひさき衛星搭載の極端紫外線分光器 EXCEED によって、イオ軌道（約 $6R_J$）の近傍に位置するイオプラズマトーラス発光の強度と分布が朝側・夕側で非対称に変動し、この変動が太陽風の動圧の急激な増加に伴っていることが確認された。この非対称な変動はイオ軌道近傍に~4-9[mV/m] の朝夕電場がかかることで生じうると見積もられている [Murakami et al., 2016]。朝夕電場があることでイオプラズマトーラスが朝側に~0.1-0.3R_J シフトし、トーラス内プラズマが夕側で断熱加熱を、朝側で断熱冷却を受ける。その結果、イオプラズマトーラスの発光分布の朝夕非対称変動が生じるとされる。ここで、朝夕電場の起源として以下の太陽風影響プロセ

スが示唆されている。まず太陽風の動圧増大によって木星磁気圏が圧縮される。これにより磁気圏-電離圏結合電流系が変調され、高緯度電離圏へ流入する沿磁力線電流が増大する。その結果、沿磁力線電流によって形成される電離圏電場が増大し、低緯度領域へと拡大侵入する。これが磁力線を介して内部磁気圏赤道面に投影されることで、その深部に位置するイオ軌道近傍にまで朝夕電場が生成される、というものである。

我々は、このシナリオを数値モデルによって定量評価するため、薄層近似を行なった 2 次元の木星電離圏ポテンシャルソルバーを開発した。沿磁力線電流量には Galileo 探査機などによる時間平均された観測結果 [Khurana, 2001] を用い、その水平方向分布には地球の電離圏モデルで採用されているガウス関数を用いた。また、電離圏の電気伝導度分布は木星超高層領域における荷電粒子の衝突周波数とサイクロトロン周波数および密度の分布から計算した。衝突周波数はイオン-H_2 衝突と電子-H_2 衝突を考慮した [Tao, 2009]。イオ軌道は、沿磁力線電流の流入領域やオーロラ発光域よりも低緯度の電離圏と結合するので、その軌道上にかかる朝夕電場の強度は電離圏電気伝導度の全球的な空間分布に大きく依存する。Galileo 探査機や Voyager 探査機による電離圏観測は観測領域が限定されていたため、本研究では Tao et al. [2014] の木星熱圏-電離圏-磁気圏結合モデルを用いて熱圏・電離圏の全球的な密度・温度分布を与えた。このモデルは、オーロラ電子の降込みに伴う加熱等を考慮しており、沿磁力線電流の流出入領域である極域の電気伝導度分布をより定量的に求めることが可能である。また、電離圏ポテンシャルの磁気圏赤道面投影には Ray et al. [2014] の磁気圏磁場モデルを用いて、$6R_J$ に位置するイオプラズマトーラスのフットプリントを求めた。このモデルは磁場フットプリントのローカルタイム変動を加味している。電離圏ポテンシャルは朝夕で非対称に分布するため、ローカルタイム変動を加味することは、イオプラズマトーラスと電離圏ポテンシャル分布の紐付けに有効である。

上記に基づく沿磁力線電流量・電気伝導度の空間分布を用いて、朝夕電場強度の分布とイオプラズマトーラスのシフト量を導出した。ただし、イオプラズマトーラス内のプラズマは等ポテンシャル線に沿ってドリフトするとした。求められた朝夕電場強度は、ひさき衛星から期待される値に比べオーダー 1 桁程度大きくなった。この差は、電離圏電気伝導度や電子密度の推定誤差によるものと考えられる (cf. Majeed et al. [1999])。そこで、今学会では、ポテンシャルソルバーを用いて、ひさき衛星観測が観測した朝夕電場強度を説明しうる電離圏の電子密度分布を導出するとともに、これらの仮定が電気伝導度や朝夕電場に与える影響を評価した結果について報告する。

可搬型分光器による木星表面構造の分光観測

岩崎 和人 [1]; 伊藤 颯 [1]; 田部 一志 [2]; 弘田 澄人 [3]; 鈴木 秀彦 [1]
[1] 明治大; [2] 月惑星研究会; [3] かわさき宙と緑の科学館

Ground-based spectroscopic observation of Jovian surface structures by using the portable spectrometer

Kazuto Iwasaki[1]; Hayate Ito[1]; Isshi Tabe[2]; Sumito Hirota[3]; Hidehiko Suzuki[1]
[1] Meiji univ.; [2] ALPO-Japan; [3] Kawasaki municipal science museum

Stripe patterns called belts or zones with various colors persist on Jovian surface. Anticyclonic vortices called an oval with various scales and colors are maintained and drifted in the boundary between zones and belts. Some ovals have different colors despite they are formed simultaneously in the same latitude region. Color changes of ovals after an interaction with other ovals have been also reported [Sanchez-Lavega et al., JGR, 2013]. The great red spot (GRS) is one of the most remarkable structures in the Jupiter and recognized since 300 years ago by sketch and photographic observations. Recently, NASA spacecraft, JUNO has revealed more complex and fine features with various colors. A close relationship between dynamics of Jovian atmosphere and local colors is well known [Sanchez-Lavega et al., JGR, 2013] though detailed mechanisms connecting them are not fully understood. Thus, the color of the each structures is thought to be one of the keys to investigate dynamics of the Jovian atmosphere.

In this study, ground-based spectroscopic observations focusing on Jovian surface structures have been conducted since December 2015. The observation is carried out by combining a telescope with a small unit for spectroscopy consists of a CCD camera and a spectrometer. The spectrometer can measure a spectrum of a selected area within an image data simultaneously obtained by the CCD camera. Dimensions and weight of the spectroscopy are only 18cm X 14cm X 4cm and 300 g, respectively. This high portability of the spectrometer enables flexible observations; we can bring the spectrometer to a public observatory which has a large telescope in a location with high clear skies rate in desired observation period. The spectra are converted and corrected to an absolute radiance at the top of atmosphere, by using a radiometric calibration data obtained with an integrating sphere and measured extinction coefficients of the local atmosphere.

In this talk, temporal variations in the spectrum of representative Jovian structures such as NEB, EZ, SEB, GRS observed by using the spectrometer during December 2015 to July 2017 are reported. A comparison with the past space-born observation conducted by the multiband camera onboard Cassini spacecraft [Ordonez-Etxeberria et al., Icarus, 2015] is also performed for verification of the observations.

木星表面には緯度毎に縞 (Belt)、帯 (Zone) と呼ばれる特徴的な縞模様が複数存在し、その境界にはオーバルと呼ばれる大小様々なスケールの渦が維持生成されている。オーバルの中には同時期・同緯度で発生したにも関わらず白色や赤褐色といった異なる色を持つものや、オーバル同士の相互作用によってみかけの色が変化するものも観測されている [Sanchez-Lavega et al., JGR, 2013]。最も著名な渦構造である大赤斑はスケッチの時代からその存在が知られていることから、そのライフタイムは 300 年以上とも言われている。最近では NASA の探査機 JUNO の近接観測により、さらに細かいスケールや複雑な構造が次々と報告されている。先行研究では各種構造の色の違いや変動は、雲頂高度の違いや雲に含まれる元素成分の違いなどに起因するなど、木星表面構造の色とダイナミクスの関係が示唆されているが詳しいメカニズムは未解明である。

そこで、本研究では表面構造の動形態と可視分光スペクトルの変化から、木星表面大気のダイナミクスを解明することを目指し、地上観測による木星表面構造の可視分光観測を 2015 年 12 月より継続して実施している。分光観測は、天体のイメージを捉える CCD カメラおよび、天体イメージの部分領域を選択して分光可能な分光器で構成された分光ユニットと大型の天体望遠鏡を組み合わせて実施している。開発した分光ユニットの外形は約 18cmX14cmX4cm 程度、重量は 300g 程度と非常にコンパクトであるため、様々な望遠鏡に取り付けが可能である。この機動性を生かし、季節ごとに晴天率の高いロケーションにある公共天文台の天体望遠鏡と組み合わせて観測を実施してきた。現在に至るまでに 7 晩の観測に成功している。得られた分光データは積分球による校正データにより絶対輝度に変換し、さらに観測時の天頂角を考慮した大気補正を施すことで、宇宙空間での絶対輝度スペクトルに変換している。

本発表では、特に NEB、EZ、SEB、GRS などの代表的な表面構造に着目し、これまでに得られた輝度スペクトルの時間変動について報告する。また、観測結果の検証のために、Ordonez-Etxeberria et al. [2015] で報告されているカッシーニ探査機による木星表面構造のバンド分光観測との比較結果についても報告する。

高速回転する薄い球殻内の熱対流により生成される表層縞帯状構造の消滅

佐々木 洋平 [1]; 石岡 圭一 [2]; 竹広 真一 [3]; 中島 健介 [4]; 石渡 正樹 [5]; 林 祥介 [6]
[1] 京大・数学; [2] 京大・理・地物; [3] 京大・数理研; [4] 九大・理・地惑; [5] 北大・理・宇宙; [6] 神戸大・理・地惑

Disappearance of surface banded structure produced by thermal convection in a rapidly rotating thin spherical shell

Youhei Sasaki[1]; Keiichi Ishioka[2]; Shin-ichi Takehiro[3]; Kensuke Nakajima[4]; Masaki Ishiwatari[5]; Yoshi-Yuki Hayashi[6]
[1] Dept. Mathematics, Kyoto Univ.; [2] Dept. of Earth and Planetary Sci., Grad. School of Sci., Kyoto Univ.; [3] Research Inst. Math. Sci., Kyoto Univ.; [4] Earth and Planetary Sciences, Kyushu University; [5] Cosmosciences, Hokkaido University; [6] Earth and Planetary Sciences, Kobe University

Surface flows of Jupiter and Saturn are characterized by the broad prograde zonal jets around the equator and the narrow alternating zonal jets in mid- and high-latitudes. Heimpel and Aurnou (2007, hereafter HA2007) proposed thermal convection in rapidly rotating thin spherical shell models and show that the equatorial prograde zonal jets and alternating zonal jets in mid- and high-latitudes can be produced simultaneously when the Rayleigh number is sufficiently large and convection becomes active even inside the tangent cylinder. However, they assume eight-fold symmetry in the longitudinal direction and calculate fluid motion only in the one-eighth sector of the whole spherical shell. Such artificial limitation of the computational domain may influence on the structure of the global flow field. For example, zonal flows may not develop efficiently due to the sufficient upward cascade of two-dimensional turbulence, or stability of mean zonal flows may change with the domain size in the longitudinal direction.

On these accounts, we performed long time numerical experiment of thermal convection in the whole thin spherical shell domain, where the experimental setup is same as that of HA2007. The result shows that the banded structure disappears and one broad eastward zonal jet appears in mid- and high- latitudes of each hemisphere, suggesting that the solution of HA2007 is not a statistically steady state but a transient state. However, it was not clear whether the difference between the characteristics of our results and HA2007 was due to the region of calculation area or the difference of the settings of hyperviscosity.

In this study, we carried out numerical experiments in which the calculation settings including hyperviscosity are unified, and the calculation area were set whole spherical shell or 1/8 sector area assuming 8 times symmetry in the longitude direction. We consider Boussinesq fluid in a spherical shell rotating with constant angular velocity. The non-dimensionalized governing equations consist of equations of continuity, motion, and temperature. The non-dimensional parameters appearing in the governing equations, the Prandtl number, the Ekman number, the modified Rayleigh number, and the radius ratio, are fixed to 0. 1, $3\text{x}10^{-6}$, 0. 05, and 0. 85, respectively. The thermal boundary condition is fixed temperature. Free-slip condition is adopted at both boundaries.

When time integration was performed in the 1/8 sector area, a strong equatorial jet and a banded structure of mid- and high-latitudes emerged. This banded structure of mid- and high-latitudes are sustained for a long time without disappearing. On the other hand, in the calculation of the whole spherical shell, once a mid- and high-latitudes banded structures were formed, further progress of time integration accelerated the mid- and high-latitudes and the banded structures were disappeared. Therefore, whether the banded structures were maintained or disappeared depends on the calculation region, not the settings of hyperviscosity. For the disappearance of this banded structures, it is expected that the angular momentum transport by the component with the wavenumbers less than 8, which can not be expressed by 1/8 sector calculation, plays an important role.

木星と土星の表層の流れは，赤道周辺の幅の広い順行ジェットと中高緯度で交互に現われる互いに逆向きの幅の狭いジェットが特徴的である． Heimpel and Aurnou (2007, 以下 HA2007) は，これまでに考えられていた深いモデルよりも薄い球殻領域内の深部対流運動を考え，レイリー数が十分大きく内球接円筒での対流が活発な場合に，赤道域の順行流と中高緯度の交互に現われる狭いジェットが共存する状態を数値的に再現した．しかしながら，彼らの研究では経度方向に 8 回対称性を仮定しており，全球の 1/8 の領域の運動しか解いていない．このような領域の制限は流れ場全体の構造に影響を与えている可能性がある．例えば，2 次元乱流的なエネルギーの逆カスケードが十分に作用し，互い違いの縞状ジェットが生成されないかもしれない．また，生成される帯状流が不安定となって縞状ジェットが壊されてしまうかもしれない．

このような問題意識のもとに, 我々はこれまで薄い球殻対流の数値計算を全球で長時間行い, 赤道域および中高緯度領域の帯状流が形成されるか否かを調べてきた. その結果, 長時間積分後には縞状構造が消滅し, 南北中高緯度に幅広の帯状流がそてぞれ 1 本ずつ出現する状態が得られた. このことは HA2007 の解は最終的な統計的平衡状態ではなく過渡的な状態であることを示唆している. しかしながら, HA2007 と我々の結果の特徴の相違が, 計算領域を全球領域にしたためなの

か, あるいは超粘性拡散パラメータの違いによるものなのかが明らかでなかった.

そこで, 本研究では超粘性拡散パラメータを含めた計算設定を統一し, 計算領域を全球領域並びに経度方向に 8 回対称性を仮定した 1/8 セクター領域とした数値実験を行った. 用いたモデルは回転する球殻中のブシネスク流体の方程式系で構成されている．方程式系に現われる無次元数であるプラントル数を 0.1，エクマン数を $3\text{x}10^{-6}$，球殻の内径外径比を 0.85，修正レイリー数を 0.05 とした．熱境界条件は温度固定である．力学的境界条件は自由すべり条件である．初期には回転系での静止状態にランダムな温度擾乱を加えた.

1/8 セクター領域にて時間積分したところ強い赤道ジェットと中高緯度の縞状構造が出現した. この中高緯度の縞状構造は, 消滅することなく長時間維持されつづけている. 一方で全球領域計算では, 中高緯度の縞状構造が一旦形成されるものの, さらに時間積分を進めると中高緯度が加速され縞状構造が消滅した. すなわち, 縞状構造が維持されるか消滅してしまうかは, 超粘性拡散設定ではなく計算領域に依存している. この縞状構造の消滅には, 1/8 セクター計算では表現できない経度方向波数 8 未満の成分による角運動量輸送が重要な役割を果たしていると予想される.

全球海惑星気候の太陽定数依存性の研究: 海洋大循環の影響の考察

河合 佑太 [1]; 高橋 芳幸 [1]; 石渡 正樹 [2]; 西澤 誠也 [3]; 竹広 真一 [4]; 中島 健介 [5]; 富田 浩文 [6]; 林 祥介 [7]
[1] 神戸大・理・惑星; [2] 北大・理・宇宙; [3] 理研 AICS; [4] 京大・数理研; [5] 九大・理・地惑; [6] 理研 AICS; [7] 神戸大・理・地惑

A study on dependence of aquaplanet climates on the solar constant: consideration of the influence of ocean general circulation

Yuta Kawai[1]; Yoshiyuki O. Takahashi[1]; Masaki Ishiwatari[2]; Seiya Nishizawa[3]; Shin-ichi Takehiro[4]; Kensuke Nakajima[5]; Hirofumi Tomita[6]; Yoshi-Yuki Hayashi[7]
[1] Department of Planetology, Kobe Univ.; [2] Cosmosciences, Hokkaido University; [3] RIKEN AICS; [4] Research Inst. Math. Sci., Kyoto Univ.; [5] Earth and Planetary Sciences, Kyushu University; [6] RIKEN AICS; [7] Earth and Planetary Sciences, Kobe University

1. Introduction

In order to understand the diversity of exoplanet climates, we have investigated aquaplanet climates with atmospheric general circulation models (AGCMs). For example, Ishiwatari et al. (2007) (hereafter, referred to as INTH07) explored the solar constant dependency of aquaplanet climates in which the limit of longwave radiation of planet and atmospheric general circulation are considered, as an extension of previous studies (e.g., Budyko, 1969) with one-dimensional energy balance models (EBMs). They found a globally ice-covered state, a partially ice-covered state and a runaway greenhouse state, and showed the multiplicity of solutions, even in an AGCM with many degrees of freedom. But they excluded the ocean general circulation. However, the development of computational science enables the studies of exoplanet climates, considered the ocean general circulation (e.g., Marshall et al., 2007). In particular, Rose (2015) (hereafter, referred to as R15) investigated the solar constant dependence of aquaplanet climates with a coupled atmosphere-ocean-sea ice model, and indicated the ocean heat transport produced a new stable equilibrium state (waterbelt state). However, he used a simplified AGCM, and did not focus on cases of large solar constant where the runaway greenhouse state may exist. In this study, as an extension of INTH07, we explore solar constant dependence of a coupled atmosphere-ocean-sea ice system on an aquaplanet. We also investigate the change of climatic regimes with the ocean general circulation, and consider the role of ocean on aquaplanet climates.

2. Model and Experimental setup

We use our developing coupled atmosphere-ocean-sea ice model. The atmospheric model is an AGCM, DCPAM, in which three-dimensional primitive equations are solved. Based on INTH07, a gray atmosphere radiation scheme (Nakajima et al., 1992), moist convective adjustment scheme and large condensation scheme (Manabe et al., 1965), and Mellor and Yamada level 2 scheme are applied. The ocean model is a zonally averaged two-dimensional ocean general circulation model in which hydrostatic Boussinesq equations are solved. The mixing due to meso-scale eddies and convection is parametrized (Gent and McWilliams, 1990; Marotzke, 1991). The sea ice model is a thermodynamics model based on Winton (2000). The surface albedo is set to 0.5 where surface temperature is below 263 K, otherwise set to 0. In order to evaluate the influence of ocean general circulation clearly, three configurations are considered: swamp, slab, and dynamic ocean. The value of solar constant, S, is specified every 50 W/m^2 in the range between 900-1600 W/m^2. The number of atmosphere model grid is 64x32x32 for S$>$1450 W/m^2, otherwise 64x32x16. The number of grid points on ocean and sea ice models is 64x60 and 64, respectively. For most of cases, the initial condition is a rest atmosphere and ocean with 280 K, while some other conditions are also used to examine the multiplicity. The time integration for swamp/slab ocean experiments is basically performed over about 300 years, and, for dynamic ocean experiment, over about 30,000 years with periodically synchronous coupling.

3. Results

The statistically equilibrium state of coupled system in a control case (S=1380 W/m^2) reproduces the atmospheric and oceanic fields qualitatively, obtained from INTH07 and R15. In the dynamic ocean experiment, three climatic regimes appear with multiplicity, as in INTH07. The regime diagrams for dynamic ocean experiment is qualitatively similar to ones for swamp/slab ocean experiments, and the ocean general circulation seems to have a dramatic impact on the climates. The significant difference from R15 is that the runaway greenhouse state is contained, and the disconnection of branch of partially ice-covered state is not found. In order to examine the detailed branch structure, we perform further numerical experiments gradually varying the solar constant.

1. はじめに

系外惑星で実現される気候の多様性の理解を深めるために, 我々は大気大循環モデルを用いて水惑星の気候を調べてきた. 例えば, Ishiwatari et al. (2007) (以後 INTH07) では, 伝統的な南北 1 次元エネルギー・バランスモデル (EBM) を用いた研究 (Budyko 1969 等) の発展として, 惑星放射の射出限界や大気大循環が陽に考慮される系で, 水惑星気候の太陽定数依

存性を調べた. EBM に比べて自由度が遥かに多い系でも, 現在地球の太陽定数付近で全球凍結解, 部分凍結解, 暴走温室解の多重性が存在することを INTH07 は示したが, 海洋大循環の影響は考慮されなかった. しかし, 近年の計算科学の発展に伴い, 地球以外の惑星気候計算にも海洋大循環が考慮できるようになってきている (Marshall et al., 2007 等). 特に, Rose (2015) (以後 R15) は, 水惑星の大気海洋海氷結合系の太陽定数依存性を調べ, 海洋熱輸送により新たな安定平衡解 (赤道非凍結解) が生じることを示唆している. しかし, 彼らは計算時間の短縮のために簡略化した大気モデルを用いている. また, 太陽定数が大きい場合は着目されなかったため, 暴走温室解までは調べられていない. 本研究では, INTH07 の発展として, INTH07 大気設定のもとで, 水惑星大気海洋海氷結合系の太陽定数依存性を調べる. また, 海洋大循環の有無による気候レジームの変化にも注目し, 水惑星気候に対する海洋の役割について考察する.

2. モデルと実験設定の記述

実験には, 系外惑星の気候探索を念頭に現在我々が開発中の大気海洋海氷結合モデルを用いる. 大気モデルは, 惑星大気大循環モデル DCPAM である. 力学過程では, 3 次元プリミティブ方程式系が擬スペクトル法によって解かれる. 放射過程は Nakajima et al. (1992) の灰色大気放射スキーム, 凝結過程は Manabe et al. (1965) の湿潤対流調節スキームと大規模凝結スキーム, 鉛直乱流混合過程は Mellor and Yamada level 2 スキームによって表現される. 海洋海氷モデルは軸対称モデルである. 力学過程では, 静力学ブジネスク方程式系が擬スペクトル法によって解かれる. 海洋の中規模渦や対流による混合は, Gent and McWilliams (1990) や Marotzke (1991) のパラメタリゼーションにより表現される. 海氷モデルは Winton (2000) の鉛直 3 層熱力学モデルであり, 海氷輸送は海氷厚さの水平拡散で表現する. 表面アルベドは表面温度が 263 K 以下では 0.5, それより高い場合は 0 に設定する. 本実験では, 海洋大循環の影響を明確に調べるために, 海洋の取り扱いとして swamp ocean, slab ocean, dynamic ocean の 3 種類を考える. 太陽定数 (S) は約 900~1600 W/m^2 の範囲で約 50 W/m^2 ごとに指定する. 大気モデルの格子点数は, 太陽定数が 1450 W/m^2 より大きい場合は 64x32x32 (T21L32), それ以下の場合は 64x32x16 (T21L16) に設定する. 海洋モデルの格子点数は 64x60, 海氷モデルの南北格子点数は 64 である. 多くの実験における初期値は 280 K 等温の静止した大気海洋とするが, 解の多重性を調べるために別の実験で得られた全球凍結解や暴走温室解を初期値とした実験も行った. 時間積分は, 基本的に, swamp/slab ocean 実験では約 300 年間, dynamic ocean 実験では周期的同期結合を用いて約 3 万年間行う.

3. 計算結果

標準ケース (S=1380 W/m^2) から得られる結合系の統計的平衡状態は, INTH07 や R15 が得た大気海洋場を定性的に再現することを確認した. dynamic ocean 実験から得られる気候レジームは, 全球凍結解, 部分凍結解, 暴走温室解の三種類であり, これらの解は多重解であることが示された. また, swamp ocean, slab ocean 実験の気候レジーム図と比較するとき, その多重性の様相は定性的には変化せず, 我々の設定では海洋大循環の影響が小さいことが分かった. R15 が得た気候レジーム図と大きく異なる点は, 暴走温室解が含まれることと, 彼らが示唆した, 海洋熱輸送した場合に生じる部分凍結解のブランチの分断が見られない点である. 現在, 部分凍結解のブランチの構造により迫るため, 部分凍結解を初期値にして太陽定数を増減させる実験を進めている.

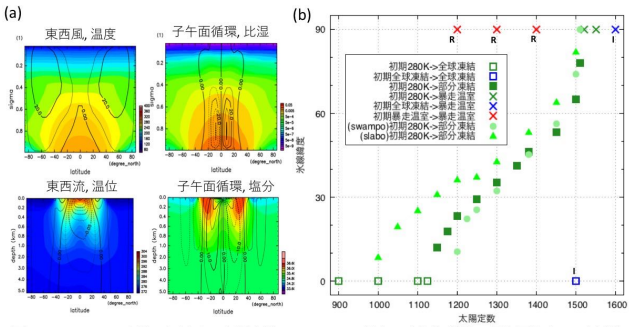

図: dynamic ocean 実験における(a)太陽定数 1380 W/m^2 の場合の大気海洋場の子午面分布, (b)氷線緯度の太陽定数依存性(初期値が全球凍結解・暴走温室解の場合は, それぞれ I, R のラベルで示している. また, swamp/slab ocean 実験における部分凍結解の点もプロットしている.)

火星極夜でのCO2過飽和に対する大気波動の影響

野口 克行 [1]; 黒田 剛史 [2]; Paetzold Martin[3]; Tellmann Silvia[3]
[1] 奈良女大・理・情報; [2] NICT; [3] ケルン大

Atmospheric CO2 supersaturation in the Martian polar nights: Role of large-scale atmospheric waves

Katsuyuki Noguchi[1]; Takeshi Kuroda[2]; Martin Paetzold[3]; Silvia Tellmann[3]
[1] Nara Women's Univ.; [2] NICT; [3] Univ. Cologne

This study aims at investigating the role of large-scale atmospheric waves (stationary waves and transient waves) on CO2 supersaturation at northern polar nights on Mars. A distinct longitudinal dependence of CO2 supersaturation was observed at high altitude levels (around 100 Pa), where a wavenumber 2 stationary wave lowered the background temperature. However, the stationary wave alone was not sufficient to cause CO2 supersaturation. We found that additional temperature disturbances caused by transient waves, namely, superposition of both waves, had a significant role in CO2 supersaturation. The MGCM (DRAMATIC) also reproduced the effect of both stationary waves and transient waves on CO2 supersaturation.

本研究では、1996年に米国が打ち上げた火星探査機 Mars Global Surveyor（MGS）における電波掩蔽観測の気温および気圧の高度分布データを用いて、火星極夜における大気中の二酸化炭素（CO2）過飽和の発生メカニズムについて調べた。これまでの観測で、火星極夜において大気主成分であるCO2が凝結するほどの低温となることが明らかになっている。そのような低温域においては、大気中でCO2の過飽和が発生していることも知られている。火星の総大気量は、極夜域でのCO2凝結を通して著しく季節変化する（20-30%程度）。そのため、CO2凝結や過飽和現象の発生メカニズムの解明は火星気象・気候を理解する上で重要である。火星大気中には地球大気と同じように様々な大気波動が存在し、局所的な低温域を作り出してCO2凝結や過飽和に寄与していると考えられる。本研究は、火星極夜に存在する比較的空間スケールの大きな大気波動（定常波・非定常波）に着目し、CO2過飽和の発生に与える影響を調べた。気温の東西平均からのずれ（偏差）とCO2過飽和が観測された場所の相関を調べたところ、CO2過飽和は波数2の定常波の気温極小域で多く発生していた。そのため、定常波によってCO2過飽和が引き起こされている可能性が示唆された。一方、東西平均だけでは非定常波の影響がわからないため、気温の東西偏差を三角関数でフィッティングし、どのような波数・周期成分を持つ大気波動がCO2過飽和を引き起こし得るか調べた。その結果、実際には定常波のみで過飽和が発生するケースは少なく、非定常波との重ね合わせで過飽和が発生するケースが多いことが明らかになった。火星大気大循環モデルDRAMATICの出力結果と比較したところ、定性的には観測結果と一致する結果が得られた。

古海洋・厚いCO2大気環境のもとでの火星古気候シミュレーション－水環境の気候に及ぼす影響

鎌田 有紘 [1]; 黒田 剛史 [2]; 笠羽 康正 [3]; 寺田 直樹 [4]; 秋葉 丈彦 [5]
[1] 東北大・理・地物; [2] NICT; [3] 東北大・理; [4] 東北大・理・地物; [5] 東北大・理・地物

Global climate simulation of early Mars with a paleo-ocean and a dense CO2 atmosphere: Impact of aquatic environment to climate

Arihiro Kamada[1]; Takeshi Kuroda[2]; Yasumasa Kasaba[3]; Naoki Terada[4]; Takehiko Akiba[5]
[1] Geophysics, Tohoku Univ.; [2] NICT; [3] Tohoku Univ.; [4] Dept. Geophys., Grad. Sch. Sci., Tohoku Univ.; [5] Geophysics,Tohoku Univ.

http://pat.gp.tohoku.ac.jp/wordpress/access/

There are many fluvial traces such as valley networks and outflow channels which are supposed to be made before ~3.8 billion years ago on the Martian surface. If those traces were made by the flow of liquid H_2O, the environment of the ancient Mars should be suitable for huge amount of liquid water. There have been several studies using 3-dimensional Mars Global Climate Models (MGCMs) to reproduce such environment of early Mars, assuming the solar insolation of ~75% of today and denser CO_2 atmosphere. However, previous studies have not reproduced the surface temperature above 273K even under the surface pressure up to ~7 bars, regardless of the existence of saturated H_2O vapor [*Forget et al*., 2013; *Wordsworth et al*., 2013].

In this study, we use a MGCM named DRAMATIC (Dynamics, RAdiation, MAterial Transport and their mutual InteraCtions) to reveal the nature of early Martian climate, focusing on the sensitivity of surface parameters. In addition to the physical processes for Martian paleo-climate similar to *Forget et al*. [2013], we have implemented the virtual ocean and lakes in the northern lowlands and wet soil in the southern highlands, making high thermal inertia of between 1,000 and 3,000(J $s^{-1/2}$ m^{-2} K^{-1}) which have never been implemented in the preceding studies. Also we have implemented a water cycle scheme assuming the phase changes among ice, liquid and vapor, including the frost of ocean below the melting point. The obliquity in the simulations is set to be the same as today's Mars (25.19 degrees),and the orbit is assumed to be circular with the radius of 1.523 AU. Furthermore, Rayleigh-friction coefficients are set to be the valid values, which reproduce wind field of today's Mars.

We performed the simulation with the averaged surface pressure (hereafter p_s) of 0.1-2.0 bars, for two cases (1) with ocean/lakes and wet soil (hereafter 'wet surface') and (2) without them (hereafter 'dry surface', assuming the dry soil which is the same as today's Mars globally). As a result, we produced higher surface temperature in 'wet surface' at all pressures, dT ~+30 K at p_s = 2.0 bars, in comparison with 'dry surface'. In the 'wet surface' simulation, the annual mean surface temperature was ~230 K at p_s = 1.0 bar and ~260 K at p_s = 2.0 bars. Although there were little precipitation and the paleo-ocean quickly froze in p_s below 1.0 bar, the paleo-ocean was maintained throughout the year in low-to-mid latitudes area in p_s above 1.0 bar with the precipitation of 1,000-3,000 mm in one Martian year (about 1.88 Terrestrial year) was shown alongside the shoreline, e.g. in the north-east of Hellas basin and at the foot of tall mountains such as Mt. Elysium, where large fluvial traces of outflow channels have been observed. Furthermore, the distribution of the amount of flowing water of the river, which is calculated by a 3-layers tank model [*Ishihara and Kobatake*,1979] and developed river flow model considering the river velocity calculated by *Manning* formula and confluence of several rivers, was also in a good consistency with the existence of fluvial traces of outflow channels on Martian surface.

大気大循環モデルを用いた火星の水循環と HDO/H2O 同位体分別のシミュレーション：観測とモデルの国際連携に向けて

黒田 剛史 [1]; 笠羽 康正 [2]
[1] NICT; [2] 東北大・理

Simulation of the water cycle and HDO/H2O isotopic fractionation on Mars using a GCM: Towards the international collaborations

Takeshi Kuroda[1]; Yasumasa Kasaba[2]
[1] NICT; [2] Tohoku Univ.

We are simulating the water cycle of the present Martian environment using a Mars general circulation model (MGCM) for the investigations of the water cycle system and related material transport on Mars in collaboration with the current and future observations. We performed the horizontal high-resolution simulations with the grid intervals of ˜67 km, showing the relationships between water transport and atmospheric dynamics more clearly than the previous low-resolution simulations (intervals of ˜300 km). Our results show the consistent seasonal and latitudinal changes of zonal-mean water vapor column density and ice opacity with observations in the run without the radiative effects of water ice clouds. Also, we have implemented the HDO/H_2O isotopic fractionations, and reproduced the qualitatively consistent seasonal and latitudinal changes of the ratio with a preceding simulation.

In this presentation, our future plans of international collaborations about the water cycle on Mars using this MGCM will be shown, including the observational missions such as ExoMars Trace Gas Orbiter and ground-based/airborne telescopes and also the intercomparison of MGCMs with water cycle in different approaches, especially in the framework of Japan-Belgium collaboration program, AMAVERO (Exploring the Atmosphere of MArs and VEnus with Remote Observations: A Belgium-Japan partnership).

MAVEN観測に基づく太陽風電場と地殻磁場が火星からの重イオン流出に与える影響の統計的研究

乾 彰悟 [1]; 関 華奈子 [2]; 堺 正太朗 [2]; 松永 和成 [3]; Brain David A.[4]; McFadden James P.[5]; 原 拓也 [5]; Halekas Jasper S.[6]; Mitchell David L.[5]; Connerney John E. P.[7]; Jakosky Bruce M.[8]
[1] 東大・理・地惑; [2] 東大理・地球惑星科学専攻; [3] 名大 ISEE; [4] LASP, Univ. of Colorado at Boulder, USA; [5] SSL, UC Berkeley; [6] Dept. Phys. & Astron., Univ. Iowa; [7] NASA GSFC; [8] LASP, CU Boulder

Effect of the crustal magnetic fields and solar wind electric fields on heavy ion outflows from Mars observed by MAVEN

Shogo Inui[1]; Kanako Seki[2]; Shotaro Sakai[2]; Kazunari Matsunaga[3]; David A. Brain[4]; James P. McFadden[5]; Takuya Hara[5]; Jasper S. Halekas[6]; David L. Mitchell[5]; John E. P. Connerney[7]; Bruce M. Jakosky[8]
[1] Earth and Planetary Science, Univ. of Tokyo; [2] Dept. Earth & Planetary Sci., Science, Univ. Tokyo; [3] ISEE, Nagoya Univ.; [4] LASP, Univ. of Colorado at Boulder, USA; [5] SSL, UC Berkeley; [6] Dept. Phys. & Astron., Univ. Iowa; [7] NASA GSFC; [8] LASP, CU Boulder

Geological studies have suggested that Mars had a warm climate and liquid water on surface about 4 billion years ago. Now, Mars has a cold surface temperature and little water on surface. Escape of greenhouse gases such as CO_2 to space is considered as the plausible reason to cause the drastic climate change. On one hand, mechanisms enabling the large amount of the CO_2 loss are far from understood. The planetary ion escape through interaction between the solar wind and the Martian upper atmosphere is one of the candidate mechanisms to achieve the atmospheric escape. Mars doesn't have global intrinsic magnetic field, but it has local crustal magnetic fields. Effects of this crustal magnetic fields on the atmospheric escape are far from understood. To understand atmospheric loss from Mars, MAVEN (Mars Atmosphere and Volatile EvolutioN) has observed the ion escape from Mars as well as space environment around Mars since November 2014. In our previous study, we investigated detailed characteristics of a dense cold ion outflow event observed in the Martian induced magnetotail based on the MAVEN observations. We suggested that the combination of the mini-magnetosphere and the downward-E hemisphere facilitates the cold ion escape from low altitude Martian ionosphere.

In this study, we report on a statistical analysis of heavy ion outflows from Mars to investigate influence of the crustal magnetic fields and the direction of solar wind electric field on the ion outflows by using the data of MAVEN. STATIC (Supra-Thermal And Thermal Ion Composition), SWIA (Solar Wind Ion Analyzer) and MAG (Magnetometer) data from November 2014 to March 2017 were used for the statistical study. We focused on the heavy ion outflows in the wake region. At first, we selected the orbits in which solar wind was stable. The stability condition of solar wind was determined by the direction of the interplanetary magnetic field (IMF). We only include the wake observations in the statistical study, if difference between IMF directions observed just before and immediately after the wake observation is less than 30 degrees. Next, we divided observed data by the location of the strongest local crustal magnetic field around east longitude of 180 degrees into 4 local time groups: noon, dawn, dusk, and night. The results show that number densities of heavy ions observed in the southern hemisphere in the MSE coordinates tend to be higher than those observed in the northern hemisphere, while there are no clear difference in number fluxes between the two hemispheres. We will also report on dependence of heavy ion outflows on other solar wind parameters.

弱い固有磁場中における火星からのイオン流出機構

堺 正太朗 [1]; 関 華奈子 [1]; 寺田 直樹 [2]; 品川 裕之 [3]; 田中 高史 [4]; 海老原 祐輔 [5]
[1] 東大理・地球惑星科学専攻; [2] 東北大・理・地物; [3] 情報通信研究機構; [4] 九大・国際宇宙天気科学教育センター; [5] 京大生存圏

The ion escape from Mars with a weak intrinsic magnetic field

Shotaro Sakai[1]; Kanako Seki[1]; Naoki Terada[2]; Hiroyuki Shinagawa[3]; Takashi Tanaka[4]; Yusuke Ebihara[5]
[1] Dept. Earth & Planetary Sci., Science, Univ. Tokyo; [2] Dept. Geophys., Grad. Sch. Sci., Tohoku Univ.; [3] NICT; [4] REPPU code Institute; [5] RISH, Kyoto Univ.

It is recognized that ancient Mars had liquid water on the surface and thick atmosphere according to the recent space missions. However, the atmosphere was lost from the planet through some escape channels, and present-day Mars only has a thin atmosphere consisting mainly of CO_2 and does not have liquid water on the surface. It means that Mars has experienced much atmospheric loss from the past through the present. One of the important mechanisms of the atmospheric loss is the ion escape from the upper atmosphere. The ion escape is mainly controlled by the solar conditions such as solar wind parameters and solar XUV (X-ray and extreme ultraviolet) irradiances, and magnetic-field configuration. A previous numerical simulation indicated that the ion escape rate was at most five orders of magnitude higher under the past active solar condition than under the present ones. The planetary magnetic field is also an important factor in determining the ion escape rate. Present-day Mars does not have an intrinsic magnetic field, but it is leaving the magnetism in its crust. The existence of crustal magnetic field suggests that Mars had a global magnetic field of interior origin in the past. We present the ion escape mechanism under a weak intrinsic magnetic field at Mars based on a three-dimensional multi-species magnetohydrodynamics (MHD) modeling.

The simulations are performed for the two different magnetic fields with (case 1) only the interplanetary magnetic field (IMF) and (case 2) the IMF and dipole field of 100 nT on the equatorial surface of the planet. Note that the Parker spiral is adopted for the IMF. The shape of the magnetosphere appears to be hybrid between the magnetosphere with strong dipole field such as Earth and the induced magnetosphere with no dipole field such as present-day Mars, when a weak dipole field is considered. The east-west component of magnetic field is predominant at the subsolar point due to the penetration of the IMF draped field into the ionosphere rather than the north-south component of the global dipole field. On the other hand, the dipole field dominates the tail region of the magnetosphere.

The ion escape flux is obtained from the ion densities and velocities calculated. In the case 1, the flux has a peak near the center of the figure (Figure 1a). It suggests the ions created around Mars are flowing down to the tail. In contrast, in the case 2 the total flux has four peaks on the y-z plane of Mars-centered Solar Orbital (MSO) coordinate system (Figure 1b). Two of them are located in the magnetic neutral sheet (a white dased line of Figure 1b), and the others are in the higher latitudes. These results show that the difference of magnetic configuration significantly changes the ion escape flux and mechanism. The four-peak structure of flux in the case 2 is brought by the magnetosphere, which is formed by the interaction between the assumed solar wind and global dipole field. The two peaks in the high latitude are associated with the cusp region. The other two peaks are seen in the flank region of plasma sheet and generated by the complex reconnection between the dipole field and the IMF around the magnetosheath. Comparisons between the two cases suggest that the ion tailward flux increases by the magnetization of the planet and ions particularly escape through four channels in the magnetotail. This could result in the ion escape rate from the upper atmosphere enhanced.

Figure 1. The total ion flux of O^+ and O_2^+ in the two different magnetic fields with (a) IMF and (b) IMF and dipole magnetic field of 100 nT on the equatorial surface on the y-z plane at x = -5 R_M of the MSO coordinate system. The white dashed line shows the magnetic neutral sheet of B_x = 0.

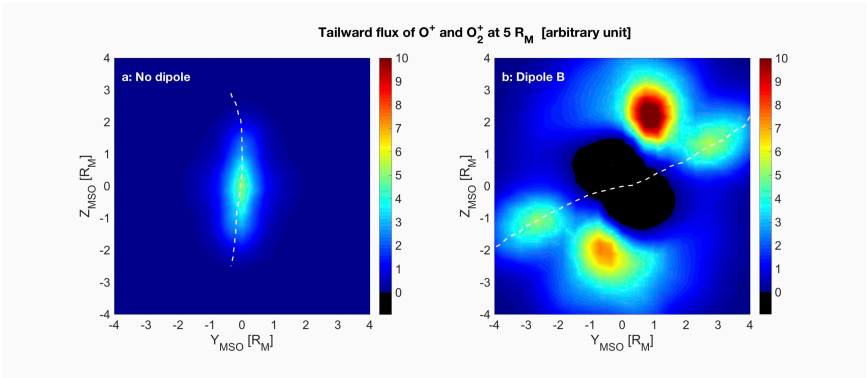

Near infrared spectral imager MacrOmega onboard MMX to investigate martian atmosphere

Hiromu Nakagawa[1]; Shohei Aoki[2]; Takeshi Imamura[3]; Kazunori Ogohara[4]; Takao M. Sato[5]; Hideo Sagawa[6]; Takeshi Sakanoi[7]; Yasumasa Kasaba[8]; Makoto Taguchi[9]; Takahiro Iwata[10]; Tomoki Nakamura[11]; Vincent Hamm[12]; Cedric Pilorget[12]; Jean-Peire Bibring[12]

[1] Geophysics, Tohoku Univ.; [2] BIRA-IASB; [3] The University of Tokyo; [4] JAXA/ISAS; [5] ISAS/JAXA; [6] Kyoto Sangyo University; [7] Grad. School of Science, Tohoku Univ.; [8] Tohoku Univ.; [9] Rikkyo Univ.; [10] ISAS/JAXA; [11] Earth science, Tohoku Univ.; [12] IAS

We start a study on a sample return missions to a martian moon to be launched in early 2020s (Mars Moon eXploration (MMX) mission). With this mission, we will give a boost to planetary science by adding new information on planetary formation and evolution processes in the part of the solar system linking its inner and outer-part. Sample analysis/remote sensing allows us to unveil the migration history of the small body that behaved as a capsule which carried water and organic compounds into the inner-solar system.

Near infrared spectral imager MacrOmega will observe hydroxide or hydrated mineral absorptions on Phobos and Deimos in the wavelength of 2.7 and 3.2 micron. By analyzing the shape of the spectra, we will distinguish between water in hydrous silicate minerals, water molecules, and water ice particles. MacrOmega will also try to detect the absorption by organic matter in the wavelength range of 3.3 and 3.5 micron. These results will support efforts to answer the question of the origin of the martian moons, and identify whether they are satellites formed by a giant impact or asteroids captured by Mars. This instrument is based on MicrOmega onboard ExoMars rover and Hayabusa2 MASCOT and modified as a spectral imager.

The equatorial-orbit of the spacecraft around Mars also offers an interesting advantage to continuously observe Mars atmosphere from a global perspective. The latest space-born measurement, MAVEN/IUVS, showed unprecedented view of Mars diurnal cloud evolution within hours. Tharsis clouds begin the day much smaller than the width of the volcanoes, but merge together in the late afternoon to span up to 2000 kilometers (Schneider et al., 2017). We will aim to perform hourly-measurements for global distribution of atmospheric/surface compounds using MarcOmega, in order to investigate the cloud/dust formations, water cycle via surface-atmosphere interaction, dynamics, and compositions.

After reaching Mars, the MMX spacecraft will enter an equatorial Phobos-orbit, a 9376 km altitude (2.76 mars radii), and a ˜7.6-hours duration. MacrOmega provides the two-dimensional map with spectral features in the wavelength range between 0.9 and 3.6 micron, in which there are the attractive objectives of atmosphere, including water vapor, water-ice cloud, CO2-ice cloud, adsorbed water in the regolith, dust, carbon monoxide, molecular oxygen airglow, and carbon dioxide. The wavelength selection is performed using an Acousto Optical Tunable Filter (AOTF) located at the entrance optics. The spectral resolution depends on the bandwidth of the AOTF (˜20 cm-1), which is suitable to retrieve the narrow feature of the atmospheric compounds. MacrOmega has an instantaneous FOV of 6x6 degree (corresponding to 600kmx600km) with 256x256 pixels, and uses a pivoting scan mirror for mapping. In this paper, we introduce the scientific capability and measurement sensitivity of the instrument. We expect the first weather satellite on Mars is an epoch-making to increase our understanding for Mars climatology.

Gravity waves in the Martian exosphere

Naoki Terada[1]; Kaori Terada[2]; Hiromu Nakagawa[3]; Francois Leblanc[4]; Alexander Medvedev[5]; Erdal Yigit[6]; Takeshi Kuroda[7]; Hitoshi Fujiwara[8]; Kanako Seki[9]

[1] Dept. Geophys., Grad. Sch. Sci., Tohoku Univ.; [2] Geophys., Tohoku Univ.; [3] Geophysics, Tohoku Univ.; [4] LATMOS-IPSL, CNRS; [5] MPS, Germany; [6] MPI; [7] NICT; [8] Faculty of Science and Technology, Seikei University; [9] Dept. Earth & Planetary Sci., Science, Univ. Tokyo

The exosphere is a collision-less region located in the uppermost layer of a planetary atmosphere. Because of efficient dissipation due to molecular diffusion (molecular viscosity and thermal conduction), any small-scale perturbations are expected to be quickly dissipated in the exosphere. However, recent MAVEN/NGIMS observations revealed that small-scale, large-amplitude perturbations are persistent even above the exobase at Mars [cf. Terada et al., 2017]. We have investigated statistical properties of these perturbations using MAVEN/NGIMS data and examined possible generation, propagation, and dissipation mechanisms using DSMC simulations of the Martian upper thermosphere-exosphere [Terada et al., 2016]. Based on MAVEN/NGIMS data obtained along satellite's tracks as well as DSMC simulations of gravity waves and acoustic waves propagating from the lower and middle atmosphere, constraints on the wavelength and frequency ranges of perturbations are obtained, which favor gravity wave modes with a very long vertical wavelength. Also investigated are properties of perturbations generated by precipitating pickup ions with DSMC simulations based on MAVEN parameters. Possible generation, propagation, and dissipation mechanisms of the exospheric perturbations are discussed based on these results.

「あかつき」でみえてきた金星大気の多彩な流れ

堀之内 武 [1]; 村上 真也 [2]; 佐藤 毅彦 [3]; 渡部 重十 [4]; 神山 徹 [5]; 小郷原 一智 [6]
[1] 北大・地球環境; [2] 宇宙研; [3] 宇宙研; [4] 北大・理・宇宙; [5] 産総研; [6] 宇宙研

Variable winds in the Venusian atmosphere as revealed by Akatsuki

Takeshi Horinouchi[1]; Shin-ya Murakami[2]; Takehiko Satoh[3]; Shigeto Watanabe[4]; Toru Kouyama[5]; Kazunori Ogohara[6]
[1] Hokkaido University; [2] ISAS/JAXA; [3] ISAS, JAXA; [4] Cosmosciences, Hokkaido Univ.; [5] AIST; [6] JAXA/ISAS

We have conducted cloud tracking using image data from Akatsuki, a Venus orbiting satellite, at multiple wavelengths. Our method provides cloud-motion vectors with unprecedented high quality. Obtained cloud top winds exhibit rich spatial and temporal variability. In the lower cloud layer, it is observed that a jet stream was formed in the equatorial region in 2016, which persisted at least over a few months. Batropically unstable vortices are found to develop to erode the shear associated with the jet. Ultraviolet imaging at two wavelengths suggested the existence of systematic vertical shear at the cloud top.

我々は、金星探査機「あかつき」の撮像観測をもとに、雲追跡による金星の流れ場の導出と、その結果を用いた金星大気の力学の研究を行っている。本講演では、これまでに明らかになった金星大気の様々な流れを紹介し、その力学的な示唆について述べる。

用いた手法は、新規に開発した自動追跡法である (Ikegawa and Horinouchi, 2016: Horinouchi et al. 2017)。本手法では、2 枚以上の画像（輝度データ）を適切に組み合わせることで、誤推定を減らし、S/N 比を増して精度を高めるものであり、さらに誤り修正のための「緩和法」にも独自の改良を加えたものである。また、誤差の指標が得られ、結果のスクリーニングが行える。「あかつき」の高品質なデータと新手法の組み合わせにより、過去の探査に基づく研究に比べて格段に高品質の雲移動ベクトルが高密度で得られている。

その成果の一つは、2 μ m カメラ IR2 の夜面観測により見いだされた、低緯度の中下層雲帯の風速のピークである。従来の限られた観測からは、中下層雲帯での風速は緯度 40 度より低緯度ではほぼ一定で時間変化も乏しいと考えられて来た。しかし、IR2 による 2016 年 7-8 月の観測からは、赤道付近にピークをもつジェット状の風速分布が見いだされ、我々はそれを「赤道ジェット」と呼ぶことにした (Horinouchi et al., 2017, accepted)。赤道ジェットは 2016 年 3 月にはみられず、それ以降に形成されたとみられる（2016 年 4-6 月は軌道の関係で夜面観測が限られた）。中下層雲帯の夜面観測は、Galileo の金星フライバイ時や Venus Express でも行われたが、風速が得られている時期は限られている。よって我々は、赤道ジェットは過去にも形成されることがあったが観測されなかったのではないかと推測している。2017 年 8 月に、赤道ジェットの脇で直径約 1000km の渦の列が発生するというイベントが発生した。これは順圧不安定擾乱とみられ、それによってジェット脇の水平シアーが減じることが観測された。より小規模な渦列とみられる擾乱も時折みられる。以上より、「静かな低緯度の中下層雲帯の流れ」というこれまでのイメージは、大きく変わるものと考えられる。

あかつきの紫外カメラ UVI は、Pioneer Venus Orbitor (PVO) などの過去の多くの探査機で採用された 0.3-0.4 μ m 帯（未知の紫外線吸収物質によって雲頂の構造が可視化される）での撮像 (中心波長 365nm) に加え、SO2 の吸収帯での撮像 (中心波長 283nm) も行う。SO2 吸収帯での雲追跡は、PVO の偏光観測による試みが一例あるものの、誤差が大きいと考えられるため、これまでほぼなかったと言ってよい。UVI データを用いた我々の雲追跡により、過去の 0.3-0.4 μ m 帯画像から報告されてきた風速の空間分布と時間変動の諸特徴が確認された。さらに、283nm の結果と比較すると、283nm 画像にみられる超回転（スーパーローテーション）のほうが 365nm 画像にみられる超回転より平均的に速いことが明らかになった（Horinouchi et al., submitted）。この結果は、雲頂付近に平均して正または負の鉛直シアーが存在することを示唆する（283nm 画像が捉える模様の高度のほうが平均して高ければ正）。

あかつきより得られる風速分布は、過去のミッションに基づく研究に比べて格段に高密度で、分布も滑らかであり、精度もよいと考えられる。今後研究を進めることで、未知の諸現象がさらにあきらかになり、金星大気の超回転のメカニズムに関する量的な示唆も得られると期待される。

高解像度金星大気シミュレーションで再現された惑星規模のストリーク構造

樫村 博基 [1]; 杉本 憲彦 [2]; 高木 征弘 [3]; 松田 佳久 [4]; 大淵 済 [5]; 榎本 剛 [6]; 中島 健介 [7]; 石渡 正樹 [8]; 佐藤 隆雄 [9]; はしもと じょーじ [10]; 佐藤 毅彦 [11]; 高橋 芳幸 [12]; 林 祥介 [13]
[1] 神戸大・理・惑星/CPS; [2] 慶大・日吉物理; [3] 京産大・理; [4] 東京学芸大
; [5] 神戸大・CPS; [6] 京大・防災研; [7] 九大・理・地惑; [8] 北大・理・宇宙; [9] 宇宙研; [10] 岡大・自然; [11] 宇宙研; [12] 神戸大・理・惑星; [13] 神戸大・理・地惑

Planetary-scale streak structures produced in a high-resolution simulation of Venus atmosphere

Hiroki Kashimura[1]; Norihiko Sugimoto[2]; Masahiro Takagi[3]; Yoshihisa Matsuda[4]; Wataru Ohfuchi[5]; Enomoto Takeshi[6]; Kensuke Nakajima[7]; Masaki Ishiwatari[8]; Takao M. Sato[9]; George Hashimoto[10]; Takehiko Satoh[11]; Yoshiyuki O. Takahashi[12]; Yoshi-Yuki Hayashi[13]
[1] Planetology/CPS, Kobe Univ.; [2] Physics, Keio Univ.; [3] Faculty of Science, Kyoto Sangyo University
; [4] Tokyo Gakugei Univ.; [5] CPS, Kobe Univ.; [6] DPRI, Kyoto Univ.; [7] Earth and Planetary Sciences, Kyushu University; [8] Cosmosciences, Hokkaido University; [9] ISAS/JAXA; [10] Okayama Univ.; [11] ISAS, JAXA; [12] Department of Planetology, Kobe Univ.; [13] Earth and Planetary Sciences, Kobe University

Night-side images of Venus taken by the IR2 camera onboard Venus Climate Orbiter/AKATSUKI has shown many features of the lower cloud layer. One prominent feature is bright planetary-scale streak structures extending from high-latitudes to low latitudes on both hemispheres (Fig. a). IR2 night-side images capture infrared radiated from the near-surface atmosphere, and the infrared can be blocked by clouds. Therefore, bright regions indicate thin-cloud regions.

We have performed a high-resolution simulation of the Venus atmosphere by a simplified general circulation model, which is based on AFES: the Atmospheric general circulation model For the Earth Simulator. The horizontal resolution is T159 (i.e., about 0.75 deg x 0.75 deg grids) and the vertical resolution is about 1 km with the model top at 120 km. In the model, the atmosphere is dry and simply forced by the solar heating with the diurnal change and Newtonian cooling that relaxes the temperature to the horizontally uniform basic temperature which has a virtual static stability of the Venus atmosphere. In the basic temperature profile, we have introduced a low-stability (0.1 K/km) layer from 55 km to 60 km, which is suggested by the recent radio occultation observation. We have explored waves (Sugimoto et al. 2014ab), polar vortex (Ando et al. 2016), and kinetic energy spectra (Kashimura et al. 2014) in the simulated atmosphere with the above model settings (some with lower resolution).

In this study, we have found that planetary-scale streak structures similar to that observed by the IR2 night-side image are produced in the vertical velocity field above the low-stability layer in the simulated atmosphere (Fig. b). Large streaks are shown by strong downward flow. This is consistent with the observation because the downward flow can decrease cloud amounts and make a thin-cloud region. Seen from above the pole, the simulated streak structure shapes a huge spiral extending from the polar vortex to low latitudes (Fig. cd). Such spiral is similar to that observed by VIRTIS onboard Venus Express. In addition, the streak structures on both hemispheres are synchronized, that is the streak structures located in the same longitude.

In this presentation, we will explore the influence of the diurnal heating and the ‘low-stability layer’ to the streak structures, and discuss a possible mechanism for their formation and synchronization.

Figure: (a) Contrast-enhanced image (for a press release) of Venus night-side taken by the IR2 camera (wavelength: 2.26 micrometers) on 25th March 2016. (b-d) Snapshot of the vertical velocity field at 60 km height simulated by AFES-Venus. Panel (b) is a view seen from same location as the spacecraft at (a). Panels (c, d) are views seen from above the poles. Note that planetary rotation direction of AFES-Venus is opposite to the real Venus, so that Panel b is displayed with a 180 deg rotation.

金星探査機あかつきの IR2 カメラは、金星の夜面を撮像することで、雲層下部の様々な特徴を明らかにしている。その中でも顕著な特徴の 1 つが、南北両半球で高緯度から低緯度にかけて延びる、惑星規模の明るいストリーク構造である (図 a)。IR2 の夜面画像が捉えているのは地表付近の大気から放射される赤外線であり、それは雲によって遮られるため、画像の明るい領域は雲の薄い領域を表している。

我々は簡易な大気大循環モデルを用いて、金星大気の高解像度シミュレーションを実施してきた。モデルは AFES (Atmospheric general circulation model For the Earth Simulator) を金星大気に対応させたものである。水平解像度は T159 (約 0.75 度 x 0.75 度格子) で、鉛直解像度は約 1 km で大気上端は高度 120 km である。モデル内の大気は乾燥しており、日変化を含む太陽加熱と水平一様なニュートン冷却で放射過程を簡単化している。ニュートン冷却の基準温度場は金星大気の静的安定度を模しており、近年の電波掩蔽観測で示唆されている低安定度層 (0.1 K/km) が高度 55 km から 60 km に

導入されている。我々はこれまでに、低解像度版の結果も含め、計算された金星大気中の、波動 (Sugimoto et al. 2014ab)、極渦 (Ando et al. 2016)、そして運動エネルギースペクトル (Kashimura et al. 2014) を解析してきた。

本研究で我々は、金星 AFES で計算された大気の低安定度層上空の鉛直流速分布が、IR2 夜面で観測された惑星規模のストリーク構造に、類似していることを確認した (図 b)。強い下降流が巨大なストリーク状に分布しており、これは観測と整合的である。なぜなら、下降流によって雲量が減り、雲の薄い領域を生み出しうるからである。極上空から見ると、モデル内のストリーク構造は、極渦から低緯度にかけて延びる螺旋を成している (図 cd)。このような螺旋構造は、Venus Express の VIRTIS が捉えた螺旋構造とも類似している。また、南北両半球のストリーク構造はおよそ同じ経度に位置しており、南北で同期している。

本発表では、さらに、ストリーク構造に対する日変化加熱・低安定度層の影響をそれぞれ調べ、ストリークを形成する力学、南北同期の要因について考察する。

図 (a) 2016 年 3 月 25 日に IR2 カメラ (波長 2.26 マイクロメートル) で撮影された金星夜面画像。ただし、コントラストを強調する処理が施された記者発表用の画像である。(b-d) 金星 AFES で計算された高度 60 km の鉛直流分布 (スナップショット)。 (b) は (a) 撮像時の探査機位置から見た場合の分布。(c, d) は極上空から見た分布。なお、金星 AFES は自転の向きが金星と逆のため、図を回転させて表示している。

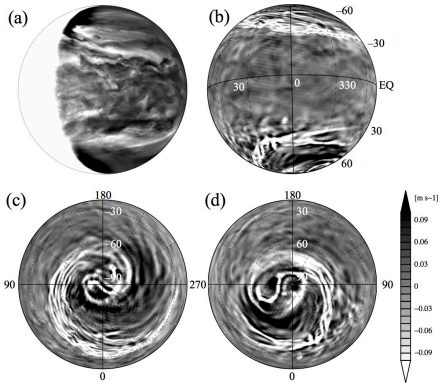

金星赤道域における熱構造の地方時依存性

安藤 紘基 [1]; 福原 哲哉 [2]; 今村 剛 [3]; 高木 征弘 [4]; 杉本 憲彦 [5]; 佐川 英夫 [6]
[1] 京産大; [2] 立教大・理; [3] 東京大学; [4] 京産大・理; [5] 慶大・日吉物理; [6] 京都産業大学

Local time dependence of the thermal structure in the Venusian equatorial region

Hiroki Ando[1]; Tetsuya Fukuhara[2]; Takeshi Imamura[3]; Masahiro Takagi[4]; Norihiko Sugimoto[5]; Hideo Sagawa[6]
[1] Kyoto Sangyo University; [2] Rikkyo Univ.; [3] The University of Tokyo; [4] Faculty of Science, Kyoto Sangyo University ; [5] Physics, Keio Univ.; [6] Kyoto Sangyo University

The radio occultation technique is one of the most useful methods to retrieve vertical temperature profiles in planetary atmospheres. Ultra-Stable Oscillator (USO) onboard Venus Climate Orbiter, Akatsuki, enables us to investigate the thermal structure of the Venus atmosphere between about 40-90 km levels. It is expected that 35 temperature profiles will be obtained by the radio occultation measurements of Akatsuki until August 2017. Static stability derived from the temperature profiles shows its local time dependence above the cloud top level at low-latitudes equatorward of 25 degrees. The vertical profiles of the static stability in the dawn and dusk regions have maxima at 77 km and 82 km levels, respectively. A general circulation model (GCM) for the Venus atmosphere (AFES-Venus) reproduced the thermal structures above the cloud top qualitatively consistent with the radio occultation measurements; the maxima of the static stability are seen both in the dawn and dusk regions, and the local maximum of the static stability in the dusk region is located at a highler level than in the dawn region. Comparing the thermal structures between the radio occultation measurements and the GCM results, it is suggested that the distribution of the static stability above the cloud top could be strongly affected by the diurnal tide. The thermal tide influences on the thermal structure as well as atmospheric motions above the cloud level. In addition, it is shown that zonally averaged zonal wind at about 80 km altitude could be roughly estimated from the radio occultation measurements using the dispersion relation of the internal gravity wave.

電波掩蔽観測とは、探査機が地上局から見て惑星の背後に隠れる、または背後から現れる時に電波を射出し、衛星の軌道運動と惑星大気の影響で受信周波数がドップラーシフトすることを利用して、高度方向の気温分布を高精度（温度測定誤差~0.1 K）・高分解能（鉛直分可能～1 km）で測定できる手法である。これは、惑星大気の鉛直構造や鉛直伝播する波動を捉えることと等価である。「あかつき」は 2016 年 3 月に金星大気の電波掩蔽観測を開始した。臼田局とインド局を共に用いることで、2017 年 8 月までに計 35 個の気温分布を取得した。

気温分布から得られた大気安定度分布を朝側と夕方側で分けると、金星雲層より上の領域において安定度の極大が見られ、極大が位置する高度は朝側で 77 km、夕方側で 82 km でありずれが生じている。この構造の成因を探るため金星大気大循環モデル AFES-Venus の計算結果と比較したところ、電波掩蔽観測の結果と定性的に整合するような構造が再現され、主に東西波数 1 の熱潮汐波が寄与していることが分かった。また、熱潮汐波の分散関係式をもとに雲層より上の高度における平均東西風の速さを推定したところ、過去の観測とほぼ整合的な値であった。これは、電波掩蔽観測によって熱潮汐波の構造を知ることができれば、これまで観測し得なかった高度域の平均的な風速分布を推定できることを示唆する。

Study on the thermal structure of the Venusian polar atmosphere

Mao Takamura[1]; Makoto Taguchi[2]; Tetsuya Fukuhara[3]; Toru Kouyama[4]; Takeshi Imamura[5]; Takao M. Sato[6]; Masahiko Futaguchi[7]; Masato Nakamura[8]; Naomoto Iwagami[9]; Makoto Suzuki[10]; Munetaka Ueno[11]; Mitsuteru SATO[12]; George Hashimoto[13]; Seiko Takagi[14]

[1] Rikkyo Univ.; [2] Rikkyo Univ.; [3] Rikkyo Univ.; [4] AIST; [5] The University of Tokyo; [6] ISAS/JAXA; [7] Toho Univ.; [8] ISAS,JAXA; [9] none; [10] ISAS, JAXA; [11] ISAS, JAXA; [12] Hokkaido Univ.; [13] Okayama Univ.; [14] Tokai Univ. TRIC

The Venus atmosphere exhibits characteristic thermal features called ’polar dipoles’ and ’polar collars’in both polar regions. The polar dipole which locates around the center of the polar region is warmer than mid-latitudes and the polar collar surrounding the polar dipole is colder than the other regions at the same altitude. These features were revealed by infrared observations of Venus by the previous missions Pioneer Venus and Venus Express. The polar dipoles and polar collars are attributed to the residual mean meridional circulation (RMMC) enhanced by the thermal tide. In the high latitudes downward advection driven by RMMC adiabatically heats the polar atmosphere inducing the warm polar dipole, and conversely, in the latitudes equatorward of the polar dipole, upward advection driven by RMMC adiabatically cools the atmosphere inducing the cold polar collar. These results are reproduced by a numerical simulation of the Venus atmospheric circulation [Ando et al., 2016].

The previous observations showed that shapes of the polar dipoles can be characterized by three patterns which are the zonal wave numbers of 0-2, and that they change with time [Garate-Lopez et al., 2013]. The rotation periods of polar dipoles were determined to be 2.5 Earth days [Piccioni et al., 2007] and 2.8-3.2 Earth days [Schofield et al., 1983] for the southern and northern polar regions, respectively. It has not been clear that the difference and variability in the rotation period is due to just a temporal variation, influence of solar activity, or other reasons. Sato et al. [2014] compared the appearances of both polar hot regions by a ground-based observation, rotation of the hot regions is synchronized between the northern and southern hemispheres. However, rotation periods of the northern and southern polar dipoles have not yet been directly compared.

The Japanese Venus orbiter Akatsuki is a planetary meteorological satellite aiming at understanding the atmosphere dynamics of Venus. The Longwave Infrared Camera (LIR), observes thermal emission from the cloud top (˜65km) [Fukuhara et al., 2011]. Since Venus Express was in a polar orbit with an apoapsis located above the south pole, it extensively investigated the southern hemisphere. On the other hand, Akatsuki is in an equatorial orbit, which is suitable for simultaneous observations of both northern and southern polar regions. Variations of thermal features in the polar regions can be retrieved from more than two successive images obtained by LIR with a time interval of several hours.

Rotation periods of polar vortices were derived using the LIR data by tracking a zonal position of maximum temperature. The rotation periods of polar vortices of southern and northern hemispheres are determined to be 3.0 - 8.2 and 1.6 - 5.5 Earth days, respectively (Fig.1). These rotation periods of southern polar vortex are significantly longer than the values observed in the past.

As a next step, we will derive rotation periods of the polar vortices for other observation periods. From these results, possibility of north-south symmetrical rotation of polar vortices, temporal variation of the rotation period and its dependences on local time and spatial resolution will be discussed. Relation between the variation in rotation period and global circulation will help to understand the dynamics of Venusian atmosphere.

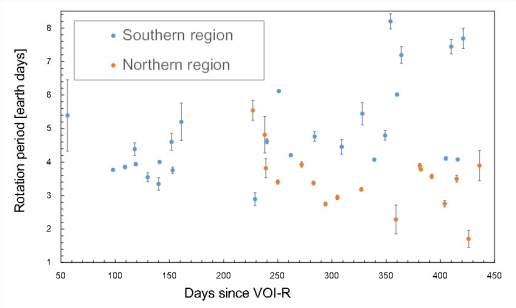

Fig.1. The rotation periods of polar vortices derived from LIR data from 50 to 450 days after Venus orbit insertion (VOI-R) of Akatsuki on Dec. 7, 2015 (Jan. 2016 ~ Feb. 2017).

Measuring the velocity deviation between the movement of planetary-scale and mesoscale cloud features using UVI/AKATSUKI images

Masataka Imai[1]; Toru Kouyama[2]; Yukihiro Takahashi[1]; Shigeto Watanabe[1]; Atsushi Yamazaki[3]; Manabu Yamada[4]; Masato Nakamura[5]; Takehiko Satoh[6]; Takeshi Imamura[7]
[1] Cosmosciences, Hokkaido Univ.; [2] AIST; [3] ISAS/JAXA; [4] PERC/Chitech; [5] ISAS,JAXA; [6] ISAS, JAXA; [7] The University of Tokyo

Venus has a global cloud layer whose thickness exceeds 30 km, and the atmosphere rotates with the speed over 100 m/s from east to west. The scattering of solar radiance and absorption in clouds cause the strong dark and bright contrast in UV range. Since the orbit insertion in December 2015, the Japanese Venus orbiter AKATSUKI continues to monitor cloud features having various spatial scale size in 283 nm SO2 and 365 nm unknown absorption bands. Depending on the AKATSUKI's highly elliptical orbit with 10.8-day period, the spatial resolution ranges from ˜50 km to ˜5 km in the equatorial region, and UVI can capture ˜100 km mesoscale cloud features over the entire visible dayside area. In contrast, the planetary-scale feature, which is often represented as Y-feature, is simultaneously observed when the orbiter is at the moderate distance from Venus and when the Sun-Venus-orbiter phase angle is smaller than 45 degree.

At the previous exploration of Venus Express, cloud top wind velocity was measured with the cloud tracking technique using the mesoscale cloud motion. This approach is widely used, and the long-term trend of wind velocity is being revealed. However, at the same time, observations of the propagation velocity and its variation of the planetary-scale feature are not well conducted because of the limitation of the observable area in the dayside. In this study, we use the ground-based telescope named Pirka and revealed the periodicity change of planetary-scale waves with a time scale of a couple of months. It is considered that the motion of the planetary-scale clouds is related to the atmospheric planetary-scale waves, and the contribution of the waves to the wind acceleration would be a key parameter to solve the generation mechanism of the mysterious super-rotation.

The purpose of this study is to clarify the motion of mesoscale and planetary-scale cloud features simultaneously using AKATSUKI UVI images. Each cloud feature can be represented as the wind and phase velocity of the planetary-scale waves, respectively. For the initial study, we used the time-consecutive and well spatially resolved UVI images taken in the orbit #32. During this orbit (from Nov. 13 to 20, 2016), 7 consecutive images were obtained in a dayside with ˜2 hr time-interval between the images and with the spatial resolution ranged from 35 km to 10 km. To investigate the typical spatial scale dividing the mesoscale and planetary-scale motion, the Gaussian-filters with sigma = 1-, 3-, 5- and 8-deg. were used to smooth geometrically mapped images, which were produced by projecting the original UVI images with 0.25 deg. resolution using the Akima interpolation. Then the mapped images were divided into 15 x 5 deg. (lon x lat) sub-images covering N50–S50. The amount of longitudinal shift between each pair of two time-consecutive bands was estimated by searching the 2D cross-correlation maximum. The final wind and phase velocity (or rotation period) for mesoscale features were determined with a small error about +/- 0.2-day period. In the case of planetary-scale features, they still were not well determined because of the unnatural correlation peak, and it was necessary to exclude the low contrast sub-images manually especially when the larger sigma at the Gaussian-filter and sub-images of higher latitudes were used. However, the visual inspection of the figures, which arrange sub-latitudinal images smoothed by the 3-deg. filter in the vertical direction (as shown in Figure 1), clearly showed the velocity deviation between the mesoscale and planetary-scale motion.

At the presentation, the methodology of our new analyses using UVI images and the results of the time variation of the velocity deviation with the time scale of a couple of months will be shown. The phase velocity of the planetary-scale features can also be compared with the results derived from our ground-based simultaneous observations using the Pirka telescope.

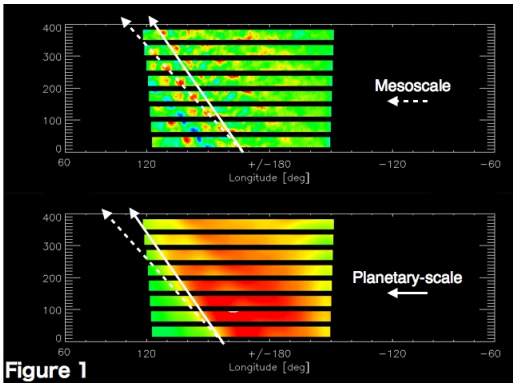

あかつき金星紫外画像に見られる地形固定構造

北原 岳彦 [1]; 今村 剛 [2]; 山崎 敦 [3]; 山田 学 [4]; 渡部 重十 [5]
[1] 東大・理・地惑; [2] 東京大学; [3] JAXA・宇宙研; [4] 千葉工大・惑星探査研究センター; [5] 北大・理・宇宙

Stationary features at Venusian cloud top observed by Akatsuki UV Imager

Takehiko Kitahara[1]; Takeshi Imamura[2]; Atsushi Yamazaki[3]; Manabu Yamada[4]; Shigeto Watanabe[5]
[1] Earth and Planetary Science, UTokyo; [2] The University of Tokyo; [3] ISAS/JAXA; [4] PERC/Chitech; [5] Cosmosciences, Hokkaido Univ.

Using the cloud image obtained with the Ultraviolet imager (UVI) on board the Venus orbiter "Akatsuki", we detect stationary features and investigate their origin. Huge bow-shaped structures extending from northern to southern high latitudes have been discovered by the Longwave infrared camera (LIR), which is also installed in Akatsuki, and such structures have been observed several times. Since they appear above certain highlands and continue to be there against the zonal wind, they are attributed to topographic gravity waves. This study shows that there exist similar features also in other wavelengths.

Variations of the vertical wind have been observed over the Aphrodite Terra (altitude 3000˜4000 m) by the VEGA balloon in 1985 (Blamont *et al*., 1986), and recently the cloud tracking using cloud images taken by VMC on bored Venus Express showed that the zonal wind speed is decreased above the Aphrodite Terra (Bertaux *et al*., 2016). These two studies suggested the existence of gravity waves and their important role in momentum transfer. Gravity waves, whose restoring force is buoyancy, are considered to be generated preferentially in the lower atmosphere and propagate upward. When they break at cloud heights, the momentum transported from the lower layer are delivered to the background atmosphere, and then the mean zonal wind is decelerated. Since this effect is an important factor for understanding the super-rotation, understanding of gravity waves is crucial. From such a viewpoint, we identify topographically-fixed structures in Akatsuki UVI images, study geographical and local time dependences and measure the horizontal wavelength. We also study how gravity waves create shading pattern and derive the wave amplitude. In addition, we compare images taken at 283 nm, where the absorption by sulfur dioxide dominates, and 365 nm, where absorption occurs due to unknown absorbers, to consider factors of difference in appearance.

We use L3 data projected onto the latitude and longitude coordinate. In order to extract structures fixed to the terrain, we apply high-pass filtering by subtracting a Gaussian-smoothed image to emphasize small structures and average multiple images taken in a particular orbit to smooth out moving features.

We analyzed the 283 nm image taken on 7th December 2015, which is the date of Venus orbit reinsertion, and identified stationary structures like scratches running in the north-south direction in low latitudes. Analyzing all L3 data of 283 nm taken before January 25, 2017, we found that all of the stationary structures appeared exclusively above highlands near the equator, and that they tend to appear around the local time from noon to the evening. The horizontal wavelengths are about 200-300 km. Bow-shaped structures were observed by LIR also in these geographical regions and local time, suggesting a common dynamical mechanism behind the stationary features observed by UVI and LIR. We also analyzed in a 365 nm image that visualizes the density of unknown absorbers. As a result, the stationary structures was unclear compared to 283 nm, and we could identified only in cases where the amplitude was particularly large or the cloud shading pattern was monotonous.

We assume that the stationary features are generated by gravity waves and we are modeling to estimate the gravity wave parameters. We set the value of sulfur dioxide and cloud scale height and calculate advection by plane wave solution of gravity wave based on the model of Chiu and Ching (1978) to estimate fluctuation in the amount of sulfur dioxide column above the cloud top. By comparing the observed brightness variation and the result of model, amplitude of atmosphere density variation can be obtained. In addition, the scale height of the unknown absorbers and the cloud can be restricted by the phase relation to the stationary features observed at multiple wavelengths by Akatsuki.

金星探査機あかつき搭載の紫外カメラ（UVI）で取得された雲画像を用いて、金星地表に対してほぼ固定した微細な模様を検出し、その起源について考察する。同じくあかつきに搭載されている赤外カメラ（LIR）により、南北にまたがる巨大な弓状構造が発見され、これまでに複数回出現していることが確認されている。これらは特定の高地上に出現し、背景風に流されることなくその場にあり続けることから、その成因は地形性の重力波によるものと考えられている。本研究は異なる波長でも似た特徴を持つ構造があることを示すものである。

これまでに 1985 年の VEGA 気球による大気観測では Aphrodite 大陸（標高 3000～4000m）上空において鉛直振動が観測され (Blamont et al., 1986)、最近は Venus Express 搭載の VMC 画像を用いた雲追跡により Aphrodite 大陸上空で東西風速が減速していることがわかった (Bertaux et al., 2016)。この２つの研究結果は、地形性重力波の存在とその影響を示唆している。重力波は浮力を復元力とする波動であり、下層大気中で励起され鉛直に伝播する。そうして下層から輸送し

てきた運動量を重力波が砕波する際に背景場に受け渡し、背景風を減速させることとなる。この効果は大気のスーパーローテーションを理解するための重要な要素となるため、金星大気重力波の更なる解明が必要とされている。そこであかつきの UVI 画像を用いて地形固定構造を確認し、発生地域とローカルタイムの傾向、および水平波長を解析する。さらに重力波が濃淡模様を作るメカニズムや重力波の振幅についても調べる。また二酸化硫黄吸収帯である 283 nm と未同定物質吸収帯である 365 nm で UVI により撮影された画像を比較し、見え方の違いの要因を考察する。

解析にはあかつきの UVI 画像を緯度・経度に展開した L3 データを用いる。まずガウシアンフィルタをかけた画像を元の画像から引くことでハイパス処理をし、小さな構造を確認しやすくする。次に地形に固定された構造を確認するため、数時間以内に連続的に撮影された画像を重ね合せて平均をとる。こうすることで移動性の構造がならされ、停滞する構造が強調される。

あかつきが 2015 年 12 月 7 日の金星再投入後に初めて撮影した 283 nm 画像を解析したところ、低緯度においていくつか南北に渡る筋状の地形固定構造が確認できた。さらに 2017 年 1 月 25 日までに撮影されたすべての 283 nm の L3 データを同様に解析した。発見できた地形固定構造はすべて赤道帯の高地上に出現しており、また発生するローカルタイムには偏りがあり、専ら昼から夕方にかけて出現していることがわかった。その東西波長は 200〜300km ほどである。同じ日時・場所において LIR でも弓状構造もしくは筋状の構造が観測されており、共通の力学現象であることが示唆される。
同様の解析を未同定吸収物質の濃淡を可視化する 365 nm 画像でも行ったところ、283 nm に比べて停滞構造は不明瞭であり、振幅が特に大きいときや背景の濃淡模様が乏しいときに限り同定することができた。

地形固定構造が重力波によるものであると仮定して重力波パラメータの推定を進めている。紫外吸収物質と雲のスケールハイトを仮定したうえで重力波の平面波解による移流を Chiu and Ching (1978) のモデルに基づいて計算し、雲頂より上の二酸化硫黄コラム量の変動を推定する。これを観測された地形固定構造と比較することで背景大気の密度振幅が求まる。また、あかつきの複数のカメラにより複数の波長で捉えられた地形固定構造から雲頂高度の変動と紫外吸収物質の変動の位相関係を求め、ここから吸収物質と雲のスケールハイトに制約を与えることができる。

あかつき電波掩蔽観測の初期成果

今村 剛 [1]; 安藤 紘基 [2]; 野口 克行 [3]; あかつき電波科学チーム 今村　剛 [4]
[1] 東京大学; [2] 京産大; [3] 奈良女大・理・情報; [4] -

Initial scientific results of Akatsuki radio occultation experiment

Takeshi Imamura[1]; Hiroki Ando[2]; Katsuyuki Noguchi[3]; Imamura Takeshi Akatsuki Radio Science Team[4]
[1] The University of Tokyo; [2] Kyoto Sangyo University; [3] Nara Women's Univ.; [4] -

http://www.astrobio.k.u-tokyo.ac.jp/imamura/

Akatsuki's radio occultation experiments are performed when the spacecraft is hidden by Venus as viewed from the tracking station. Analysis of the recorded signals yields temperature profiles, sulfuric acid vapor profiles, and the ionospheric electron density profiles. A uniqueness of Akatsuki's observation is that the location probed by radio occultation cluster in the low latitude thanks to the equatorial orbit. 35 atmospheric profiles have been observed till 2017 and interesting features related to localtime dependence and possible long-term variation are seen. We plan to obtain data under wider range of conditions in the coming years and compare them with imaging data obtained by onboard cameras.

金星探査機あかつきの電波掩蔽観測により気温の高度分布、硫酸蒸気の高度分布、電離圏電子密度の高度分布が得られている。2017 年までに 18 回の掩蔽機会をとらえ、探査機が地球から見て金星に隠れるときと再度現れるときを合わせて 35 箇所の大気構造を観測した。あかつきの軌道は従来の金星探査機のような極軌道ではなく赤道周回軌道であるため、低緯度を重点的に観測することが可能である。また掩蔽の際に電波が低緯度大気に対して垂直に近い方向に動き、水平方向にあまり動かないため、水平一様を仮定する解法が有効となり精度が向上する。このような特質を活かして、低緯度大気を主な対象として新たな発見がもたらされつつある。たとえば顕著なローカルタイム依存性が雲層内からその上の中間圏にかけての温度分布に見られており、熱潮汐波の影響のほか、夜間の雲頂の放射冷却が雲層内の対流に及ぼす影響がうかがわれる。また 1980 年代初めまでの観測データをもとに作られた Venus International Reference Atmosphere に比べて低高度の気圧と気温が低めとなっている。今後はより幅広い条件でデータ取得してこのような特徴を掘り下げるとともに、撮像データとの比較により新たな研究テーマを開拓する。

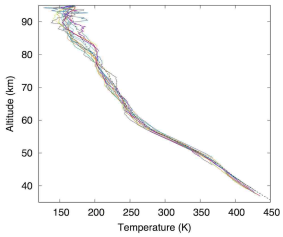

ひさき・あかつきの金星同時観測による金星大気の上下結合の研究

奈良 佑亮 [1]; 今村 剛 [2]; 吉川 一朗 [3]; 吉岡 和夫 [4]; 益永 圭 [5]; 山崎 敦 [6]; 山田 学 [7]; 渡部 重十 [8]; Lee Yeon Joo[9]
[1] 東大・新領域; [2] 東京大学; [3] 東大・理・地惑; [4] 東大・理; [5] 東大・理
; [6] JAXA・宇宙研; [7] 千葉工大・惑星探査研究センター; [8] 北大・理・宇宙; [9] JAXA/ISAS

Study on vertical coupling of Venusian atmosphere with HISAKI and Akatsuki

Yusuke Nara[1]; Takeshi Imamura[2]; Ichiro Yoshikawa[3]; Kazuo Yoshioka[4]; Kei Masunaga[5]; Atsushi Yamazaki[6]; Manabu Yamada[7]; Shigeto Watanabe[8]; Yeon Joo Lee[9]
[1] GSFS, Univ. Tokyo; [2] The University of Tokyo; [3] EPS, Univ. of Tokyo; [4] The Univ. of Tokyo; [5] Univ. Tokyo; [6] ISAS/JAXA; [7] PERC/Chitech; [8] Cosmosciences, Hokkaido Univ.; [9] JAXA/ISAS

Until HISAKI started to observe Venus, disturbances in the thermosphere have been hardly measured. Because of high temporal resolution of observation by HISAKI, periodicities in Venusian thermosphere have been detected (Masunaga et al., 2015; 2017). On the other hand, Akatsuki observes Venusian cloud layer. Combining these observations, vertical structure of Venusian atmosphere can be extracted.

Since 2013, HISAKI have observed planets such as Jupiter, Venus, Mars and Mercury, Moon, and comets with spectroscope in the extreme ultraviolet wavelength range. When observing Venus, it measures emissions of atoms, ions and molecules excited by photoelectron impacts and sunlight. Owing to its temporal resolution higher than any prior observations, HISAKI can measure the temporal variations in emissions. Since 2015, Akatsuki observes Venusian cloud layer with various band pass filters and with high spatial resolution.

During June 2017, HISAKI and Akatsuki observed Venus. We present the primary result of comparison between temporal variations of dayglow in the thermosphere observed by HISAKI and cloud brightness by Akatsuki by focusing on the variation of several days. The period of about 2.6 days in common with the two observations has been detected. We also discuss the candidate for a wave which the detected period is attributed to.

これまで金星上層大気の変動について観測的な証拠が不十分であったが、極端紫外線領域で金星を継続的に高時間分解能の観測を行うひさき衛星によりその変動を捉えられるようになった (Masunaga et al., 2015; 2017) 。また、金星探査機あかつきが雲層の観測を行っており、「ひさき」、「あかつき」の観測データを組み合わせることで雲層と熱圏を結び、大気の上下結合の理解につながることが期待できる。

地球周回衛星「ひさき」は 2013 年より、木星、金星、火星、水星といった惑星や月、彗星を極端紫外波長域で分光観測している。金星観測においては、熱圏での電子衝突や太陽光に励起された原子・イオン・分子の発光を観測する。さらに、「ひさき」はこれまでの衛星にない高時間分解で観測を実施しているため、発光の時間変動を捉えられる。金星探査機「あかつき」は 2015 年に金星の周回軌道に投入され、主に撮像により雲層の観測を行っている。「あかつき」は高空間分解能の画像を取得しており、模様の追跡による風速場の導出などが可能である。

2017 年 6 月、「ひさき」と「あかつき」は同時に金星を観測した。「ひさき」により得られた高度約 130 km での酸素原子の発光強度、「あかつき」により得られた高度約 70 km の未同定物質による吸収を受けた紫外線の太陽散乱光強度の時間変動を 1 日から 10 日程度の周期変動に着目して解析し、上層大気への波動の伝播の可能性を探っている。「ひさき」と「あかつき」の観測データに約 2.6 日の共通する周期性が確認された。本発表では、その初期結果と上層大気へ伝播しうる波動の候補を議論する。

あかつき搭載LACによる金星雷放電捜索の現状

高橋 幸弘 [1]; 今井 正尭 [1]; 佐藤 光輝 [2]
[1] 北大・理・宇宙; [2] 北大・理

Update of lightning hunt in Venus with LAC onboard Akatsuki

Yukihiro Takahashi[1]; Masataka Imai[1]; Mitsuteru SATO[2]
[1] Cosmosciences, Hokkaido Univ.; [2] Hokkaido Univ.

LAC on board Akatsuki, Venus climate orbiter, is the first sensor optimized for the lightning flash detection in planets other than the Earth so that it can identify the optical flash caused by electrical discharge in the atmosphere of Venus and could conclude the 30-year discussion on the existence of lightning in Venus. Unique performance of LAC compared to other equipments used in the previous studies of Venus is the high-speed sampling rate at 30 kHz for all 32 pixels of APD matrix, enabling us to distinguish the optical lightning flash from other pulsing noises. We selected OI 777 nm line for lightning detection, which is expected to be the most prominent emission in CO2-dominant atmosphere based on the laboratory experiments.

After checking the sound condition of high-voltage system for the APD detector after the second attempt of the insertion of Akatsuki into the orbit around Venus on December 7, 2015, the regular operation of LAC at nominal high-voltage of 300 V for lightning hunt was started on December 1, 2016. Due to the elongated orbit than that planned originally, we have an umbra for about 30 min to observe the lightning flash in the night side of Venus every 10 days.

Up to now, July 9, 2017, we have examined 13 times observations with total observation time about 4 hours, but could not find any lightning signals. If the spacecraft is located at a distance of 5,500 km from Venus surface, the threshold of triggering is 1/20 of the average of the Earth lightning flash and the instant field-of-view is 1/500 of the whole

globe. Here we discuss the upper limit of the lightning occurrence rate in Venus, assuming homogeneous occurrence over whole globe, which might be compared with the estimations by previous studies. However, in order to confirm the occurrence ratio reported by Hansell et al. (1995), one of the representative estimation, we need to accumulate total observation period by 3 times than we did.

次世代赤外ヘテロダイン分光器MILAHIに導入する中間赤外ファイバーの評価と金星中間圏風速・温度場のリトリーバル手法の確立

高見 康介 [1]; 中川 広務 [1]; 佐川 英夫 [2]; Krause Pia[3]; 青木 翔平 [4]; 笠羽 康正 [5]; 村田 功 [6]; 平原 靖大 [7]; Benderov Oleg[8]; 片桐 崇史 [9]
[1] 東北大・理・地球物理; [2] 京都産業大学; [3] University of Cologne; [4] BIRA-IASB; [5] 東北大・理; [6] 東北大院・環境; [7] 名大・院・環境・地球惑星; [8] MIPT; [9] 東北大・工

Evaluation of optical fiber for MILAHI and Verification of the retrieval method for wind and temperature in Venusian mesosphere

Kosuke Takami[1]; Hiromu Nakagawa[1]; Hideo Sagawa[2]; Pia Krause[3]; Shohei Aoki[4]; Yasumasa Kasaba[5]; Isao Murata[6]; Yasuhiro Hirahara[7]; Oleg Benderov[8]; Takashi Katagiri[9]
[1] Geophysics, Tohoku Univ.; [2] Kyoto Sangyo University; [3] University of Cologne; [4] BIRA-IASB; [5] Tohoku Univ.; [6] Environmental Studies, Tohoku Univ.; [7] Earth&Planetary Sciences, Nagoya Univ.; [8] MIPT; [9] Engineering, Tohoku Univ.

Spatial and temporal variations of the thermal structure in Venusian mesosphere (above 70 km) were found by Venus Express (VEX) (Patzold et al., 2007; Bougher et al., 2015; Mahieux et al., 2015). This altitude is considered as the region where the global dynamics change from superrotation to the sub-solar to anti-solar flow, suggesting that any variations on the thermal structure might be related to the variations on the dynamics. However, the wind velocity in this region have not been understood due to difficulty of observation for the altitude range of 70 - 95 km. CO_2 absorption spectra in 10 um band fully resolved by mid-infrared (MIR) heterodyne spectrometers, are an effective tracer to observe the mesosphere, and are retrieved for wind velocity and temperature by radiative transfer and inverse calculation (Nakagawa et al., 2016). Then, we are able to study the relationship between mesospheric wind and temperature variations.

We retrieved the wind velocity and temperature from the heterodyne spectroscopic data obtained on March 20 - 29 by THIS (developed by University of Cologne) and on May 18 - 20 by HIPWAC (developed by NASA) in 2012. We detected the sensitivities of the altitude range of 85 - 100 km with the altitude resolution of 10 km and the uncertainties of +/-33 - 54 m/s, and of the altitude range of 70 - 95 km with the altitude resolution of 5 km and the uncertainties of +/-0.6 - 13 K from retrievals of wind velocity and temperature, respectively. In addition, we estimated the dependences on initial guess of inverse calculation. The dependences of wind velocity and temperature are +/-10 - 35 m/s and +/-3 - 5 K, respectively. The dependences do not influence the retrieval results because they are within the maximum of the retrieval uncertainties. The retrieved vertical temperature profile well agreed with the previous result of MIR heterodyne spectrometers (Stangier et al., 2015) and of radio occultation experiments by VeRa/VEX in the altitude range of 75 - 90 km. The study verified the method of the retrieval for Venusian mesospheric wind velocity and temperature. The understanding of Venusian mesosphere will be progressed with long-term observations by MIR heterodyne spectroscopy.

We have developed the Mid-Infrared LAser Heterodyne Instrument (MILAHI) attached on Tohoku University 60 cm diameter telescope at Mt. Haleakala. The instrument had been recently upgraded with a fast Fourier transform spectrometer of 2.5 GHz range. The test observation of this upgraded instrumentation was conducted against Venus in May, 2017. We also started the test of MIR fiber optics in collaboration with Moscow Institute of Physics and Technology (MIPT) for the future development of the instruments on lander, orbiter and ground-based observations . Fiber technology has the advantages for reduction of mass and size due to simplification of optics, and simplification of the light path alignment. In addition, it is also enable us to observe several wavelengths due to easy reconnection of multiple laser sources, and to retrieve the physical parameters in several altitudes due to observations of absorption in different optical thickness. The optical fibers for near-IR had well developed and will be implemented for the instrument on ExoMars platform (Rodin et al., 2015). The optical fibers for MIR are more challenging because of its low transmission. Furthermore, smaller core diameter is needed to transmit single-mode for heterodyne system. The MIR fibers developed in Tohoku University are Ag-covered hollow fibers with inner and outer diameter of 1 and 1.6 mm, respectively. High transmission of laser source with loss rate less than 0.5 dB/m could be achieved by this large core size. We also confirmed the single-mode transmission with small numerical aperture due to diminishment of other modes. In this study, we discuss the feasibility of the MIR fibers as a key component of future MIR heterodyne spectrometer.

欧州の金星探査機 Venus Express(VEX) の電波掩蔽観測によって、金星中間圏・下部熱圏（高度 70 km より上方）における熱構造の時間・空間的変動が明らかになった (Patzold et al., 2007; Bougher et al., 2015; Mahieux et al., 2015)。また、中間圏は大気循環がスーパーローテーションから昼夜間対流に遷移する領域と考えられており、温度構造の時間・空間変動には風速場との相関関係があると推測されるが、高度 70 - 95 km のにおける風速の観測は難しく、理論的にも観測的にも理解が進んでいない。CO_2 の 10 um 帯のスペクトルは、雲層の上に分布する CO_2 大気が雲頂からの背景放射を吸収することで形成されるため、その吸収線には中間圏領域の情報が含まれている。このスペクトルを $3X10^7$ の高周波数分解能（1MHz）を達成する中間赤外ヘテロダイン分光器を用いて観測し、また放射伝達計算と反転解析を行うことで中間圏の視線方向の風速と温度鉛直分布を導出することができ (Nakagawa et al., 2016)、中間圏の風速場の変動と温度構造の変動の相関関係を議論することが可能になる。

我々の先の研究では、2012 年 3 月 20 - 29 日の THIS（ケルン大学開発）と 5 月 18 - 20 日の HIPWAC（NASA 開発）の 2 つの中間赤外ヘテロダイン分光観測から風速と温度を導出した。風速解析は、誤差+/-33 - 54 m/s の範囲で高度 85 - 100 km に高度分解能 10 km で 1 つまたは 2 つの高度に感度を持つことがわかった。温度解析では、高度分解能 5 km で 70 - 95 km の温度鉛直分布を誤差+/-0.6 - 13 K で得られた。反転解析の初期値依存性の評価を行ったところ、風速が+/-10 - 35 m/s、温度が+/-3 - 10 K であった。この結果より、それぞれの初期値依存性は解析誤差の最大値の範囲内に収まっており、初期値依存性による解析結果への影響は十分小さいことがわかった。また、温度分布について、中間赤外ヘテロダイン分光観測 (Stangier et al., 2015) と電波掩蔽観測 VeRa/VEX の先行研究と高度 75 - 90 km の範囲でよく一致した。本研究により、中間圏の風速と温度の導出手法が確立され今後の中間赤外ヘテロダイン分光の長期観測により中間圏の理解が進むと期待される。

この目的のため、我々はハレアカラ山頂に位置する東北大学 60cm 望遠鏡に東北大学開発の Mid-Infrared LAser Heterodyne Instrument (MILAHI) を設置し地球型惑星の長期的な観測の実現に向けて開発を進めている。2017 年 5 月には、2.5 GHz の高速フーリエ変換分光器を導入し長期観測の準備を整え、金星試験観測を行った。現在では、Moscow Institute of Physics and Technology (MIPT) と共同で惑星着陸機や周回軌道衛星、地上観測の観測器に中間赤外ファイバーを導入するための試験を行っている。ファイバー技術は、光学系の簡易化による装置の軽量、小型化、光路調整の簡易化に繋がる。また、ファイバーの繋ぎ換えのみでレーザー光源を簡単に換えられるため、複数波長で異なる光学的厚みの吸収線を観測でき様々な高度での大気物理量の導出が可能となる。近赤外ファイバーの技術はすでに確立されており、ExoMars の火星着陸機に搭載することが決定されているが (Rodin et al., 2015)、中間赤外ファイバーは、伝送率が悪く今までは実用段階に達していなかった。また、ヘテロダイン分光に用いられるファイバーは、伝送モードがシングルモードになる必要があり、コア径が小さいものでなければならない。東北大学工学部で開発されている銀コーティングの内径 1 mm、外径 1.6 mm の中空ファイバーは、損失特性が CO_2 レーザー光源で 0.5 db/m 以下の高伝送を達成できている。加えて、内径が大きいながらも入射開口数を小さくすることで基底モード以外のモードが十分に減衰しシングルモードの伝送が可能であることが確認された。本発表では、ヘテロダイン分光器の重要な要素として中間赤外ファイバーの可能性について議論する。

Evaluation of JACOSPAR applied to OMEGA / MEx : a fully spherical radiative transfer code with multi-scattering by aerosols

Masashi Toyooka[1]; Arnaud Mahieux[2]; Shohei Aoki[2]; Hiromu Nakagawa[3]; Yasumasa Kasaba[4]; Hironobu Iwabuchi[5]
[1] Tohoku Univ.; [2] BIRA-IASB; [3] Geophysics, Tohoku Univ.; [4] Tohoku Univ.; [5] CAOS, Tohoku Univ.

JACOSPAR (Iwabuchi et al., 2006, 2009) is a fast radiative transfer (RT) model that considers refraction and multiple scattering of light by aerosols in the spherical atmosphere. This can be used for the limb observation of the planetary atmosphere. It had been a difficulty for RT models to consider spherical atmosphere and multiple scatterings by aerosols at the same time for a huge calculation amounts.

JACOSPAR have mainly two characteristics to calculate the radiance effectively. One is that it uses backward Monte Carlo method that treats absorption and scattering of the radiation as a probability process of the model photons from observed point to the radiation source. Another is that it adopts dependent sampling method (Marchuk et al., 1980). With this method, the radiance for a given wavenumbers and interpolates the radiance for the other wavenumbers, reducing the calculation amounts.

The atmospheric escape of Mars is gathering a lot of attention from researchers. Maltagliati et al. (2011) found the super-saturation of water vapor around 30-50 km observed by SPICAM/MEx. Recently an introduction of water vapor around 60km altitude was found to increase the escape rate of the hydrogen atom by a factor of several (Chaffin et al., 2017). However, the researches directly retrieved the vertical profile of the water are not so many (with SPICAM/MEx Fedorova et al., 2009, Maltagliati et al. 2011, 2013). The more studies about the water vapor vertical profile will give us more information about physical and photochemical process of Martian hydrological cycle and atmospheric escapes.

In our research, we will apply the JACOSPAR to the observation of OMEGA/MEx and evaluate the obtained water vapor vertical profiles with this model by comparing previous studies (Maltagliati et al. 2011, 2013).

This study is intended to be applied to the Nadir and Occultation for Mars Discovery spectrometer (NOMAD) instrument onboard Trace Gas Orbiter (Vandaele et al., 2015), which was successfully inserted into Mars orbit on October 2016 and science operations to begin in 2018..

超小型火星探査機搭載THzヘテロダイン分光システムの開発検討

松本 怜 [1]; 西田 侑治 [2]; 真鍋 武嗣 [3]; 前澤 裕之 [4]; 笠井 康子 [5]; 黒田 剛史 [5]; 落合 啓 [5]; Larsson Richard[5]; 佐藤 滋 [5]; 今村 剛 [6]; 和地 瞭良 [6]; 阪上 遼 [6]; 高橋 亮平 [6]; 中須賀 真一 [6]; 長谷川 豊 [7]; 西堀 俊幸 [8]; 佐川 英夫 [9]; 笠羽 康正 [10]
[1] 大阪府大・理・物; [2] 大府大・理・物; [3] 大阪府大・工・航空宇宙; [4] なし; [5] NICT; [6] 東京大学; [7] JAXA/ISAS; [8] なし; [9] 京都産業大学; [10] 東北大・理

THz-band Heterodyne Spectroscopy Sensing System on board Mars Micro-satellite Lander/Orbiter

Satoshi Matsumoto[1]; Yuji Nishida[2]; Takeshi Manabe[3]; Hiroyuki Maezawa[4]; Yasuko Kasai[5]; Takeshi Kuroda[5]; Satoshi Ochiai[5]; Richard Larsson[5]; Shigeru Sato[5]; Takeshi Imamura[6]; Akifumi Wachi[6]; Ryo Sakagami[6]; Ryohei Takahashi[6]; Shin-ich Nakasuka[6]; Yutaka Hasegawa[7]; Toshiyuki Nishibori[8]; Hideo Sagawa[9]; Yasumasa Kasaba[10]
[1] Osaka Prefecture Univ; [2] OPU; [3] Aerospace Engineering, Osaka Prefecture Univ.; [4] none; [5] NICT; [6] The University of Tokyo; [7] JAXA/ISAS; [8] JAXA; [9] Kyoto Sangyo University; [10] Tohoku Univ.

Recently the heterodyne instrument for the HIFI (Heterodyne Instrument for the Far Infrared) on board Herschel space observatory (European Space Agency) indicated that the mixing ratio of molecular oxygen in the Martian atmosphere shows the increase at the lower atmosphere. The NASA's infrared telescope and Mars rover, Curiosity have also discovered the concentration of Methane on Mars. For understanding of the sources of these species, it is crucial to reveal the chemical reaction network of the Martian atmosphere as well as the presence or absence of life. We have started to study the development of the 0.4 THz band heterodyne spectroscopic system for the remote sensing of the minor constituents such as O_2, H_2O, O_3, CO, their isotopes, and so on in the Martian atmosphere through the night- and day-time and the four seasons. At present, we are planning to install this THz system on the Mars micro-satellite orbiter and lander under consideration by Nakasuka group of the University of Tokyo.

Thanks to the high frequency resolution THz band heterodyne spectroscopy is the powerful tool to derive altitude distributions of the minor constituents and less affected by absorption and scattering of aerosol/dusts in the lower altitude, without the back ground sources like the Sun.

In this mission due to the budget limitations of the weight, space, and electric power, it's vital to optimize the thermal and structural design and components of the system. For the frontend Schottky barrier diode mixer devices implemented with frequency multiplying local oscillators (Virginia diode Inc.) are utilized. Input RF signals are divided to right and left handed polarized waves with the novel waveguide-type circular polarizer, which will allow us to estimate the magnetic field near the ground of Mars by observing the difference of the polarized spectral line profiles induced by the Zeeman effect.

One of the good landing candidate sites in the low latitude plains area, Isidis Planitia, has the surface temperature from 190 - 280 K and 0.7 % atmospheric pressure as the Earth's one according to the Mars Climate Database. With this in mind for the case of lander the thermo-fluid simulations of the THz sensing system were performed. In this presentation we will discuss the design of the THz band heterodyne sensing system, the results of 3D high frequency electromagnetic simulations of the newly designed circular polarizer, and the 3D-thermal simulations of the system.

ハーシェル宇宙望遠鏡 (European Space Agency) の HIFI (Heterodyne Instrument for the Far Infrared) により、火星大気において酸素分子の混合比が低高度において増加する傾向が捉えられた。また、局所的なメタンの発生も NASA の赤外望遠鏡や火星探査車キュリオシティによって観測されている。しかし、これらはいずれも、その起源が未解明であり、生物起源である可能性も含め、火星環境における基本的な化学反応ネットワークの理解が急務な課題となっている。我々は、東京大学工学系研究科の中須賀研究チームが検討を進めている超小型火星衛星による周回機や着陸機により、火星大気中の O_2、H_2O、O_3、CO やそれらの関連同位体分子などの昼夜・四季を通じた観測、Zeeman 効果による低高度の火星磁場の計測、惑星における酸素などのバイオマーカーのポテンシャルを探るべく、0.4 THz 帯ヘテロダイン分光システムの開発検討を進めている。

THz 帯ヘテロダイン分光は、高い周波数分解能により惑星大気の微量分子の高度分布を高精度に導出できる他、エアロゾル/ダストの影響を受けにくく火星全体を覆うようなダストストーム発生時でも低高度まで見通して大気の観測が可能であること、背景光源が不要であり昼夜の面を問わず大気を観測できる強みがある。受信機には新規の円偏波分離デバイスと SBD ミクサと逓倍型の固体局部発振器を内蔵した常温のヘテロダイン検出器を、分光計にはマックスプランク研究所のチャープ変換型分光計を採用する計画である。超小型衛星であるため、現在の検討段階で搭載できるバジェットは 7kg 程度以下の制限があり、システムや構造、熱設計の検討が重要となる。Mars Climate Database を用いて調べたところ、着陸機の着陸候補地の 1 つである火星の低緯度地域のイシディス平原は、1 公転周期の季節変動と日照変化によって地表の温度は 190〜280 K 程度、高度 0.5 m 付近の気温は 200〜250 K 程度まで変動することがわかった。ローバーを想定した火星の大気圧程度の流体も考慮した 3 次元熱解析シミュレーションを実施したところ、夜間はヘテロダイン検出器の許容動作範囲内に収まらない可能性があることが分かった。また、火星大気圧下の熱伝達の影響や、シールドの輻射率を変えることでシステムの外気への輻射冷却による影響を調べた。昼夜間の温度変動を許容動作範囲内で抑えるべ

く、ヒーターや熱伝導を効果的に使うなどのさらなる検討を進めている。本講演では、これら熱流体解析の結果や、THz ヘテロダイン分光システムの検討状況、セプタム型の円偏波分離デバイスの 3 次元高周波電磁界解析の結果などについて報告する。

Exploring the Atmosphere of MArs and VEnus with Remote Observations: A Belgium-Japan partnership (AMAVERO)

Yasumasa Kasaba[1]; Hiromu Nakagawa[2]; Hideo Sagawa[3]; Takeshi Kuroda[4]; Takeshi Imamura[5]; Ann Carine VANDAELE[6]; Shohei Aoki[7]; Isao Murata[8]; Naoki Terada[9]; Takeshi Sakanoi[10]; Kosuke Takami[2]; Sae Aizawa[11]; Masashi Toyooka[12]; Takehiko Akiba[13]; Yasuko Kasai[4]; Atsushi Yamazaki[14]; Takao M. Sato[15]; Hiroyuki Maezawa[16]; Makoto Taguchi[17]; Severine ROBERT[6]; Valerie WILQUET[6]; Arnaud MAHIEUX[6]
[1] Tohoku Univ.; [2] Geophysics, Tohoku Univ.; [3] Kyoto Sangyo University; [4] NICT; [5] The University of Tokyo; [6] BISA; [7] BIRA-IASB; [8] Environmental Studies, Tohoku Univ.; [9] Dept. Geophys., Grad. Sch. Sci., Tohoku Univ.; [10] Grad. School of Science, Tohoku Univ.; [11] Geophysics, Tohoku Univ; [12] Tohoku Univ.; [13] Geophysics,Tohoku Univ.; [14] ISAS/JAXA; [15] ISAS/JAXA; [16] none; [17] Rikkyo Univ.

http://c.gp.tohoku.ac.jp/~www/amavero.html

Recent successful explorations of Mars and Venus atmospheres by numerous spacecraft and ground-based telescopes have suggested their active photochemistry and dynamics on the planets. Characteristics of spatial and temporal variations of temperature, wind, and atmospheric constituents are essential to understand the photochemistry and dynamics. However, (1) "3D distributions (i.e., spatial variation + vertical profiles)" of temperature, wind, and trace gases on Mars, and (2) those at the middle atmosphere (from the cloud top to the upper atmosphere, 60-140 km) of Venus, are still poorly understood.

In 2017-2018 FY, Japan-Belgium collaboration program, AMAVERO (Exploring the Atmosphere of MArs and VEnus with Remote Observations: A Belgium-Japan partnership) is running. In this project, we study those aspects by collecting unique observational datasets from Belgium and Japan. Belgian side provides the data taken by European Mars orbiter Mars Express (MEx) and Trace Gas Orbiter (TGO), and Venus Orbiter Venus Express (VEx). From Japan, we provide the data taken by ground-based and space-borne telescopes with Japanese Venus Orbiter Akatsuki. Moreover, we share tools to analyze the observational datasets, and develop the numerical models of the atmospheres to interpret the observational results.

In the spring in 2017, we sent scientists from Japan to Belgium and initiated the following researches based on the exchange of young research staffs, postdocs, and graduate school students: (1) Collaboration of ground-based observation data, taken by ALMA sub-mm array, SOFIA IR airborne telescope, and MIRAHI IR heterodyne spectrometer. (2) Development of Limb retrieval code JACOSPAR for the utilization to ExoMars Trace Gas Orbiter and its test application for H2O vertical profile derived from Mars Express data. (3) Distribution and dynamics of Venusian atmosphere observed by Akatsuki IR imagers. (4) The intercomparison of MGCMs with water cycle in different approaches.

This project was generated from the long-term collaborations between Japan and European groups for Mars and Venus sciences associated with Mars Express (2003-), Venus Express (2005-2015), CrossDrive project (Collaborative Virtual Environments for Mars Science Analysis and Rover Target Planning, 2014-2016), ExoMars Trace Gas Orbiter (2016-), with groundbased and numerical simulation works. Any proposals which enhance the activities are welcomed.

月・惑星探査用飛行時間型質量分析装置の開発

今井 優介 [1]; 齋藤 義文 [2]; 齋藤 直昭 [3]; 横田 勝一郎 [2]
[1] 東大・理・地球惑星; [2] 宇宙研; [3] 産総研

Development of TOF-MS for in-situ K-Ar dating

Yusuke Imai[1]; Yoshifumi Saito[2]; Naoaki Saito[3]; Shoichiro Yokota[2]
[1] Dept. Earth & Planet. Sci, Univ. Tokyo; [2] ISAS; [3] AIST

In-situ material measurement in planetary exploration is quite important in understanding origin and evolution of the planets. For the purpose of performing in-situ elemental analysis, mass spectrometers are installed, for example, on NASA's Curiosity rover and the ESA's Rosetta spacecraft. However, we still do not have a mass spectrometer that is suitable for the future planetary exploration. Therefore, we have decided to develop a Time Of Flight Mass Spectrometer (TOF-MS) aiming at using for the future planetary exploration. The mass spectrometer that we are developing can also be used for in-situ Potassium-Argon (K-Ar) isochron dating. The instrument for Potassium-Argon (K-Ar) isochron dating is the combination of a laser-induced breakdown spectroscopy (LIBS) for the K concentration measurement and a mass spectrometer for the Ar isotopic measurement. Considering that the instrument should be installed on a planetary lander, there exists limitation on the weight, size and power etc, it is necessary to design a small size mass spectrometer which has a mass resolution capable of the Ar isotopic measurement. In order to minimize the variation of the initial position and initial energy of the ionized ions for maximizing the mass resolution, we have decided to adopt a single-stage reflectron with two-stage acceleration part. We have analytically optimized the design parameters of the reflectron. By using SIMION charged particle simulation software we have confirmed that mass resolution of our TOF-MS is high enough for Ar isotopic measurement. We are aiming to develop the multi-reflector type TOF-MS which has the potential to increase mass resolution under the size constraint. Compared to the single-reflector TOF-MS, the flight path becomes about three times longer which makes the mass resolution of the TOF-MS improved. However, as the flight length increases, variations in the flight path of the ions increase and the detection rate decreases. In order to solve this problem, we have decided to use electron lens for reducing ion dispersion. Under the same conditions as the single-reflector TOF-MS, we confirmed improvement of mass resolution about three times as compared with the single-reflector TOF-MS. We will mainly report the design of the multi-reflector type TOF-MS as well as the current status of our single-reflector TOF-MS development.

月・惑星探査におけるその場の質量分析は、月・惑星の進化を理解する上で非常に重要であると考えられる。近年の太陽系探査において、NASA の火星探査機「Curiosity」や ESA の彗星探査機「Rosetta」にはその場での元素分析を行うための質量分析器が搭載されている。しかし、ISAS では月・惑星の岩石試料の計測を目的とした質量分析器は未開発である。そこで我々は月・惑星の探査を想定した TOF-MS(Time-Of-Flight Mass Spectrometer:飛行時間型質量分析器) の開発を進めている。また、本 TOF-MS はその場 K-Ar 年代測定への応用も想定している。その場 K-Ar 年代測定により、クレーター年代学で生じる不確定性を減らし、火星の気候変動や月の進化の過程に制限を設けることができる可能性がある。

我々が TOF-MS の使用を検討しているその場 K-Ar 年代測定は、K 濃度測定を行う LIBS(Laser Induced Breakdown Spectroscopy:レーザ誘起絶縁破壊分光装置) と Ar 同位体測定行う TOF-MS から構成されている。着陸機搭載を想定すると、重量、サイズ（直径 10[cm]、全長 20[cm] 程度）、電圧（数 [kV]）などに制約があり、その条件下で Ar 同位体測定が可能な質量分解能の TOF-MS を設計する必要がある。TOF-MS において、イオンの初期位置や初期エネルギーのばらつきを抑え、高い質量分解能を得るために、我々はイオンを反射させるリフレクター方式の TOF-MS を採用し、先行研究で試作した試験モデルの改良を進めている。先行研究で試作した試験モデルでは、イオン源で生成したイオンの加速を行うイオン加速部は 1 段、リフレクトロンのイオン反射部は 2 段の構成であったが、最適な設計を目指した性能比較試験を行うため、本研究のモデルでは、加速部を 2 段、反射部を 1 段の構成に変更した。イオンの初期位置や初期エネルギーのばらつきに依らず飛行時間が収束することを条件にして求めた解析解から、装置の寸法や印加電圧等のパラメータを設定した。これらのパラメータを基に粒子シミュレーションソフト SIMION を用いて Ar イオンの飛行時間と検出器への到達率を求め、前述のサイズ、印加電圧の条件において、Ar 同位体計測に必要な質量分解能が達成可能である事を確認した。その上で、限られた容積で質量分解能を向上させることを目指して、反射を複数回行うマルチリフレクター型の TOF-MS の開発を目指している。それまでの一回反射の TOF-MS と比べ、3 回反射のマルチリフレクター型の TOF-MS はイオンの飛行時間が約 3 倍となり、分解能が向上する。しかし、飛行時間が増加するとイオンの飛行経路のばらつきが増え、検出率が低下する。そのため、レンズを用いてイオンの飛行経路のばらつきを抑える設計とした。一回反射の TOF-MS と同様に SIMION を用いて Ar イオンの飛行時間と検出器への到達率を求め、前述のサイズ、印加電圧の条件において、一回反射の TOF-MS と比べ約三倍の質量分解能の向上を確認した。

本発表では、主にマルチリフレクター型の TOF-MS の設計について報告する他、Ar 同位体計測用の 1 回反射型 TOF-MS の開発状況を報告する。

新規開発ファイバ分光装置による金星紫外観測

山田 学 [1]; 鍵谷 将人 [2]; 山崎 敦 [3]
[1] 千葉工大・惑星探査研究センター; [2] 東北大・理・惑星プラズマ大気研究センター; [3] JAXA・宇宙研

Observation of Venus cloud tops with new developed fiber IFU

Manabu Yamada[1]; Masato Kagitani[2]; Atsushi Yamazaki[3]
[1] PERC/Chitech; [2] PPARC, Tohoku Univ; [3] ISAS/JAXA

Venus is covered with thick clouds made of sulfuric acid on the whole planet, and in visible light it has poor features. On the other hand, in ultraviolet light of the wavelength from 200 to 500 nm, it has clear features showing high speed wind blowing so called “super rotation”. From 200 nm to 320 nm, absorption can be well explained by SO_2 existence, but absorber have not yet identified at wavelengths longer than 320 nm. Although previous observations were carried out by using only one band with a center wavelength of 365 nm, it may be possible to clarify the nature and number of this unknown absorber by comparing the difference of the spatial structure between different wavelengths.

We have developed a spectral imager with new developed integral field unit (IFU).Such an instrument can produce data cube that includes spatial distribution with spectral information made by unknown absorber in cloud top of Venus. The observation of Venus with the spectral imager was made at Haleakala Observatory in Hawaii from 21 to 26 June 2017. We employed the spectral imager coupled to a 60cm reflective Coude telescope and succeeded obtain data cube from near 330nm to 450nm. We report the method of analysis using the data cube and a preliminary result from the observation.

金星は全球が分厚い硫酸の雲におおわれており、可視光で見る金星は特徴に乏しい。一方、金星の上層雲には太陽放射のうち 200nm から 500nm の波長を吸収する物質が含まれており、高速の風が吹き荒れているさまを見せる雲の模様を作り出す。200nm から 320nm は SO_2 による吸収で良く説明できるが、320nm より長い波長での吸収を担う物質はいまだ同定されていない。これまで実施された観測は主に 365nm を中心波長とする単バンドしか使っていなかったが、異なる波長の空間構造の違いを比較することでこの非同定吸収物質の性質や数を明らかにできる可能性がある。

我々はファイバアレイを用いた分光イメージャを開発してきた。分光イメージングは同時に連続した波長で二次元の画像を取得でき、金星の非同定吸収物質による吸収を観測するのに利用できる。ハレアカラ観測所の 60T 望遠鏡に新たに開発した分光イメージャをとりつけ、2017 年 06 月 21 日から 6 月 26 日までの観測を実施した。およそ 330nm から 400nm までの分光データを取得することに成功した。本発表では、二次元分光データの解析手法および、紫外付近の各波長でみた金星雲層空間構造の初期解析結果を示す。

Comparison of Akatsuki radio occultation experiments with thermal infrared image obtained by LIR

Tetsuya Fukuhara[1]; Hiroki Ando[2]; Masahiro Takagi[3]; Takeshi Imamura[4]; Makoto Taguchi[5]; Tetsuya Fukuhara Akatsuki RS/LIR team[6]

[1] Rikkyo Univ.; [2] Kyoto Sangyo University; [3] Faculty of Science, Kyoto Sangyo University ; [4] The University of Tokyo; [5] Rikkyo Univ.; [6] -

Venus climate orbiter called Akatsuki which failed to be inserted into Venus orbit in 2010 has been successfully re-orbited on December 2015, and instruments onboard the spacecraft has finally started observation of Venus. The longwave infrared camera (LIR) detects thermal emission with wavelengths of 8 - 12 micron from Venus disk regardless of day or night side, and represents horizontal distribution of the brightness temperature at the cloud top. LIR has continuously archived more than eight thousands images without serious fault for two Venusian years. The radio occultation experiment termed Radio Science (RS) retrieves the atmospheric pressure, the temperature, the sulfuric acid vapor mixing ratio, and the electron density. Akatsuki mainly probes the low and middle latitude regions with the near-equatorial orbit in contrast to the previous radio occultation experiments such as Venus Express in a polar orbit. Vertical temperature profiles by RS observation were successfully obtained at altitude of 38 - 85 km by July 2017. On the other hand, the cloud-top altitude observed by LIR would be roughly ˜65 km in accordance with the contribution function of Venus atmosphere simulated under situation of typical cloud distribution. However, it is difficult to retrieve an actual cloud-top altitude except for the comparing with the vertical temperature profile synchronously observed. LIR images have been synchronously acquired with most of RS observations as a basic strategy for Akatsuki observation. Thus, we could acquire several data sets in which LIR and the radio occultation experiments observed same region. The data set covered low latitude in the morning and southern mid latitude in the midnight. Since LIR image included background bias depending on baffle temperature at observation, it was canceled by using deep-space images acquired on orbit with different baffle temperature. Furthermore, limb-darkening effect which is generally seen in the thermal infrared images is considered when absolute brightness temperature is estimated from LIR observation. Thus, the cloud-top altitudes in the LIR images were deduced by the comparison with the RS observations. It showed some atmospheric features depending on the local time and latitude. A variability which is caused by thermal tides at the cloud top layer may be included. We are carefully considering the result obtained by our observation.

あかつきIR1カメラから明らかにする金星雲変動

高木 聖子 [1]; あかつき IR1 チーム 岩上　直幹 [2]
[1] 東海大、TRIC; [2] -

The variation of Venus cloud observed by IR1 camera onboard AKATSUKI

Seiko Takagi[1]; Iwagami Naomoto AKATSUKI IR1 team[2]
[1] Tokai Univ. TRIC; [2] -

Near infrared (0.986 um) dayside image of Venus has taken by solid state imaging (SSI) of the Galileo spacecraft (NASA). It appears almost flat, there are some small-scale features with a contrast of 3 % [Belton et al., 1991]. In Takagi et al.(2011), it may be calculated that the source of the contrast of the order of 3 % in near infrared Venus dayside image is due to variation in the cloud optical thickness.

On December 7, 2015, AKATSUKI (JAXA) approached Venus and the Venus orbit insertion was successful. After the Venus orbit insertion, many 0.90 um Venus dayside images were taken by the 1 um near infrared camera (IR1) onboard AKATUSKI.

In this study, patterns of cloud optical thickness variation are investigated from 0.90 um Venus dayside images taken by IR1 and radiative transfer calculation. Furthermore, we will examine Venus meteorological some change contribute to cloud variation.

大気の窓領域である近赤外波長を用いた金星昼面撮像観測では、雲の光学的厚さの増減を金星表面のコントラストとしてとらえることができる [Takagi et al., 2011]。木星探査機 Galileo/SSI (NASA) により得られた金星昼面近赤外画像 (0.986 um) では、金星表面のコントラストはわずか 3 %と示されている [Belton et al., 1991]。

金星探査機あかつき (JAXA) は、2015 年 12 月に金星周回軌道投入に成功した。搭載された近赤外カメラ IR1 は、軌道投入後約 1 年間、波長 0.90 um における金星昼面撮像を行い、かつて木星探査機 Galileo/SSI が得たものと整合的な昼面画像を多数取得している。

本研究では、IR1 カメラが取得した 0.90 um 昼面放射輝度および放射輸送計算を用いて、雲の光学的厚さの変動傾向を全球的に知る。また、雲の変動に寄与する金星の気象変化について考察する。

金星大気重力波イベントのALMA/金星探査機「あかつき」の連携観測プロジェクトの進歩報告

青木 亮輔 [1]; 徳田 一起 [2]; 前澤 裕之 [3]; 田口 真 [4]; 福原 哲哉 [5]; 佐川 英夫 [6]; 西合 一矢 [7]; 佐藤 隆雄 [8]; Lee Yeon Joo[9]; 今村 剛 [10]; 中村 正人 [11]
[1] 大府大・理・物理; [2] 大阪府立大/国立天文台; [3] なし; [4] 立教大・理・物理; [5] 立教大・理; [6] 京都産業大学; [7] 国立天文台; [8] 宇宙研; [9] JAXA/ISAS; [10] 東京大学; [11] 宇宙研

Synergetic observations of bow-shaped structures on Venus with ALMA and Venus Climate Orbiter "Akatsuki"

Ryosuke Aoki[1]; Kazuki Tokuda[2]; Hiroyuki Maezawa[3]; Makoto Taguchi[4]; Tetsuya Fukuhara[5]; Hideo Sagawa[6]; Kazuya Saigo[7]; Takao M. Sato[8]; Yeon Joo Lee[9]; Takeshi Imamura[10]; Masato Nakamura[11]
[1] Physical Science, Osaka Prefecture University; [2] Osaka Prefecture University/NAOJ Chile Obeservatory; [3] none; [4] Rikkyo Univ.; [5] Rikkyo Univ.; [6] Kyoto Sangyo University; [7] NAOJ; [8] ISAS/JAXA; [9] JAXA/ISAS; [10] The University of Tokyo; [11] ISAS,JAXA

We are monitoring the carbon monoxide (CO) in the middle atmosphere of the terrestrial planets in the solar system using our ground-based 10 m-radio telescope, and we found that the Venusian atmosphere has short-term changes of CO mixing ratio at an altitude of about 80 km. In December 9, 2015, the longwave infrared (LIR; 10 micrometre) band camera on board Venus Climate Orbiter "Akatsuki" (JAXA), which traces the temperature of the cloud top at around 65 km altitude, discovered the bow-shaped structures generated by atmospheric gravity waves on Venus. The huge bow-shaped structures appear on the western region of Aphrodite Terra with high reproducibility. Such dynamical and convective fluctuations induced by atmospheric gravity waves may cause the short-term variations of CO mixing ratio in the Venusian middle atmosphere.

For better understandings of three dimensional chemical and dynamical network links between the lower and upper atmosphere via H^2SO_4 clouds of Venus, in November 20 and December 1, 2016 and May 14, 2017 we carried out the synergetic observations with Akatsuki and ALMA toward the western highland of Aphrodite. ALMA executed the observations of ^{12}CO and ^{13}CO line at 200 GHz band (Band 6) and ^{12}CO, ^{13}CO, HDO, SO, and SO_2 line at 300 GHz band (Band 7). In Dec. 1, 2016 the LIR camera of Akatsuki at the perihelion succeeded to shoot the images of a part of the bow shaped structure. The spatial resolutions for the Band 7 and Band 6 are 0.27 and 0.40 arcsecond under the C40-4 antenna configuration, respectively, which allow us to resolve the bow-shaped structure spatially. ALMA in Cycle 4 consists of fifty 12m antenna arrays and Atacama compact arrays (twelve 7m antenna arrays and four 12m single dish antennas) to provide a good coverage of the UV plane. Each synergetic observation was carried out within a single day synchronizing the all antennas because the dynamical patterns induced by high speed winds on Venus change quickly. Now the delivery of the quality assurance (QA2) data of ALMA has gradually started.

In this conference, we will talk about the synergetic mission with Akatsuki and ALMA, and the current status of the data analysis.

金星探査機「あかつき」とアタカマ大型ミリ波サブミリ波干渉計 (ALMA) を用いた金星の連携観測について報告する。

我々は 10 m 電波望遠鏡を用いて太陽系地球型惑星の大気の監視を推進しており、金星の高度 80 km 付近の一酸化炭素の全球平均が短期スケールで変動する様子を捉えている。2015 年 12 月、「あかつき」衛星 (JAXA) の中間赤外カメラ (LIR：波長 10 μ m)(高度 65 km 付近の雲頂温度を観測) が巨大な弓状構造を捉えることに成功した。この弓状構造はアフロディーテ大陸で発生する大気重力波が作り出すと考えられている。一酸化炭素の変動は、こうした大気重力波イベントが化学物質の輸送状態にもたらす変化として見えている可能性もある。「あかつき」衛星の赤外線や紫外線のセンサーは低層大気から雲頂にかけての温度や CO、SO_2 などの存在量・速度場を捉えることができ、一方で ALMA のミリ波・サブミリ波のヘテロダイン分光観測では、高度 75 km から 110 km の CO や HDO、SO_2 などの微量分子を捉えることができる。そこで我々は、「あかつき」衛星と ALMA の連携観測を実施し、大気重力波イベント時とイベントの無い時期について、これら分子種の 3 次元分布（高度・緯度・経度方向など）を観測し、金星のダイナミクスと大気化学反応ネットワークのリンクに迫る。

これまでに 2016 年 11 月 20 日、12 月 1 日、2017 年 5 月 14 日の 3 回に渡り「あかつき」衛星と ALMA の連携観測を実施した。11 月 20 日はアフロディーテ大陸西部が夕方頃にさしかかり惑星大気重力波が発生する時期と予想されたが、この時は近金点での LIR カメラの撮像の範囲で弓状構造を確認することはできなかった。一方 12 月 1 日は、弓状構造の一部を連続撮像することに成功した。5 月 14 日は、アフロディーテ大陸西部が明け方に差し掛かる時期であり、重力波が発生しない reference case として観測を行った。ALMA の 50 台の 12 m 望遠鏡群と 12 台の 7 m 望遠鏡群の干渉計システム、4 台の 12 m 単一望遠鏡により UV 空間をカバーするが、通常これらアンテナ群は独立にオペレーションされる。しかし金星の高速の輸送により大気の時間変動が早いことから、すべての望遠鏡を連動させる同時観測を試み成功した。12 月 1 日は、ALMA は C40-4 の配列で、金星の 16 秒角の視直径に対して空間分解能は 300 GHz 帯 (^{12}CO,^{13}CO,HDO,SO,SO_2) で 0.27 秒角、200 GHz 帯 (^{12}CO,^{13}CO) で 0.40 秒角となっているので、弓状構造を十分空間的に分解し、かつ resolve-out の問題を回避して広がりを抑えることができるアンテナ配置となっている。現在 ALMA の QA2 データ配信が始まっており、本発表ではこれらの観測と解析状況について報告する。

金星大気大循環モデルによる3次元金星雲分布および大規模運動への結合の研究

秋葉 丈彦 [1]; 黒田 剛史 [2]; 高橋 正明 [3]; 池田 恒平 [4]; 笠羽 康正 [5]; 寺田 直樹 [6]; 鎌田 有紘 [7]
[1] 東北大・理・地物; [2] NICT; [3] 東大・大気海洋研; [4] 環境研; [5] 東北大・理; [6] 東北大・理・地物; [7] 東北大・理・地物

Study of the Venusian cloud distributions and their link to the global dynamics: a Venusian general circulation model

Takehiko Akiba[1]; Takeshi Kuroda[2]; Masaaki Takahashi[3]; Kohei Ikeda[4]; Yasumasa Kasaba[5]; Naoki Terada[6]; Arihiro Kamada[7]
[1] Geophysics,Tohoku Univ.; [2] NICT; [3] AORI, Univ. of Tokyo; [4] NIES; [5] Tohoku Univ.; [6] Dept. Geophys., Grad. Sch. Sci., Tohoku Univ.; [7] Geophysics, Tohoku Univ.

Venus is covered with sulfuric acid clouds in about 48 and 70 km altitude, and the radiative effects of clouds may impact on the and atmospheric motion like superrotation (very fast zonal wind than rotation speed). To understand the mechanism, we have developed a Venus General Cirulation Model (VGCM) which takes the formation and advection of clouds into account based on CCSR/NIES/FRCGC MIROC. The model has a radiative transfer scheme which realistically calculate the effects of sulfuric acid clouds and molecules (Ikada, 2011), and the implementations of the cloud processes (condensation/evaporation of sulfuric acid vapor/clouds, advection and gravitational sedimentation of clouds) and chemical processes related to sulfuric acid vapor have been implemented (Itoh, 2016). Itoh (2016) suggested that sulfuric acid vapor is lifted upward into the upper cloud layer in the equatorial atmosphere and change into sulfuric acid clouds there followed by the transport poleward by meridional circulation, but the radiative effects of clouds did not reflect the simulated cloud distributions, considering the horizontally uniform cloud distributions with observed vertical distributions for each mode (Haus and Arnold, 2010)

In this study, we have improved the radiative processes of sulfuric acid clouds in theVGCM to interact with the simulated cloud distributions. Now we are able to calculate the radiative effects of clouds from the simulated distributions at each time step. The effects of unknown UV absorber, which is considered as the one of factors which make the heating in cloud layer, have been considered by increasing the absorptions of UV-visible wavelengths relating to the optical thickness of mode 1 sulfuric acid cloud in the upper cloud layer (Tomasko et al., 1980; Crisp,1986). It is the first trial on the VGCM which allows to understand the interactions between radiative effect of the clouds and the cloud distribution in the both aspects of atmospheric circulation and cloud formation (hereafter Simulation A). The simulation is started from the equilibrium states of wind, pressure, and temperature fields simulated by Itoh (2016) and horizontally uniform cloud distributions with observed vertical distributions shown by Haus and Arnold (2010). The results are compared with the one of Itoh (2016) (hereafter Simulation B).

In Simulation A, zonal wind with the velocity of about 50 m/s was shown above equator in 50˜65 km altitude. Comparing solar heating from each Simulation, the heating layer above 65 km altitude which exists in Simulation B was not made in Simulation A, in which the heating by solar radiation reached to downward by ˜10 km more, which resulted in the lifting of mode 1 clouds upward. It may be explained that the solar radiation reaches and clouds get heated more deeply in Simulation A, and then the thermal tide due to this heating accelerates zonal wind. In both Simulations A and B, zonal winds of 50 m/s in Simulation A and 100 m/s in Simulation B, respectively, were seen above mid-latitude and 65˜70km altitude, which may support the theoretical study that meridional circulation excites the zonal wind.

Quantitatively, zonal wind velocity in Simulation A was weak, about a half of the observed data in low- and mid-latitudes in the cloud layer. The meridional circulation in Simulation A was weaker than in Simulation B, which may result that the cloud top altitude in Simulation A was lower than that in simulation B for 3 km and the cloud total mass at cloud top (about 65km altitude) in Simulation A was about a half of that in Simulation B, making more sulfuric acid vapor below the cloud layer. The results in Simulation A suggest the relationship among weaker meridional circulation, less heating and enhancement of the sedimentation and evaporation of clouds, which may be because of the wrong evaluation of the effects of unknown UV absorber.

金星の雲は高度約48 -70kmで全球を覆っており、大規模循環に放射効果等を介して影響を与えうる。我々はCCSR/NIES/FRCGC MIROCをもとに開発された金星大気大循環モデル (以降 VGCM) に硫酸雲の生成・消滅過程を加え、金星雲の自律的再現およびあかつき探査機観測との比較を目指した研究を行っている。このVGCMは金星大気における現実的な大気分子及び硫酸雲の放射効果を計算可能な放射スキームを実装しており (池田, 2011)、これに硫酸雲の凝縮／蒸発、重力沈降過程を組み込むことで、赤道付近での硫酸蒸気の上昇と雲の凝結生成、雲の子午面循環による中・高緯度域への輸送といった硫酸雲層の維持・循環の再現をみている (伊藤, 2016)。本研究では、本コードに対して凝縮／蒸発と移流による雲分布変化の放射過程への反映を試みた。伊藤 (2016) では Haus and Arnold (2010) 雲モデルの硫酸雲混合比を基に時空間で固定された光学的厚さを用いて放射効果を計算していたが、本研究ではそれぞれの時間ステップで出力される雲の混合比を基に計算を行えるよう改良し、これに基づいた雲の放射効果を計算するスキームとした。雲層内の加熱に大きく起因すると考えられているUV absorberの効果については、雲層上部のモード1の硫酸雲の光学的厚さに対応し、紫外～可視領域の吸収を強めることで評価する（Tomasko et al., 1980; Crisp,1986）、自律的な雲過程と放射計算への反映を行うシ

ミュレーションは初であり、雲の生成・消滅・輸送に伴う雲分布の変動が放射に影響を与え、これが大気循環にフィードバックされる一連の機構を再現しうる (以後計算 A とする)。初期状態として、平衡状態の風速・気温場に観測に基づく鉛直分布に基づいた水平一様の雲及び硫酸蒸気分布を与えた。

本講演では、放射計算に雲分布を反映させていない伊藤 (2016) の結果 (以後計算 B とする) との、東西風速度場の分布の違い、雲分布の違いを評価する。東西風速度場を比較すると、計算 A において、高度 50〜65 km (雲層下層〜中層) の赤道上空で風速 50 m/s 程度の強く吹くセルが出現した。太陽放射による加熱率を比較すると、計算 B で発生していた高度 65 km での加熱層（最大 8.5 K/day）が現れず、加熱の深さを見ると計算 A のほうが雲による太陽光吸収によってより 10 km 程度下層まで加熱されている。この結果は雲分布を放射に対応させることにより、モード 1 の雲が上層に運ばれる結果を反映したと考えられる。赤道上での東西風のセルとこの加熱層の位置関係から、この加熱の日周期性による熱潮汐波が東西風を加速させる理論を支持していると推測される。 また、計算 A・B とも高度 65〜70 ☒ (雲層中層〜上層) 中緯度にて強く吹く（計算 A で 50m/s、計算 B で 100m/s）セルが確認され、子午面循環によって東西風が加速される理論も支持する結果となった。

定量的には、計算 A で生成された東西風の強さは赤道上・中緯度上空のセルでいずれも 50 m/s と観測値の半分程度の大きさとなっていた。計算 A では計算 B と比べて子午面循環が弱く、 そのため雲の分布をみると、計算 A では雲頂が計算 B より高度で約 3 km 下がっており、また雲の全体量を見ると、計算 A の雲は雲頂 (高度 65 km) で 計算 B の半分となっており、その分は雲層より下の層での硫酸蒸気として安定して存在していた。このことから雲層内の子午面循環が弱まることに関連して加熱の弱化と雲の蒸発・沈降が起こっていることが考えられ、その原因としては加熱の要素の一つと考えられている unknown UV absorber の効果 が正しく計算されていない可能性がある。

A numerical simulation of the large-scale stationary gravity waves in the Venus atmosphere

Takeru Yamada[1]; Takeshi Imamura[2]; Tetsuya Fukuhara[3]; Makoto Taguchi[4]
[1] Physics, Rikkyo Univ.; [2] The University of Tokyo; [3] Rikkyo Univ.; [4] Rikkyo Univ.

The Longwave Infrared Camera onboard Akatsuki observed a bow-shaped stationary temperature feature on December 7, 2015 [Fukuhara et al., 2017]. It extended from the northern polar region to the southern polar region across the equator, and stayed near the evening terminator for four earth days at least in contrast to the background wind speed of about 100 m s^{-1} at the cloud-top level. The prominent feature disappears in the different local time. A simple numerical simulation suggested that the stationary feature may be caused by a gravity wave propagated from near the surface. However, conditions the wave propagation is permitted are still unknown. Hence, we attempted to reproduce the wave propagation in the numerical simulation, and investigated a contribution of the Venus cloud layer at the altitude of 45 - 55 km where the static stability is relatively low.

A nonlinear primitive equation model in spherical geometry was used based on Imamura [2006]. The vertical log pressure level was divided to 100 sections from 5 km (66.65 x 10^{5} Pa) to 109 km (66.65 x 10^{-1} Pa). The grids of longitude and latitude are 3 degrees. The basic zonal wind, which increases monotonically from 1.3 m s^{-1} at 5 km to 94 m s^{-1} at 69 km, was given based on the Schubert and Walterscheid [1984]. Radiative transfer was represented by time constant with Newtonian cooling based on Crisp. [1989]. We gave a forced temperature disturbance of 2 K on the bottom boundary with a Gaussian-shaped function with a half width of about 6 degree on the equator. Thus, the bow-shaped stationary temperature feature at the cloud-top layer was reproduced in the simulation. When the static stability at the cloud layer decreased to nearly zero from the nominal value, the amplitude of the temperature at the bow shape decreased. The static stability at the cloud layer may be one of the conditions of the bow-shaped structure appearing at the cloud top.

大気大循環モデルを用いた地球気候の太陽定数依存性に関する数値実験

松田 幸樹 [1]; 石渡 正樹 [2]; 高橋 芳幸 [3]; 林 祥介 [4]
[1] 神戸大・理; [2] 北大・理・宇宙; [3] 神戸大・理・惑星; [4] 神戸大・理・地惑

Numerical experiments on dependence of the Earth's climate on the solar constant by the use of a GCM

Koki Matsuda[1]; Masaki Ishiwatari[2]; Yoshiyuki O. Takahashi[3]; Yoshi-Yuki Hayashi[4]
[1] Science, Kobe Univ; [2] Cosmosciences, Hokkaido University; [3] Department of Planetology, Kobe Univ.; [4] Earth and Planetary Sciences, Kobe University

A solar constant is one of important parameters causing diversity of the planetary climate. For example, in previous studies by the use of one-dimensional energy balance models (EBMs), the planet's climate was studied (e.g., Budyko, 1969). These studies showed globally ice-covered states, partially ice-covered states, and ice-free states appeared as changing the solar constant. In addition, the existence of multiple states with a solar constant was also shown. A planetary climate was also studied by the use of general circulation models (GCMs) (e.g., Ishiwatari et al., 2007). This study confirmed the three states, which had been shown by EBMs in previous studies, appear in GCMs. Moreover, the existence of the runaway greenhouse state, which had not been shown in EBMs, was confirmed. In the previous studies, however, effects of land-ocean distribution and atmospheric composition were not considered. In this study, we assume the atmospheric composition and the land-ocean distribution same as those of the present Earth, and show dependence of the Earth's climate and some physical variables on the solar constant.

In the experiments, we use a planetary atmosphere general circulation model, DCPAM5. Dynamics process is calculated by solving the primitive equations with a spectral method. For radiative process, the Earth radiative model by Chou et al. (2001) is used. Condensation process is represented by Relaxed Arakawa-Schubert scheme (Mootrhi and Suarez, 1992). Vertical turbulent mixing process is represented by the Mellor and Yamada (1982) level 2.5 scheme. Cloud process is represented by forecasting mixing ratios of a cloud ice and a cloud water, with considering advection, turbulent mixing, production by condensation, and loss with fixed time constants. On the land surface, the surface and soil temperatures are calculated by a soil heat conduction model, and the soil moisture is calculated by a bucket model (Manabe, 1969). For the ocean, a slab ocean with depth of 60 m is assumed. The surface albedo of the ocean is set to 0.6 where the surface temperature is below 271.15 K, while it is set to 0.1 where the surface temperature is above 271.15 K. We use data of ETOPO1 (Amante and Eakins, 2009) and Matthews (1983, 1984, 1985) for topography and surface albedo distribution, respectively. As for ozone distribution, we use a zonal mean value of climatology of CMIP5 simulations. Resolution used in this study is a longitude-latitude grid size of about 5.6 degrees, and 26 vertical levels. By the use of the model, we performed 15 experiments with various solar constants and two initial conditions to explore dependence of the Earth's climate on the solar constant. The given solar constant ranges from 1100 Wm^{-2} to 1500 Wm^{-2}, and two initial conditions are isothermal atmospheres of 280 K or 200 K.

The results of the experiments confirmed existence of globally ice-covered states, partially ice-covered states, and ice-free states, that had been discovered by previous studies by the use of EBMs and GCMs. Moreover, we found the climate regime diagram is different between in the southern hemisphere and in the northern hemisphere, because of the difference in the land-ocean distribution. We examined the change of meridional circulation as changing the solar constant. As the solar constant increases, the upward flow region of meridional circulation moves southward, and the strength of meridional circulation does not increase monotonically. The strength of meridional circulation has the maximum when a planet is in a partially ice-covered state in both hemispheres. Moreover, examination of the strength of meridional circulation in a partially ice-covered state show, as the solar constant increases, the circulation becomes week in the southern hemisphere, but become strong in the northern hemisphere.

As a next step, we will confirm the existence of a runaway green house state, and a large ice cap and small ice cap instabilities.

惑星気候の多様性を考える上で, 太陽定数は重要なパラメータの一つである. 南北 1 次元エネルギーバランスモデル (EBM) を用いた先行研究 (例えば, Budyko, 1969) において, 惑星気候の太陽定数依存性が調べられた. それによると, 太陽定数に応じて全球凍結状態, 部分凍結状態, 氷なし状態という 3 つの状態が現れること, および, ある太陽定数に対して複数の状態 (多重解) が解となることが示された. また, 大気大循環や惑星放射の射出限界を陽に計算できる大気大循環モデル (GCM) を用いた先行研究においても, 惑星気候の太陽定数依存性が調べられ, EBM で得られた 3 つの状態や多重解が現れることが確認された (例えば, Ishiwatari et al., 2007). さらに, GCM を用いた研究では, EBM では見られなかった暴走温室状態が存在することが確認された. 上記で挙げた 2 つの先行研究では, 海陸分布や大気組成の影響を考慮していない. 本研究では, 地球の海陸分布と大気組成を考慮した大気大循環モデルを用いて, 地球気候の太陽定数依存性を明らかにし, 様々な物理量の太陽定数依存性について考察する.

実験には惑星大気大循環モデル DCPAM を用いる. 力学過程は, プリミティブ方程式系をスペクトル法を用いて解くことで計算される. 放射過程は, Chou et al. (2001) 等による地球放射モデルを用いる. 凝結過程は, Relaxed Arakawa-Schubert (Moorthi and Suarez, 1992) で表現される. 鉛直乱流混合過程は, Mellor and Yamada (1982) level 2.5 により表現される. 雲は, 移流, 乱流混合, 凝結による生成, 定数時定数による消滅を考慮して雲水・雲氷混合比を予報することで, 表現される.

陸面では, 土壌熱伝導モデルにより土壌温度を計算し, バケツモデル (Manabe, 1969) により土壌水分を計算する. 海は, 60 m の深さを持つ板海として取り扱う. 海表面アルベドは, 海表面温度が 271.15 K よりも低い時には 0.6 とし, 271.15 K より高い時には 0.1 とする. 地形データは ETOPO1 (Amante and Eakins, 2009) を使用する. 陸面アルベド分布は Matthews (1983, 1984, 1985) によるものを使用する. オゾン分布は CMIP5 設定の気候値の東西平均を使用する. 本研究で行った実験で用いた解像度は, 緯度経度格子間隔が約 5.6 度であり, 鉛直方向の大気層数が 26 である. このモデルを用いて, 地球の気候の太陽定数依存性を調べるために, 様々な太陽定数と二つの初期条件を与えて 15 個の実験を実施した. 与えた太陽定数の範囲は 1100 Wm^{-2} から 1500 Wm^{-2} であり, 初期条件は 280 K および 200 K の等温大気である.

上記の設定で実験を行ったところ, 全球凍結状態, 部分凍結状態, 氷なし状態が存在することが確認された. また, 地球の海陸分布を考慮すると, 気候レジーム図が南北半球で異なることがわかった. また, 太陽定数の変化に伴う子午面循環の変化について調べた. 太陽定数が増加すると, 子午面循環の上昇域が南方向へ移動する. 子午面循環の強度は単調増加せず. 南北半球ともに部分凍結状態が最大となる. 部分凍結状態の中で子午面循環の強度を比較すると, 南半球では太陽定数大きくなるにつれて弱くなるが, 北半球では太陽定数が変化してもあまり変化しない.

今後は, 暴走温室状態の有無や大氷冠不安定や小氷冠不安定の有無を確認する予定である.

火星大気熱赤外センサデータの4次元格子化による解析と可視化の環境整備

野口 克行 [1]; 上田 真由 [2]; 林 寛生 [3]
[1] 奈良女大・理・情報; [2] 奈良女・理・環境; [3] 富士通 FIP

4D Gridding of MRO-MCS Data for Easier Analysis and Visualization

Katsuyuki Noguchi[1]; Mayu Ueda[2]; Hiroo Hayashi[3]
[1] Nara Women's Univ.; [2] NWU; [3] Fujitsu FIP

We present a method to process data obtained by Mars Climate Sounder (MCS) onboard Mars Reconnaissance Orbiter (MRO) in order to simplify analysis and visualization of the MRO-MCS data, which consists of a huge number (> 1,000,000) of vertical profiles of atmospheric physical parameters retrieved. The method includes two steps; the first step is the format conversion of original text data into netCDF (Network Common Data Form), and the second step is 4D gridding of the data to be available for use by various analysis tools. Results of visualization of the data by Grid Analysis and Display System (GrADS) will be presented. We also show preliminary results of the analysis on the relation among temperature, water ice clouds and dust observed by MRO-MCS.

本講演では、米国の火星探査機 Mars Reconnaissance Orbiter（MRO）搭載の Mars Climate Sounder（MCS）による気温、ダスト、水氷雲等の観測データの利用拡大を目的としたデータ解析環境整備について紹介する。このデータは NASA の Planetary Data System（PDS）から公開されているが、観測プロファイル数が膨大（100 万本以上）でデータ量が非常に大きく、1 つのテキストファイルに数時間毎の複数観測プロファイルが含まれているためにデータ構造が取り扱いにくい。そこで、まずデータフォーマットを Network Common Data Form（netCDF）に変換し、さらに地球の大気・海洋科学分野で広く使われている Grid Analysis and Display System（GrADS）で扱えるようにデータの 4 次元格子化を行うことで、データの可搬性・可読性を向上させるとともにデータ解析と可視化を容易にした。講演では、このようにして整備したデータを利用した初期解析結果についても紹介する。

Global structure of Mercury’s magnetosphere and heavy ion precipitation on Mercury

Manabu Yagi[1]; Kanako Seki[2]; Yosuke Matsumoto[3]; Dominique Delcourt[4]; Francois Leblanc[5]
[1] AICS, RIKEN; [2] Dept. Earth & Planetary Sci., Science, Univ. Tokyo; [3] Chiba University; [4] LPP, Ecole Polytechnique, CNRS; [5] LATMOS-IPSL, CNRS

From Mariner 10 and MESSENGER observations, Mercury’s magnetosphere is thought to be a miniature of the Earth’s magnetosphere. While these two magnetospheres have several characteristics in common, some critical differences are also evident. First, there is no atmospheric layer, but only tenuous exosphere. Second, center of dipole field is shifted to northward about 485km, which is equivalent to 0.2 Mercury’s radius. Kinetic effects of heavy ions will also be important in Mercury’s magnetosphere, because Mercury’s magnetosphere is relatively small compared to the large Larmor radii. Trajectory tracings is one of the methods to estimate the contribution of heavy ions which originate from the exosphere, while the results of the simulation are quite sensitive to the electric and magnetic field. Hence, it is important to provide a realistic field model in the trajectory tracings. In order to construct a large scale structure, we developed a MHD simulation code, and adopted it to the global simulation of Mercury’s magnetosphere. In this study, we performed MHD simulations with various kinds of solar wind parameters to investigate the interaction between solar wind plasma and offset dipole of Mercury. IMF conditions comes from Parker Spiral which has strong Bx and By component at the Mercury’s orbit, and fluctuations are added in By and Bz components. In the results of MHD simulations, global configuration of magnetosphere shows strong north-south asymmetry due to dipole offset and IMF-Bx in addition to dawn-dusk asymmetry which comes from IMF-By. IMF Bx also affects to the intensity ratio of north and south cusp pressure, while IMF By component ’twist’ the cusp region to longitudinal direction. In the presentation, we will also discuss the heavy ion distribution and precipitation on Mercury obtained by trajectory tracings of test particles. The identification of the cusp region and heavy ion precipitation region is important not only for the understanding of magnetospheric physics itself, but also making a proposal to the observational plan of spacecraft such as Bepi-Colombo.

弱磁場天体の小型磁気圏形成に関する全粒子シミュレーション

沖 知起 [1]; 臼井 英之 [2]; 寺田 直樹 [3]; 関 華奈子 [4]; 加藤 雄人 [5]; 三宅 洋平 [6]; 八木 学 [7]
[1] 神大・システム・計算; [2] 神戸大・システム情報; [3] 東北大・理・地物; [4] 東大理・地球惑星科学専攻; [5] 東北大・理・地球物理; [6] 神戸大学; [7] AICS, RIKEN

Full PIC simulation on the formation of small magnetosphere of a weakly magnetized body

Satoki Oki[1]; Hideyuki Usui[2]; Naoki Terada[3]; Kanako Seki[4]; Yuto Katoh[5]; Yohei Miyake[6]; Manabu Yagi[7]
[1] Kobe Univ.; [2] System informatics, Kobe Univ; [3] Dept. Geophys., Grad. Sch. Sci., Tohoku Univ.; [4] Dept. Earth & Planetary Sci., Science, Univ. Tokyo; [5] Dept. Geophys., Grad. Sch. Sci., Tohoku Univ.; [6] Kobe Univ.; [7] AICS, RIKEN

The objectives of this research is to study a small magnetosphere formed by the interaction between a weakly magnetized small body and the solar wind, to understand the formation of each region of the magnetosphere, and to examine the dependency of each plasma phenomena on the intensity of the intrinsic magnetic field by performing three-dimensional particle simulation. Based on the previous observations, it is well known that Mercury, the magnetic dipole moment of which is around 1/2000 of that of the Earth, has a small (i.e. 1/20 of that of the Earth) magnetosphere. The Mercury magnetosphere has been studied by MHD and hybrid particle simulations so far. However, there is still room for argument of kinetics including electron dynamics on the formation of magnetosphere. In this study, we focus on the parameters of Mercury environment and investigate the kinetic phenomena in the small magnetosphere by performing full particle simulations.

In the simulation model, we have a small body with a small magnetic dipole moment, and introduce the magnetized plasma flow corresponding to the solar wind. When we define Dp as the distance between the dipole center and a position where the solar wind dynamic pressure balances the magnetic pressure at the dayside, we provided a dipole moment that gives the ratio D_p/L_i being comparable to or a bit larger than the unity, where L_i denotes the ion inertia length. In the preliminary simulation results, we could confirm the fundamental physics in the small magnetosphere such as the formation of a small-scale magnetosphere with asymmetric density profile between the dawn and dusk regions, the dependence on the direction of IMF direction. We describe the details of these phenomena. We will investigate how the formation of small magnetosphere varies when the D_p/L_i changes.

Meanwhile, mercury owns no ionosphere but an exosphere. We are interested in the formation of exo-ionosphere which can be represented by the spatial distribution of the Na+ ions. In future research, we will consider the contributions of heavy ions and photo-electrons with a certain scale height, and analyze their dynamics in the Mercury environment.

本研究の目的は、弱い固有磁場を持つ天体と太陽風の相互作用によって形成される小型磁気圏を 3 次元全粒子電磁シミュレーションにより再現し、各磁気圏領域の形成を運動論的観点から理解するとともに、磁場ダイポールモーメント強度に対する依存性を明らかにすることである。地球より小規模の磁気圏を持つ天体として水星がよく知られている。これまでの観測から、水星の固有磁場を形成する磁気モーメントは地球のものよりも約 2000 倍程度小さく、地球磁気圏の約 1/20 のサイズの小型磁気圏が形成されると予想されている。水星磁気圏の巨視的構造については、磁気流体力学 (MHD) シミュレーションを用いたモデル化も試みられているが、磁気圏各領域形成におけるイオンや電子の運動論的効果の重要性はまだ議論が進んでいない。そこで本研究では、水星環境パラメータを念頭に置き、電子及びイオンを粒子として扱う全粒子プラズマモデルによる小型磁気圏形成シミュレーションを行った。シミュレーションモデルでは、磁気ダイポールを持つ小型球体を中央に置き、領域境界から太陽風に相当する磁化プラズマ流を流す。昼間側において、ダイポール中心から磁気圧と太陽風動圧が釣り合う点までの距離を D_p とすると、標準モデルでは、D_p に対するイオン慣性長の比が 1 前後となるような磁気ダイポールを球体に与える。これまでに実施したシミュレーション結果により、小型磁気圏の形成、朝方夕方の磁気圏構造の非対称性、昼間側磁気圏境界層幅の IMF 方向の依存性などが明らかになった。本発表ではまずこれらの詳細について示す。先行研究において電子を流体として扱うハイブリッド粒子シミュレーションによる小型磁気圏形成解析が行われたが、本研究では、イオンのみならず電子の運動論的効果が小型磁気圏形成にどのように影響するかについても着目する。また、小型磁気圏形成が、D_p 対するイオン慣性長の比にどのように依存するかについても調べたい。

一方、水星には電離圏が存在せず、希薄な外圏大気が存在する。明確な電離圏がない磁気圏の電流構造において外圏起源のイオン（Na^+ など）がどのような役割を果たすかは興味深い。

今後、今回形成した磁気圏環境下に、あるスケールハイトを持つ重イオンや光電子の空間分布を導入し、小型磁気圏環境におけるそれらの分布及びダイナミクスを解き明かすことも計画している。

Loss process due to elastic collisions between magnetospheric keV electrons and neutral H2O molecules in the Enceladus torus

Hiroyasu Tadokoro[1]; Yuto Katoh[2]
[1] Musashino University; [2] Dept. Geophys., Grad. Sch. Sci., Tohoku Univ.

Water group neutrals (H_2O, OH, and O) in Saturn's inner magnetosphere play the dominant role in loss of energetic electrons and ions because of abundance of the neutrals [e.g., Paranicas et al., 2007,2008; Sittler et al., 2008]. The previous studies suggested that the neutral cloud originated from Enceladus contributes to loss processes of plasma in the inner magnetosphere. However, little has been reported on a quantitative study of the electron loss process due to electron-neutral collisions. Tadokoro et al., [2014] examined the variation of 1keV electron pitch angle distribution due to elastic collisions with the dense region of H_2O originated from Enceladus using one-dimensional test-particle simulation. The result showed that the electrons of ˜11.4% to the total number of equatoriall electrons at the initial condition are lost in ˜380sec, corresponding to the co-rotating electron flux tube passes the dense H_2O region in the vicinity of Enceladus. Next remaining issue is a calculation of energy dependent electron loss rate. We show the loss rate of electrons with 500eV-50keV and the comparison of the loss rate between the high (in the vicinity of Enceladus) and low (in the Enceladus torus) H_2O density regions.

ひさき衛星による木星磁気圏観測とグローバルMHDシミュレーションの連携解析の概要

木村 智樹 [1]; 深沢 圭一郎 [2]; 村上 豪 [3]; 北 元 [4]; 垰 千尋 [5]; 土屋 史紀 [6]
[1] RIKEN; [2] 京大・メディアセンター; [3] ISAS/JAXA; [4] 東北大・理・惑星プラズマ大気; [5] 情報通信研究機構; [6] 東北大・理・惑星プラズマ大気

Overview of the synergetic analysis of the global MHD simulation and Hisaki monitoring for Jupiter's magnetosphere

Tomoki Kimura[1]; Keiichiro Fukazawa[2]; Go Murakami[3]; Hajime Kita[4]; Chihiro Tao[5]; Fuminori Tsuchiya[6]
[1] RIKEN; [2] ACCMS, Kyoto Univ.; [3] ISAS/JAXA; [4] Tohoku Univ.; [5] NICT; [6] Planet. Plasma Atmos. Res. Cent., Tohoku Univ.

The Hisaki satellite has been monitoring our solar system bodies with the first-ever long continuity since its launch in September 2013. New dynamics in the planetary plasmas and atmospheres were discovered in the continuous monitoring. This study investigates the physical origin for the observed dynamics of Jupiter's aurora and plasma torus in comparison with the global magnetohydrodynamic simulation established by Fukazawa et al. [2005]. Variabilities in essential electromagnetic parameters (e.g., velocity distribution), which are likely associated with the solar wind and other conditions, are extracted from the MHD simulation. We are now quantitatively evaluating whether the extracted parameters can reproduce the observed auroral and torus dynamics. Here we report the progress in our project from the last year to the present.

２０１３年９月の打ち上げ以降、惑星分光観測衛星ひさきは、太陽系の惑星環境を、史上最も連続的に長期監視している。蓄積された大量の監視データから、今までの時間的に疎な観測では得られなかった、新しい惑星プラズマ加速・加熱過程や、大気物理の動力学が発見された。本研究では、ひさきの木星磁気圏観測で発見された、オーロラやイオプラズマトーラスの巨視的変動を物理的に解釈するため、Fukazawa et al. (2005) で確立されたグローバル MHD シミュレーションを解析し、観測を再現しうる磁気圏変動の特定を試みる。太陽風等に起因した、磁気圏内流速分布等の物理量の変動を抽出し、それらが観測されたオーロラやプラズマトーラスのダイナミクスを再現しうるか定量的検証を行っている。本発表では、昨年から現在までの取り組みの概要を報告する。

Solar wind influence on Jupiter’s inner magnetosphere derived from the global MHD simulation

Go Murakami[1]; Tomoki Kimura[2]; Keiichiro Fukazawa[3]; Chihiro Tao[4]; Hajime Kita[5]; Fuminori Tsuchiya[6]; Kazuo Yoshioka[7]

[1] ISAS/JAXA; [2] RIKEN; [3] ACCMS, Kyoto Univ.; [4] NICT; [5] Tohoku Univ.; [6] Planet. Plasma Atmos. Res. Cent., Tohoku Univ.; [7] The Univ. of Tokyo

Dawn-dusk asymmetric features in Jupiter’s inner magnetosphere, i.e., Io plasma torus (IPT), have been reported. Presence of dawn-to-dusk electric field is one of the leading explanations of the asymmetry. The extreme ultraviolet spectroscopy of IPT by Hisaki revealed that such a dawn-dusk asymmetry clearly responses to a rapid increase of solar wind dynamic pressure. However, the physical process of such a response and generating an intense electric field in Jupiter’s inner magnetosphere still remains unclear. Here we investigate the physical mechanism between the solar wind and Jupiter’s inner magnetosphere by using 3-dimensional global magnetohydrodynamic (MHD) simulation. We have calculated several cases with different solar wind conditions and compared the results with Hisaki observations. We found clear dependence of the field-aligned currents (FACs) from the mid-magnetosphere (~20-30 Rj) to the ionosphere on the solar wind dynamic pressure. Such FACs generates an additional electric potential pattern in the ionosphere and forms an electric field even in the inner magnetosphere. Thus our result agrees with the Hisaki observations and the scenario that dawn-to-dusk electric field is generated by the magnetosphere-ionosphere (M-I) coupling via FACs. This suggests that the solar wind influence can penetrate into Jupiter’s inner magnetosphere from the mid-magnetosphere via FACs.

Global MHDシミュレーションを用いた木星オーロラの太陽風応答に関する研究

北 元 [1]; 木村 智樹 [2]; 深沢 圭一郎 [3]; 垰 千尋 [4]; 村上 豪 [5]; 土屋 史紀 [6]
[1] 東北大・理・惑星プラズマ大気; [2] RIKEN; [3] 京大・メディアセンター; [4] 情報通信研究機構; [5] ISAS/JAXA; [6] 東北大・理・惑星プラズマ大気

Investigation of physical mechanisms of the solar wind control of Jovian aurora based on the global MHD simulation

Hajime Kita[1]; Tomoki Kimura[2]; Keiichiro Fukazawa[3]; Chihiro Tao[4]; Go Murakami[5]; Fuminori Tsuchiya[6]
[1] Tohoku Univ.; [2] RIKEN; [3] ACCMS, Kyoto Univ.; [4] NICT; [5] ISAS/JAXA; [6] Planet. Plasma Atmos. Res. Cent., Tohoku Univ.

The solar wind control on Jovian ultraviolet (UV) aurora is one of the unresolved issues in the Jovian system. Previous Hubble Space Telescope and ground based observations showed that the UV aurora and solar wind dynamic pressure had a positive correlation. Hisaki is an Earth-orbiting satellite, which monitoring planetary atmospheres and magnetospheres by the spectrometer EXCEED (Extreme Ultraviolet Spectroscope for Exospheric Dynamics). We have reported the statistical relationship between the total power of the Jovian UV aurora and the solar wind properties found from long-term monitoring by Hisaki EXCEED. Superposed epoch analysis indicates that auroral total power increases when the solar wind dynamic pressure increases. In addition to that, the auroral total power shows a positive correlation with the duration of a quiescent interval of the solar wind that is present before a rise in the dynamic pressure, more than with the amplitude of dynamic pressure increase.

This study investigates the physical mechanisms of the solar wind control on Jovian UV aurora based on the global magnetohydrodynamic simulation. We have calculated different cases of the dynamic pressure and the quiescent interval of the solar wind, which enable us to discuss the possible scenario for the solar wind response of Jovian magnetosphere.

Initial results show that the angular velocity profile becomes steeper when the dynamic pressure increases, which suggests that the magnetosphere-ionosphere coupling current (Hill current) becomes stronger. In addition to that, the field aligned current based on the method proposed by Hasegawa and Sato [1979] increases with a rise of the dynamic pressure. These characteristics are consistent with the observation result of Hisaki EXCEED. We will also discuss the dependence of the angular velocity distribution and the field aligned current with respect to the quiescent interval of the solar wind.

磁気圏グローバルモデルを用いた木星オーロラ増光時の磁気圏ダイナミクス

垰 千尋 [1]; 深沢 圭一郎 [2]; 木村 智樹 [3]; 北 元 [4]; 土屋 史紀 [5]; 村上 豪 [6]
[1] 情報通信研究機構; [2] 京大・メディアセンター; [3] RIKEN; [4] 東北大・理・惑星プラズマ大気; [5] 東北大・理・惑星プラズマ大気; [6] ISAS/JAXA

Magnetospheric dynamics during Jupiter auroral enhancements using a global magnetospheric model

Chihiro Tao[1]; Keiichiro Fukazawa[2]; Tomoki Kimura[3]; Hajime Kita[4]; Fuminori Tsuchiya[5]; Go Murakami[6]
[1] NICT; [2] ACCMS, Kyoto Univ.; [3] RIKEN; [4] Tohoku Univ.; [5] Planet. Plasma Atmos. Res. Cent., Tohoku Univ.; [6] ISAS/JAXA

The effect of solar wind variations on the rotation-dominated Jupiter magnetosphere have been investigated using various observations and simulations, while its physical mechanism of the auroral enhancements during solar wind dynamic pressure enhancements is not fully understood. Continuous monitoring of Jupiter auroral spectra using a spectrometer EXCEED (Extreme Ultraviolet Spectroscope for Exospheric Dynamics) on board the planetary space telescope Hisaki reveals the variations of aurora and precipitating auroral electrons during solar wind dynamic pressure enhancements. Application of the electron acceleration theory to the observed parameters suggests enhancements of magnetospheric source currents during the magnetospheric compression. This source current enhancement is proposed to be contributed by the source plasma variation or source position change [Tao et al., 2016JGR].

In order to evaluate the magnetospheric plasma variation during the solar wind compression, we have investigated the magnetospheric dynamics using a magnetohydrodynamic (MHD) simulation model of the Jovian magnetosphere [e.g., Ogino et al., 1998; Fukazawa et al., 2006]. The magnetospheric compression at middle-magnetosphere is traced by a conservation of the magnetic flux of equipotential shell regions. Variations of the magnetospheric plasma density, temperature, and source current density are derived in each shell with various solar wind dynamic pressure values. Dawn-dusk asymmetry of the equipotential shell is seen for the larger pressure case, due to the magnetospheric plasma convection. Variation of the parameters and comparison with the observation will be discussed in the presentation.

すばる望遠鏡補償光学系で観測された木星極域のパッチ状赤外オーロラ

渡辺 はるな [1]; 笠羽 康正 [2]; 坂野井 健 [3]; 鍵谷 将人 [4]; 北 元 [5]; 垰 千尋 [6]
[1] 東北大・理・地球物理; [2] 東北大・理; [3] 東北大・理; [4] 東北大・理・惑星プラズマ大気研究センター; [5] 東北大・理・惑星プラズマ大気; [6] 情報通信研究機構

IR patch-like aurora in Jupiter's polar region observed with SUBARU adaptive optic system

Haruna Watanabe[1]; Yasumasa Kasaba[2]; Takeshi Sakanoi[3]; Masato Kagitani[4]; Hajime Kita[5]; Chihiro Tao[6]
[1] Geophysics, Tohoku Univ.; [2] Tohoku Univ.; [3] Grad. School of Science, Tohoku Univ.; [4] PPARC, Tohoku Univ; [5] Tohoku Univ.; [6] NICT

The observations of Jovian auroras in the UV and IR range have revealed the morphology and their dynamics. Compared to main oval and satellite footprint mapping to (sub-)corotation region in Jupiter's magnetosphere, polar emissions are more variable in time and morphology, and they exhibit generally strong local time effects. Polar emissions are of great interest because their mapping to Jupiter's outer magnetosphere. It is suggested that the polar emissions in UV and IR show similar morphology in general [Radioti et al., 2013]. Jupiter's UV aurora is result of emission from excited atomic and molecular hydrogen, as precipitated electrons excite these species, occurring over a timescale of 10^{-2} sec. On the other hand, Jupiter's IR aurora emission is from $H_3{}^+$. In upper atmosphere $H_3{}^+$ is produced through ionization of H_2 and some ion chemistry, and thermalized in the neutral atmosphere, and then produces infrared ro-vibrational emission. So the timescale of IR auroral emission is longer than that of UV. The ion chemistry have a time scale of 10^{-2}~10^4 sec, and could play a key role to determine the total timescale of IR emission [Tao et al., 2012].

In the past imaging observation of Jupiter's IR aurora, the time resolution was ~25-30 min [Satoh and Connerney, 1999], and the spatial resolution was ~1 arcsec. Therefore, none of the observed aurora has significant variations on timescales less than 30 min and they are stable over ~90 min [Stallard et al., 2016]. But the auroral variability with shorter timescale may occur on the model calculation [Tao et al., 2012]. So the ground observation could image continuously for a long time with higher time resolution and spatial resolution should be realized.

In this study, we performed the Jovian IR auroral observation with IRCS (Infrared Camera and Spectrograph) attached on the SUBARU telescope at Mauna Kea, Hawaii on 25 May 2016 (3:16-9:56 UT). We took image data of the Jovian $H_3{}^+$ lines near 3.4 um using the H3P narrow-band filter. The time resolution was 45~110 sec. The Adaptive Optics instrument (AO188) attached to SUBARU provided us a high spatial resolution image of Jovian IR aurora with ~0.1 arcsec. The observation of Jovian IR aurora like this, in high spatial resolution and time resolution, is the first trial. Primary data reduction (dark, flat, sky) were finished and we calculated the absolute value of radiance using standard star ksi Vir. The emission intensity, there was brightness profile along the main oval, was ~5-9$*10^5$ W/m^2/str. Radioti et al. (2013) used the data observed by NSFCAM/IRTF and calculated the intensity. Compered to it, our result is larger in nearly one order. To determine the center of Jovian disc, we detected the duskside limb, observed clearly than dawnside because of the Sun direction, by fitting to curved line of Jovian disk limb estimated with plate scale. The error of fitting was estimated to be smaller than +/-2 pixels (0.106 arcsec). Then we calculated geographical longitude and latitude corresponding to each pixels and made the polar projection image. The location of main oval corresponded with the VIP4 30 R_j oval (magnetic coordinates). Additionally, from analysis of the data observed from 6:53 to 8:03, the emission patches were found in dayside polar region. The size of patches was ~3600-6000 km for latitudinal direction, and ~2800-4400 km for longitudinal direction. They blink in a few minutes and with amplitude of +/-15%, and are seen to move anti-rotation direction. The speed of moving was ~5.3-8.0 km/s. Considering that the timescale of change in thermospheric temperature or $H_3{}^+$ dynamic transport are 10^4-10^5 sec, these blinking emission corresponded to $H_3{}^+$ density change by particle precipitation. In this presentation, we report the detailed analysis results, and the study of observed polar emission using auroral emission model of Tao et al. [2011].

木星オーロラは、これまでのハッブル宇宙望遠鏡等による紫外観測や地上大型望遠鏡の赤外観測によってその分布や発光強度が明らかにされてきた。木星磁気圏プラズマの共回転および準共回転領域に起源を持つメインオーバルや衛星フットプリントのオーロラに比べて、ポーラーキャップの発光は時間・空間変化に富みローカルタイム依存性が見られる領域である。ポーラーキャップは 30R_j 以上の外部磁気圏或いは太陽風と接続した磁力線に繋がっていると考えられる。また、木星オーロラは紫外と赤外でおよそ同じ分布が見られている [Radioti et al., 2013]。紫外オーロラは磁気圏から降り込む電子が木星 H_2 大気と衝突することによる直接励起による発光であり、電子の降りこみに対する応答は早く、10^{-2} 秒程度である。一方赤外オーロラについては、電子の降りこみ等によって $H_3{}^+$ が生成され、さらに大気と降りこみ粒子の衝突やジュール加熱等で高温となっている H_2 大気中で $H_3{}^+$ が熱励起されることにより起こる発光であることから、電子降りこみに対する応答は紫外発光に比べてゆるやかである。その過程の中でも発光タイムスケールを大きく左右するのが化学反応であり、そのタイムスケールは 10^{-2}~10^4 秒である [Tao et al., 2012]。

今までの赤外オーロラの撮像観測は、紫外オーロラの観測に比べて時間・空間分解能ともに粗いものであった（撮像の場合の時間分解能はおよそ 25~30 分 [Satoh and Connerney, 1999]、空間分解能は 1 秒角程度）。それゆえ 30 分よりも短いタイムスケールでの赤外オーロラの変動の研究成果はほとんどなく、主に 90 分以上の長時間変動が報告されている [e.g.,

Stallard et al., 2016]。しかし、極域の紫外発光は数秒~数分スケールの変化が見られており、モデル計算から 30 分よりも短いタイムスケールの変動が起こる可能性が指摘されている [Tao et al., 2012]。赤外発光やそれが反映する大気は、紫外発光の短時間変動に対応して変化するのかについて、より高時間・高空間分解能で連続観測が可能な地上赤外観測が必要とされている。

我々は 2016 年 5 月 25 日（3:16-9:56 UT）にハワイ・マウナケア山頂のすばる望遠鏡赤外分光撮像装置 IRCS で木星赤外 H_3^+ オーロラの観測を行った。H3P narrow-band filter を用いて、H_3^+ イオンの輝線が含まれる 3.4 um 付近の波長域で撮像した。時間分解能は 45~110 秒であった。本研究の特長として、補償光学装置 AO188 を用いることにより、今まで行われてきた赤外オーロラ撮像よりも高い空間分解能（~0.1 秒角）を実現することができた。これほどの高い分解能および短い時間間隔での木星赤外撮像は初の試みであり、赤外オーロラの微細構造や時間変化を初めて観測することができた。観測データの一次処理（ダークノイズ除去、フラット補正、スカイ成分差し引き）を行った。さらに標準星 ksi Vir を用いて、絶対光強度を求めた。メインオーバルの明るさは場所によって異なり、5-9$*10^{-5}$ W/m^2/str であった。Radioti et al. (2013) では、NFSCAM/IRTF による観測データ（フィルター中心波長は同じく 3.4um）から絶対強度を求めており、それと比較すると桁 1 つに満たない程度、私たちの結果のほうが明るかった。次に、太陽光に照らされてディスクの夕方側リムを、プレートスケールから見積もられた木星ディスク曲線をリムにフィッティングすることで検出し、ディスク中心を定めた。フィッティングの誤差は+/-2 ピクセル（0.106 秒角）以下であることを確認した。次に、ディスク上の各画素の地理緯度経度を算出し、極座標マッピングを行った。これに VIP4 磁場モデルに基づく磁気座標を重ねた結果、メインオーバルの位置が VIP4 モデルの 30R_j に対応していることが確認された。また 6:53 － 8:03（UT）の画像データの解析から、昼側ポーラーキャップ領域にパッチ状の発光が存在することが分かった。パッチは緯度方向に~3600-6000km、経度方向には大きいもので~4400km、小さいもので~2800km 程度の広がりをもって見えていた。それらは数分のタイムスケール、および+/-15%の振幅で明滅し、昼側から夕方側ポーラーキャップ領域へと移動した。移動速度は~5.3-8.0 km/s 程度であった。熱圏の温度変化や H_3^+ 輸送の時定数は、10^4-10^5 秒と長いことから、今回観測された赤外の明滅発光変動は、オーロラ電子降り込みによる H_3^+ の密度変化に応答したものと考えられる。本発表では詳細な解析結果と、オーロラ発光モデル（Tao et al., 2011）を用いて、発光強度変動をもたらした降りこみ粒子や木星大気の変化について考察した結果を述べる。

Global MHD simulation of Jovian magnetosphere with recent supercomputer systems for observations and micro scale simulations

Keiichiro Fukazawa[1]; Yuto Katoh[2]; Tomoki Kimura[3]; Fuminori Tsuchiya[4]; Go Murakami[5]; Hajime Kita[6]; Chihiro Tao[7]; Ken T. Murata[7]

[1] ACCMS, Kyoto Univ.; [2] Dept. Geophys., Grad. Sch. Sci., Tohoku Univ.; [3] RIKEN; [4] Planet. Plasma Atmos. Res. Cent., Tohoku Univ.; [5] ISAS/JAXA; [6] Tohoku Univ.; [7] NICT

Planetary magnetospheres are very large, while phenomena within them occur on meso- and micro-scales. These scales range from 10s of planetary radii to kilometers. To understand dynamics in these multi-scale systems numerical simulations have been performed by using the supercomputer systems. We have studied the magnetospheres of Jupiter by using 3-dimensional magnetohydrodynamic (MHD) simulations for a long time, however, we have only obtained the phenomena not reaching the limits of the MHD approximation and simulation results under the specific solar wind conditions.

Recently thanks to the progress of supercomputer system, we can perform the simulation of Jovian magnetosphere with 1000 times large grid points of our previous simulation in 10 years ago. In other words, 1000 times cases of the our previous simulation can be performed at present. Considering these situations, it may be possible to connect the high resolution global (macro) simulation with micro simulation in the Jovian magnetosphere. In addition, performing a lot of parameter survey type simulations make quantitative comparison study of simulations and observations. Thus, in this study we perform the high-resolution simulation of Jovian magnetosphere to connect the electro-hybrid simulation, and low-resolution simulation under the various solar wind conditions to compare the Hisaki and Juno observation results.

For the high-resolution simulation to avoid the numerical effect to the simulation results from the irregular grid spacing, we simulated the global magnetosphere using the regular Cartesian gird with 0.15 RJ grid spacing and 7 RJ inner boundary. From these simulation settings, we can provide the magnetic field around 20 RJ from Jupiter as a background field of electro-hybrid simulation. To examine these simulation results, we found the wavy configuration along the magnetopause. This is the first time to see the wavy configuration in our global Jovian magnetospheric simulation and the wavy configuration seems to be caused by the Kelvin Helmholtz instability. In our previous simulation the resolution is not enough to catch the configuration.

In the parameter survey type simulations, we have obtained a lot of simulation results with 0.01 ˜0.09 nPa solar wind dynamic pressure and some IMF cases. These simulation data are open for the registered user to download the raw data. Comparing these data with Hisaki observation results, the relation of changing the solar dynamic pressure with emission of aurora is examined.

HISAKI衛星で観測された2015年イオ火山イベントにおけるイオトーラス中硫黄イオンのSystem IV周期の変動

荒川 崚 [1]; 三澤 浩昭 [2]; 土屋 史紀 [3]; 鍵谷 将人 [4]; 吉川 一朗 [5]; 吉岡 和夫 [6]; 鈴木 文晴 [7]; 木村 智樹 [8]; 村上 豪 [9]; 山崎 敦 [10]
[1] 東北大・理・地球物理; [2] 東北大・理・惑星プラズマ大気研究センター; [3] 東北大・理・惑星プラズマ大気; [4] 東北大・理・惑星プラズマ大気研究センター; [5] 東大・理・地惑; [6] 東大・理; [7] 東大・新・複雑; [8] RIKEN; [9] ISAS/JAXA; [10] JAXA・宇宙研

Variations of System IV period of the sulfur ions in the Io torus for the volcanic event in 2015 observed by HISAKI satellite

Ryo Arakawa[1]; Hiroaki Misawa[2]; Fuminori Tsuchiya[3]; Masato Kagitani[4]; Ichiro Yoshikawa[5]; Kazuo Yoshioka[6]; Fumiharu Suzuki[7]; Tomoki Kimura[8]; Go Murakami[9]; Atsushi Yamazaki[10]
[1] Geophysics, Tohoku Univ.; [2] PPARC, Tohoku Univ.; [3] Planet. Plasma Atmos. Res. Cent., Tohoku Univ.; [4] PPARC, Tohoku Univ; [5] EPS, Univ. of Tokyo; [6] The Univ. of Tokyo; [7] Complexity Science, Univ. of Tokyo; [8] RIKEN; [9] ISAS/JAXA; [10] ISAS/JAXA

http://www.sgepss.org/

Io plasma torus (IPT) consists of dissociated and ionized volcanic gas originated from Jupiter's moon Io, which distribute along Io's rotation orbit. The plasma corotates by the corotation electric field in the Jovian rotation period (9.925 h) called System III. However previous ground-based and probe observations of Io plasma torus (IPT) in visible, near-infrared and extreme ultraviolet (EUV) wavelengths have detected a periodic time variation whose period is longer than System III Jupiter's rotation period (9.925 h). It has been called System IV period. The *dual hot electron model* in which hot electron populations has two azimuthal variations rotating at System III and System IV periods is proposed to account for the System IV period measured by the Cassini UVIS observation (Steffl et al., 2008). While it is interpreted that the System III period of hot electron populations corresponds to azimuthal modulation of the efficiency of the electron acceleration (Hess et al., 2011), little progress has been made in explaining an origin of the System IV period.

The Cassini UVIS observation of IPT was made after the end of Io's volcanic eruption in 2000. It is reported that the System IV period derived from the Cassini observation was 10.07 h, which was shorter than the typical period of 10.21h (Steffl et al., 2006). However, the causal relationship between plasma source enhancement due to the volcanic event and change in the System IV period is not clear from the Cassini observation. Here, we analyzed time variations in intensities of EUV emissions from IPT obtained by the HISAKI satellite to understand the mechanism responsible for the System IV period and the influence of Io volcanic activity on IPT.

The observation period used in this study is from December 2014 to the middle of May 2015. During this period, enhancement of Io volcanic activity from January to March 2015 (here after 'volcanic period') was reported from the observation of Iogenic sodium emission (Yoneda et al., 2015). To find variations of the System IV period in the EUV brightness, the System III longitude at peak EUV intensity was derived by the fitting the HISAKI Level-2 data (S II 76.5 nm + 126 nm, S III 68 nm, and S IV 65.7 nm + 140.5 nm) with a sinusoidal function which consists of sum of two sinusoidal curves whose periods are System III (9.925 h) and the Io orbital period (42.456 h). The time variation in the phase of the System III component indicates the System IV period, which was derived as a mean value for a certain period. From this analysis, the System IV periods of S II before and after the volcanic event (Dec. 1, - Dec. 23, 2014 and April. 21 - May 14, 2015, respectively) were 10.16+-0.008 h and 10.03+-0.006 h, respectively. On the other hands during the volcanic event, the System IV period of S II was 9.95+-0.003 h for Mar. 11 - Apr. 20. This is the first observational evidence which shows that the System IV period has shortened after the enhancement of Io volcanic activity.

Origin of the System IV period has been discussed with sub-corotation of plasma in IPT. Since the sub-corotation occurs due to mass loading of newly picked-up ions into IPT, it is expected that the System IV period becomes long during the volcanic event. However, the result derived from the HISAKI observation shows the opposite feature and will give important information to constrain the origin of the System IV period.

The EUV intensity depends on not only ion density but electron density and temperature. To investigate the contribution of each plasma parameter to the appearance of System IV period, we will derive time variation in plasma parameters in IPT from the HISAKI data with plasma diagnosis analysis. This analysis enable us to confirm the dual hot electron model and constrain the origin of the System IV period.

衛星イオ起源の火山性ガスが解離・電離することにより、イオの軌道に沿ってトーラス状に分布したイオプラズマトーラス (IPT) が形成される。プラズマは木星の共回転電場により System III と呼ばれる木星自転周期（9.925 時間）で共回転している。しかし、過去の可視・近赤外・極端紫外の波長域における発光強度の観測からは、木星の自転周期よりも長い周期変動が観測されてきた。この周期は「System IV 周期」と呼ばれている。Cassini 探査機の紫外分光器 UVIS に

よって観測された System IV 周期の存在を説明するために Steffl らは、System III 周期と System IV 周期で回転する高温電子の二つの経度方向分布が同時に存在するとした「Dual hot electron model」(Steffl et al., 2008) を提案した。System III 周期成分の起源は、木星磁場の不均一性により生じる電子の加速効率の経度変調により生じると解釈されている（Hess et al., 2011）一方で、System IV 周期成分の起源については、様々な提案がされているが、未解明である。

Cassini による IPT の観測は、2000 年に発生したイオの火山噴火活動の終結時に開始された。この観測から求められた System IV 周期は 10.07 時間で、典型的な周期 (10.21 時間) よりも短いことが報告されている (Steffl et al., 2006）が、観測期間の制約のため、火山活動によるプラズマの増大と System IV 周期の変化の相互関係をこの観測から求めることは出来なかった。そこで、本研究ではイオの火山活動による IPT の変化と System IV 周期性との関係を明らかにし、さらにその周期が生じるメカニズムを理解するため、HISAKI 衛星で観測された IPT の極端紫外線 (EUV) 発光強度の時間変動を解析した。

本研究で用いたデータの観測期間は 2014 年 12 月から 2015 年 5 月半ばである。この期間中の 2015 年 1 月から 3 月にかけて、イオの火山活動の活発化がイオ起源のナトリウム発光の観測から報告されている（Yoneda et al., 2015)。この時期の System IV 周期とその変動を以下の手順で導出した。（１）HISAKI の Level-2 データから、S II 76.5 nm + 126 nm , S III 68 nm, S IV 65.7 nm + 140.5 nm における硫黄イオンの発光強度の時系列を抽出する。（２）データウィンドウ 5 日の時系列データに、第 1 項が System III 周期、第 2 項がイオの公転周期 (42.456 時間) の 2 つのサインカーブの線形結合の関数でフィッティングする。第 1 項の位相の時間変化が System IV 周期に対応し、任意期間のこの位相変化率の平均値から System IV 周期を求めた。この解析から火山活動増大の前後（2014 年 12 月 1 日から 12 月 23 日、及び、2015 年 4 月 21 日から 5 月 14 日）における S II 76.5 nm + 126 nm の System IV 周期は、それぞれ 10.16 ＋－ 0.008 時間と 10.03 ＋－ 0.006 時間であった。一方で火山活動増大期（2015 年 3 月 11 日から 4 月 20 日）の S II 76.5 nm + 126 nm の System IV 周期は 9.95 ＋－ 0.003 時間であった。これは、イオの火山活動の活発化により System IV 周期が短くなることを示す初めての観測的証拠である。

System IV 周期の起源は IPT 中のプラズマの準共回転と関連付けて議論されてきた。プラズマの準共回転は IPT 中に新たにピックアップされたイオンの質量供給により起こっているので、火山活動の増大中は共回転からの遅延が大きくなり、System IV 周期が長くなることが予想される。しかしながら、本研究で得られた HISAKI による観測結果はこの予想とは異なっており、System IV 周期の起源を考察する上で重要な情報となる。

EUV 発光強度は IPT 中のイオン密度に加え、イオンの励起率を決めている電子温度・電子密度に依存する。発光強度の System IV 周期の変動がどのプラズマパラメータにより生じているのかを調べるため、プラズマ診断手法 (Yoshioka et al. 2014) を用いてプラズマパラメータの時系列を求め、その周期変動特性の導出を進めている。この解析により、先行研究で提示された Dual hot electron model の確認を行うとともに、System IV 周期生成過程に制約を与えることが期待される。

Variation of ion and electron temperature on Io plasma torus after an outburst measured with Hisaki and ground-based observations

Masato Kagitani[1]; Fuminori Tsuchiya[2]; Mizuki Yoneda[3]; Kazuo Yoshioka[4]; Tomoki Kimura[5]; Go Murakami[6]; Chihiro Tao[7]; Yamazaki Atsushi Hisaki (SPRINT-A) project team[8]
[1] PPARC, Tohoku Univ; [2] Planet. Plasma Atmos. Res. Cent., Tohoku Univ.; [3] none; [4] The Univ. of Tokyo; [5] RIKEN; [6] ISAS/JAXA; [7] NICT; [8] -

Volcanic gases (mainly composed of SO_2, SO and S) originated from jovian satellite Io are ionized by interaction with magnetospheric plasma and then form a donut-shaped region called Io plasma torus. Ion pickup is the most significant energy source on the plasma torus thought, additional energy source by hot electron is needed to explain energy balance on the neutral cloud theory (e.g. *Daleamere and Bagenal,* 2003). In fact, in-site measurements by Galileo indicates some injections of energetic particles in the middle magnetosphere. Recent EUV spectroscopy from the space shows fraction of hot electron increases as increase of radial distance in the plasma torus (*Yoshioka et al.,* 2014; *Steffl et al.,* 2004). On this study, we focus on variability of electron temperature derived from EUV diagnostics measured by HISAKI/EXCEED after a volcanic outburst in 2015, as well as ion temperatures parallel and perpendicular to the magnetic field measured from the ground-based spectroscopy.

The ground-based observation of sulfur ion emission, [SII] 671.6nm and 673.1nm from Io plasma torus was made at Haleakala Observatory in Hawaii from November 2014 through May 2015 with the high-dispersion spectrograph (R = 67,000) with an integral field unit (IFU) coupled to a 40-cm Schmidt-Cassegrain telescope. The IFU consist of 96 optical fibers (core/crad/jacket diameter are 50/125/250 micro-meters, respectively). The fibers are arranged in 12 by 8 array at the telescope focus which makes high-resolution spectroscopy over field-of-view of 41”” by 61” with a spatial resolution of 5.1” on the sky. Two-dimensional Doppler measurements enables to derive spatial distribution of [SII] emissions as well as their temperatures parallel and perpendicular to the magnetic field. We also made observation of neutral sodium cloud extending up to several hundred of jovian radii as a proxy of supply of neutral particles from Io (*Yoneda et al.,* 2015).

We also employee EUV spectroscopy of Io plasma torus with EUV space telescope Hisaki EXCEED from December 2014 through May 2015. We have made spectral fitting as the following method. First, we made series of EUV spectra averaged over five days. Next, assuming azimuthal homogeneity of Io plasma torus, Abel inversion is made to reduce line-of-sight integration effect. Then, we made fitting of observed EUV spectra (60 - 140 nm) with CHIANTI model spectra by changing electron density and temperature, mixing ratio of ions (S^+, S^{++}, S^{+++}, O^+ and O^{++}) and fraction of hot electron (Te = 100 eV).

Based on observation of neutral sodium cloud (Yoneda et al., 2015), neutral supply started to increase at around DOY= 10, was at maximum at around DOY = 50, and has backed into the initial levels at around DOY = 120. In contrast, plasma diagnostics indicates that hot electron fraction at 7.0 jovian radii was less than 2 % before DOY = 50, started to increase after DOY = 50, and have reached 8(+/-1) % at DOY = 110. In addition, ion temperatures from ground-based observation started to increase after DOY=50 as similar tread of increase of hot electron fraction. EUV emission from aurora was also activated after DOY = 50 as increase of hot electron fraction on the plasma torus.

We also tried to reproduce the observed variation of electron and ion temperatures and densities using 0-dimensional time evolution model. The model calculates mass and energy balances in the torus under given conditions of neutral supply and transportation timescale as made by *Delamere and Bagenal,* 2003. Though hot electron fraction derived from plasma diagnostics is 5-10 times as much as that from the model, the mode with variable hot electron fraction reproduces the observed variation of ion mixing ratio and plasma temperatures well. The result indicates that the injection of hot electron from the outer magnetosphere (and/or local generation of hot electron) is activated after the outburst.

A study on long-term variation of Jupiter’s synchrotron radiation associated with solar wind

Sooman Han[1]; Go Murakami[2]; Atsushi Yamazaki[3]; Hajime Kita[4]; Fuminori Tsuchiya[5]; Masato Nakamura[6]
[1] EPS, UTokyo; [2] ISAS/JAXA; [3] ISAS/JAXA; [4] Tohoku Univ.; [5] Planet. Plasma Atmos. Res. Cent., Tohoku Univ.; [6] ISAS,JAXA

Jovian Radiation belt is a layer of energetic particles (˜few tens MeV). Jupiter’s synchrotron radiation (JSR) observation is a main tool for determining physical process therein, and various diffusion models have been proposed to account for the observed JSR’s short-term and long-term variations observed in the past. As for the long-term variation, where the total JSR flux density varies by 20-30% over a few years, it is known to be well correlated with solar wind ram pressure [Bolton et al. 1989] with lag time of 2 years, but its reason still remains unknown.

Amid the situation, Extreme ultraviolet spectroscope HISAKI has found evidence of electric field inside the magnetosphere-large-scale convection electric field associated the solar wind [Murakami et al. 2016], from which one can expect enhanced radial diffusion inside the magnetosphere.

In this study, I show the result of my numerical calculation on radial diffusion driven by the estimated convection electric field and synchrotron radiation variation resulted therefrom and suggest that the long term variation with 2 years lag time can possibly explained by solar-wind-driven convection electric field.

Study of the correlation between nKOM and reconnection in the Jovian magnetosphere: Inward radial transport in the magnetosphere

Takahiro Mizuguchi[1]; Hiroaki Misawa[2]; Fuminori Tsuchiya[1]; Takahiro Obara[3]
[1] Planet. Plasma Atmos. Res. Cent., Tohoku Univ.; [2] PPARC, Tohoku Univ.; [3] PPARC, Tohoku University

Jupiter has the largest magnetosphere in the planets of our solar system, which has been produced by its rapid rotation period (about 10 hours), strong intrinsic magnetic field and internal source of heavy plasma originated from Io plasma torus (IPT).

The observations by the Galileo orbiter revealed that there were quasi-periodic phenomena in the Jovian magnetotail, such as radial flow bursts of energetic particles [Krupp et al., 1998, Woch et al., 1998] and the variation of radial and north-south component of the magnetic fields [Krupp et al., 1998], which imply occurrences of magnetic reconnections and the periodic thinning and thickening of the plasma sheet. The signatures of these events were similar to the terrestrial substorm, so they are called ””substorm-like events (SLE)”” [Woch et al., 1998].

It is also known that there are radio emissions from the Jovian magnetosphere which correlate with SLE. In the preceding studies, Louarn et al. (2001, 2014) reported the narrow-band KilOMetric radiation (nKOM) and the HectOMetric radiation (HOM) correlated with inward flow burst and variation of the north-south component of the magnetic field during SLE. X-lines where the SLEs are thought to start were located at around 60-80 Jovian radii (R_J) region from Jupiter [Woch et al., 2002], while the source of nKOM is suggested to be located at the outer edge of the IPT (6-10 R_J) [Reiner et al., 1993]. The report implies that the generation process of nKOM relates to the reconnection at the magnetotail. However, it has not been revealed well yet how inner (6-10 R_J) and outer (60-80 R_J) magnetospheres couple each other during SLE.

The purpose of this study is to reveal coupling processes of the formation of nKOM at the inner magnetosphere (6-10 R_J) and the reconnection at the magnetotail (60-80 R_J). To study this process is important in order to understand the inward radial transport of energy and/or plasma in the Jovian magnetosphere and the proceeding processes of the global dynamics of the Jovian magnetosphere (as suggested by Kivelson et al. (2005)).

Louarn et al.(2015) suggested that the role of reconnection in the mechanism of radial inward transport was not clarified. Although reconnection thought to be trigger of inward radial transport, statistical analysis shows signatures of inward plasma flows reaching at inner magnetosphere (such as increase of southward magnetic field) were rare.

In this study, we have used nKOM which can be observed by remote sensing and have compared reconnection in the magnetotail region and characteristics of nKOM at the inner magnetosphere. We have obtained intensity of each nKOM event and have compared it with variation of B_r, radial component of magnetic field, as a parameter of SLE. As a result, there was correlation between the intensity of nKOM and the variation of B_r which corresponds each nKOM event.

This indicates there is relation between the energy stocked as stretching of magnetic field and the energy input towards the inner magnetosphere by the result of reconnection. We think this is one of evidences indicating inward radial transport of energy in the Jovian magnetosphere. We will discuss the energy balance and the time series of each phenomenon during SLE in order to explain this relation. We will also discuss the physical processes of this relation in order to consider the role of reconnection for inward radial transport of energy and the coupling processes of the formation of nKOM in the inner magnetosphere and the reconnection in the magnetotail region.

木星ヘクトメータ電波の発生特性の再考

三澤 浩昭 [1]; 水口 岳宏 [2]; 土屋 史紀 [2]
[1] 東北大・理・惑星プラズマ大気研究センター; [2] 東北大・理・惑星プラズマ大気

Reconsideration of source characteristics of Jupiter's hectometric auroral radio emission

Hiroaki Misawa[1]; Takahiro Mizuguchi[2]; Fuminori Tsuchiya[2]
[1] PPARC, Tohoku Univ.; [2] Planet. Plasma Atmos. Res. Cent., Tohoku Univ.

http://pparc.gp.tohoku.ac.jp/

It is known that Jupiter's auroral radio emission in the hectometric wave range (HOM) shows two type occurrence components. One is a component relating to solar wind variations (sw-HOM) appearing around CML (Central Melian system III Longitude of an observer) ~180deg when solar wind pressure enhances. The other one is generally more intense than sw-HOM and has no or weak relation with solar wind variations (nsw-HOM) appearing around CML ~110deg and ~280deg for major components when De (Jovicentric declination of an observer) ~-1deg (Nakagawa et al., 2000; Nakagawa, 2003). The nsw-HOM is thought to be generated by some internal processes initiated by the rapid planetary rotation and massive magnetospheric plasma, however precise source processes have not been revealed well.

We have reanalyzed occurrence characteristics of HOM using the WIND/WAVES data to investigate precise relation between occurrence of nsw-HOM and Jupiter's magnetospheric variations, such as plasma and magnetic field variations observed by the Galileo Jupiter orbiter and variations of Iogenic volcanic gases/plasmas obtained from the Earth based observations. As a preliminary result, a minor component of the nsw-HOM appearing around CML~340deg likely relates to magnetic reconfiguration events occurred in the Jovian outer magnetosphere, and enhancement of the major nsw-HOM sometimes lasts for more than a few days seemingly without relation to the magnetospheric variations (and also solar wind variations). In the presentation, we will show the precise occurrence characteristics of HOM and discuss their possible source processes including a comparison study of HOM with Jupiter's auroral appearance nature.

Acknowledgements: We would greatly appreciate M. Kaiser, J.-L. Bougeret and the WIND/WAVES team for providing the radio wave data.